TÉCNICO LISBOA

Deployment of 5G Radio Networks in Brownfield Scenarios

Maria dos Santos Magalhães de Carvalho Ferreira

Thesis to obtain the Master of Science Degree in

Telecommunications and Informatics Engineering

Supervisor: Prof. Luís Manuel de Jesus Sousa Correia

Examination Committee

Chairperson: Prof. Ricardo Jorge Fernandes Chaves

Supervisors: Prof. Luís Manuel de Jesus Sousa Correia

Members of Committee: Prof. António Manuel Raminhos Cordeiro Grilo

Eng. Ricardo Jorge Dinis

July 2022

I declare that this document is an original work of my own authorship and that it fulfils all the requirements of the Code of Conduct and Good Practices of the *Universidade de Lisboa*.

To my family and friends

Acknowledgements

First of all, I would like to thank Professor Luis M. Correia for providing me the opportunity to develop a thesis guided by him, for all the weekly meetings held, for learning and sharing information, for his constant availability to support and clarify doubts and for all the involvement and commitment throughout the course of the thesis.

I would also like to thank Eng. Ricardo Dinis, from NOS, for the support and the availability that allowed the development of the thesis, making it more interesting, as well as the sharing of ideas and the information analysis carried out together.

To all members of the Grow community, especially Afonso Carvalho, Beatriz Ferreira, Marco Failache, and Sofia Patrício for their companionship during this period and knowledge sharing and all the pleasant atmosphere created during the online meetings.

I would like specially to thank all my family and friends who have supported me throughout my academic journey, thank them for all the care and love provided, for encouraging me not to give up in bad times, and for being there even when a pandemic got in the way.

Last but not least, to my boyfriend, Hugo Cruz, for having supported me at all times, for listening to me, and for having been a pillar throughout the several years together, especially the year of development of this thesis.

My deepest appreciation to you all,

Maria Ferreira

Abstract

The main objective of this thesis was to develop an evaluation model of the deployment of 5G radio networks, focusing on subjects such as coverage, capacity, and performance parameters, over existing ones from previous generations, i.e., in a brownfield scenario. The proposed model considers coverage and capacity planning characteristics related to 5G-NR, using both the 700 and the 3 500 MHz bands. Simulations were conducted in three different types of environments (urban, suburban and rural). Different traffic profiles were equally considered in order to simulate a mobile communications network that encompasses the new services introduced by 5G NR. The increase in the total number of users influences the number of served users, that is, when cell capacity is exceeded some users are deactivated. With the use of other bands and different bandwidths, it is verified that with the increase in the total number of users in the 2.6 GHz band, it is possible to have an addition of 4% in relation to the number of users served compared to the 0.7 GHz one. As for the 3.5 GHz band, with the increase in the total number of users, it is seen that it is possible to support a total number of served users 20% higher than the reference band.

Keywords

5G-NR, Brownfield, Dimensioning, Coverage, Capacity.

Resumo

O objetivo desta tese é desenvolver um modelo de avaliação da implementação de redes de rádio 5G, com foco em temas como cobertura, capacidade e parâmetros de desempenho, sobre as gerações já existentes, ou seja, num cenário *brownfield*. O modelo proposto considera as características de cobertura e planeamento de capacidade relacionadas com o 5G-NR, utiliza as bandas de 0,7 e 3,5 GHz. Simulações foram realizadas em três tipos diferentes de ambiente (urbano, suburbano e rural). Diferentes perfis de tráfego foram igualmente considerados para simular uma rede de comunicações móveis que englobe os novos serviços introduzidos pelo 5G NR. O aumento do número total de utilizadores influencia o número de utilizadores servidos, ou seja, quando a capacidade da célula é excedida, alguns utilizadores são desativados. Com a utilização de outras bandas e diferentes larguras de banda, verifica-se que com o aumento do número total de utilizadores na banda de 2,6 GHz, é possível ter um acréscimo de 4% em relação ao número de utilizadores servidos quando comparado com a banda de 0,7 GHz. Quanto à banda de 3,5 GHz, com o aumento do número total de utilizadores, verifica-se que é possível suportar um número total de utilizadores servidos 20% superior à banda de referência.

Palavras-chave

5G-NR, Co-localização com sistemas anteriores, Dimensionamento, Cobertura, Capacidade.

Table of Contents

List of Figures

List of Tables

List of Acronyms

16QAM	Quadrature Amplitude Modulation (4 bits per symbol)
256QAM	Quadrature Amplitude Modulation (8 bits per symbol)
3G	Third Generation
3GPP	3rd Generation Partnership Project
4G	Fourth Generation
5G	Fifth Generation
5GC	Fifth Generation Core
64QAM	Quadrature Amplitude Modulation (6 bits per symbol)
AF	Application Function
AMF	Access and Mobility Management Function
AN	Access Network
AR	Augmented Reality
ART	Augmented Reality
ASICs	Application Specific Integrated Circuits
AUSF	Authentication Server Function
BPSK	Binary Phase Shift Keying
BS	Base Station
BW	Bandwidth
BWP	Bandwidth Parts
CN	Core Network
CP	Control Plane
DL	Downlink
DN	Data Network
EIRP	Effective Isotropic Radiated Power
EMA	E-mail
eMBB	Enhanced Mobile Broadband
eNB	Evolved Node-B
EN-DC	E-ULTRA-ER Dual Connectivity
en-gNB	enhanced next generation Node B
EPC	Evolved Packet Core Network
E-ULTRA	Evolved Universal Terrestrial Radio Access
FAU	Factory Automation
FDD	Frequency Division Duplex
FR2	Frequency Range 2

FTF	File Transfer
FTP	File Transfer Protocol
GB	Giga-Byte
GPS	Global Positioning System
HRND	Heuristic Radio Network Dimensioning
HSS	Home Subscription Server
IMT	International Mobile Telecommunications
IoT	Internet of Things
IT	Information Technology
ITS	Intelligent Transport System
ITU-R	International Telecommunication Union - Radiocommunication
KPI	Key Performance Indicator
LTE	Long Term Evolution
MAPL	Maximum Allowed Path Loss
MIMO	Multiple-Input Multiple-Output
MME	Mobility Management Entity
mMIMO	Massive Multiple-Input Multiple-Output
mMTC	Massive Machine Type Communication
MT	Mobile Terminal
MUS	Music
NB	Node-B
NEF	Network Exposure Function
NF	Network Func
NFV	Network Function Virtualisation
NG-RAN	New Generation Radio Access Network
NR	New Radio
NRF	Network Repository Function
NSA	Non-standalone
NSSAAF	Network Slice Specific Authentication and Authorisation Function
NSSF	Network Slice Selection Function
OFDM	Orthogonal Frequency Division Multiplexing
OFDMA	Orthogonal Frequency Division Multiple Access
OH	Okumura-Hata
P2P	Peer-to-Peer
PCF	Policy Control Function
PCRF	Policy and Charging Resource Function
PDU	Protocol Data Unit
PER	Packet Error Rate
PGW	Packet Data Network Gateway
PGW-C	Packet Data Network Gateway - Control

PGW-U	Packet Data Network Gateway - User
PRB	Physical Resource Block
QoE	Quality of Experience
QoS	Quality of Service
QPSK	Quadrature Phase Shift Keying (2 bits per symbol)
RAN	Radio Access Network
RAT	Radio Access Technology
RB	Resource Block
RF	Radio Frequency
RSU	Remote Surgery
RTG	Real-Time Gaming
SA	Standalone
SC	Single Carrier
SC-FDMA	Single Carrier Frequency Division Multiple Access
SCP	Service Communication Proxy
SCS	Subcarrier Spaces
SGW	Service Gateway
SINR	Signal-to-Interference-plus-Noise Ratio
SLA	Service Level Agreement
SMF	Session Management Function
SMS	Short Message Service
SNW	Social Networking
TDD	Time Division Duplex
UDM	Unified Data Management
UE	User Equipment
UL	Uplink
UP	User Plane
UPF	User Plane Function
uRLLC	Ultra-Reliable Low Latency Communication
V2V	Vehicle to Vehicle
VCF	Video Conference
VOI	Voice
VR	Virtual Reality
VST	Video Streaming
WBW	Web Browsing
WI	Wallfisch-Ikegami
WIN II	Winner II

List of Symbols

α_{pd}	Average power decay
β	path loss exponent
Δf	Subcarrier Spacing
δ	Phase difference
η	Cell load factor
η_{cell}	Overload of a cell
$\eta_{u,cell}$	Percentage of active served users
θ	Angle between the positive half of the Z-axis and the observation point
θ_B	3 dB beamwidth in degrees
λ	Wavelength
μ	Numerology
$\rho_{N,min}$	SNR requirement for a given throughput
ρ_{IN}	SNR value
ϕ	Beam's azimuth angle
A_{cell}	Area of a cell
B_{RB}	Bandwidth per RB, which depends on the SCS
$B_{i,k}$	Fading channel gain for donor cell
$B_{j,k}$	Fading channel gain for neighbouring cell
B	Dependency path loss variable

$D_{i,k}$	Distances from user to donor BS
$d_{j,k}$	Distances from user to neighbouring cells
d_a	Interspacing between elements in an antenna array
d_{max}	Maximum UE distance from BS
E_a	Field radiated by a single element
E	Electric field
F_N	Noise figure of the receiver
F_{aa}	Antenna array factor
f^j	Scaling factor, can take the values 1, 0.8, 0.75, and 0.4
G_{TMA}	TMA gain
G_{div}	Diversity gain
G_r	Gain of the receiving antenna
G_t	Gain of the transmitting antenna
I_m	Interference margin
I_{max}	Maximum current in the antenna
I_{mp}	Excitation coefficient
J	Number of aggregated component carriers in a band or band combination
k	Free space wave number
$\overline{L_{p_{ind}}}$	Indoor path loss
L'_p	Path loss given by the sum of the outdoors and indoors path loss
L_A	Correction factor related to the frequency, BS and UE antenna height, dependent on the propagation scenario

L_B	Correction factor related to the BS antenna height
L_C	Propagation scenario correction factor
L_c	Losses in the cable between the transmitter and the antenna
$L_{p,ref}$	Reference path loss, reference for 1 km distance
$L_{p,max}$	MAPL given by the Link Budget computation
L_u	Losses due to the user's body
L	Constant depending on the infrastructure of sender and receiver
l	Dipole's half length
M_{SF}	Slow-fading margin
M	Modulations served in the cell
m	Order of modulation
$\overline{N_{RB,required}}$	Total number of required RBs in the respective cell
$\overline{N^{M}_{RB,required}}$	Total number of required RBs in the respective cell per modulation
$\overline{N^{M}_{RB}}$	Total number of RBs for a modulation
$\overline{N_{RB,users,s}}$	Number of RBs allocated in the BS for a user for a specific service
$N_{f\ th}$	Number of floors theoretical calculation
N_f	Number of floors
$N_{RB,cell}$	Total number of RBs in the respective cell
N_{RB}	Number of RB
$N^{frame,\mu}_{slot}$	Number of slots in a frame
$N^{subframe,\mu}_{slot}$	Number of slots in a subframe
N^{slot}_{symb}	Number of OFDM symbols in a slot
$N_{u,cell}$	Number of active users in the cell

$N_{u,s}$	Number of active users in the service s.
N_u	Total number of users in the system
N_{MIMO}	MIMO order
$N_{PRB}^{BW^j,\mu}$	Maximum RB allocation in bandwidth BW^j with numerology μ, where BW^j is the UE supported maximum bandwidth in the given band
N_{RB}^u	Number of RB per user
N_{SC}^{RB}	Number of subcarriers per RB
N_a	Number of dipole elements of the array
N_{beams}	Number of beams
N_{ele}	Number of radiating elements
$N_{n,cell}$	Number of neighbouring cells
$N_{streams}$	Number of streams, in case of MIMO (2x2 MIMO means the number of streams is 2)
N_{symb}^{SF}	Number of symbols per sub-frame (14 for normal CP or 12 for extended CP)
$N_{u,cell}^M$	number of users accommodated in a cell
N_u^M	number of users served by the modulation M
$N_{users,cell}$	Number of users in a cell
N	Noise power
O^j	Overhead
$p_{traffic,s}$	Percentage of traffic per service
$P_{u,s}$	Subscriber usage percentage of a service *s*
P_i	Transmit power of donor BS
P_{EIRP}	Effective Isotropic Radiated Power
P_{Rx}^{DL}	Receiver input power at DL

P_{Rx}^{UL}	Receiver input power at UL
P_{Tx}	Transmitter output power
P_j	Transmit power of neighbouring BS
$P_{r,min}$	Received power
P_t	Power fed to the transmitting antenna
P_t^{DL}	Power feed to the antenna in the DL
P_t^{UL}	Power feed to the antenna in the UL
Q_m^j	Maximum supported modulation order
$\overline{R_{b,cell}}$	Average user consumption in all services
$\overline{R_{b,RB}^M}$	Average throughput per RB of each modulation M
$\overline{R_{b,users,s}}$	Average throughput per user of a service s
R_{16}	Cell 16-QAM radius
R_{64}	Cell 64-QAM radius
R_{256}	Cell 256-QAM radius
R_Q	Cell QPSK radius
R_b	Throughput per RB
R_{max}	Maximum code rate
r	Distance between the antenna and the observation point
T_{SF}	Sub-frame period
T_s^{μ}	Average OFDM symbol duration in a subframe for numerology μ
u_θ	Unit vector
v_{Layers}^j	Maximum number of supported layers
y_m	Position in the y-axis of the radiating element

Z_0	Free space impedance
z_p	Position in the z-axis of the radiating element

Chapter 1

Introduction

In this chapter, a brief summary of the work is introduced, establishing the scope in which it is inserted, the contributions that it brings, and establishing goals to be achieved by the contributions. The brief state of the art on this subject is also presented.

1.1 Overview

Every new generation of wireless networks delivers faster speeds and more functionality to our devices, 4th Generation (4G) delivering the speeds that most users enjoy nowadays. But as more users come online, 4G networks have practically reached their capacity limit. Nowadays, users increasingly want more data for their smartphones and devices, due to mobile applications' enormous popularity (such as WhatsApp, Facebook, Netflix and Google Drive). It was predicted by [Cisc20] that in 2023 the number of internet users will be two-thirds of the total population, which means 5.3 billion internet users, compared to 2018 when there were 3.9 billion users (51% of the population); it is also considered that an increase of about 15% internet users will occur, as seen in Figure 1.1.

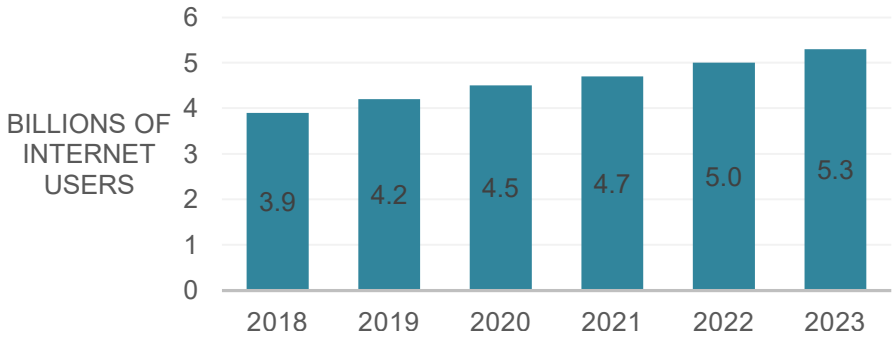

Figure 1.1. Global Internet user growth (extract from [Cisc20]).

Currently, one has the 5th Generation (5G) as the next generation of wireless mobile communications, that will be able to handle a thousand more GB in traffic than previous generations and will be ten times faster than 4G Long Term Evolution (LTE). The fifth generation hit the market by the end of 2018 and will continue to expand at a worldwide level. This evolution will allow the connection of even more devices to the current mobile network, not only the usual devices such as smartphones but also smart TVs, wearables and Internet of Things (IoT) ones. This means that these devices will be connected to wireless networks instead of using a physical connection, such as the optical fibre used for most devices nowadays.

IoT will endure some vast transformations. IoT is a growing network of internet-connected physical devices, having the ability to connect and share massive volumes of information. 5G technology is intended to bring higher speeds, improved connectivity and ultra-low latency. These benefits will improve IoT's effectiveness. Existing applications, products and features will get enhanced, and one can also witness the origin of various new IoT use cases. Another breakthrough advantage of using 5G is the speed at which data is transferred. Considering the speed of transmitting data and resolved latency issues, organisations are expected to start deploying more connected devices. As mentioned before, the implementation of 5G technology can prove to be an advantage for many applications, such as autonomous driving. As driverless cars have cameras and sensors required to use Global Positioning System (GPS) and other sources in real-time, low latency and speed are critical for a good functioning. The telecommunications industry will also get benefitted, as there will be a massive raise in wireless

communications, which will be enabled by IoT.

Considering that latency in most applications can reach 50 to 100 ms, the 4G network can deliver this type of latency without being noticed and without being a problem. However, for some applications, 50 ms of latency can be a barrier, that may be possible to overcome if latency is brought down to subhuman detectable levels like 20 ms or less. Since 5G can deliver this low-latency performance, these applications become possible. There are a lot of applications that need this kind of haptic feedback. Latency is a big factor in the virtual world, such as the responsiveness speed needed in multiplayer video games, or the sensitivity of complex simulations in manufacturing or engineering, or the safety of autonomous vehicles and remote surgery, and all these examples will occur over a wireless network.

To deliver these latency levels, mobile network operators invigorating the Core Network (CN) Virtualisation, apply the principles of Information Technology (IT) Virtualisations, like servers or storage in a data centre, to the network node. The Core Network needs to aggregate traffic, authenticate users, control calls and switching and invoking gateways in services. In a traditional network, this is all done in dedicated hardware, Application Specific Integrated Circuits (ASICs), that are normally centralised. With Network Virtualisation, the operator can deploy smaller, low-cost standardised hardware. By turning to software, Core Network functions will become rapidly and remotely configurable, and can be adapted for a specific demanding case. This solution can also decrease latency because virtual network nodes can be decentralised and located closer to customers. In short, Network Virtualisation allows more flexibility, easily configurable and better performance regarding, for example, reduced latency.

One of the most known IoT proposals is to transform cities into Smart Cities, since by connecting the proper data, problems like traffic congestion issues, noise, crime and pollution can be solved. However, this cannot be achieved using the 4G network, and therefore 5G was created with considerations in key parameters. 5G got improvements at the spectrum level, which is being more efficiently used, a decrease in the latency levels, the availability of higher throughputs, the decrease in the power consumption and the larger capacity.

1.2 Motivation and Report structure

This subsection is based on [3GPP20b] and [ITUR15]. The new 5G radio (NR) provides benefits in three major areas of services, Figure 1.2, Ultra Reliable Low Latency Communication (uRLLC), Massive Machine Type Communication (mMTC) and the Enhanced Mobile Broadband (eMBB), recommended by the International Mobile Telecommunications (IMT) and afterwards defined by the 3rd Generation Partnership Project (3GPP). 3GPP was created for standards development, used by various generations of mobile networks, from the 3rd Generation (3G) to 5G [ANAC20b]. It is expected that traffic growth in the next years will be enormous, ten times higher than the current throughputs, and even more in massive scenarios if applications such as Virtual Reality (VR) or Augmented Reality (AR) are used in a more common way.

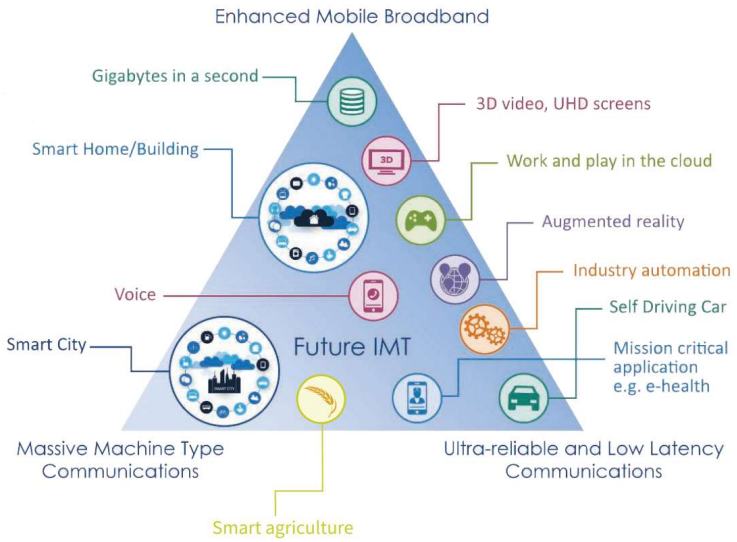

Figure 1.2. Evolution across three major releases (extract from [ANAC20b]).

This thesis was developed in collaboration with NOS, a Portuguese telecommunications operator. The main objective of this thesis was to develop an evaluation model of the deployment of 5G radio networks, focusing on subjects as coverage, capacity, and performance parameters, over existing ones from previous generations, i.e., in a brownfield scenario.

The dissertation is composed of 5 chapters, including the current one. The present chapter contains a brief overview of the problem and the motivations behind the developed work.

Chapter 2 provides fundamental information about the thesis, starting by focusing on the architecture, presenting the 5G standalone and non-standalone perspectives, the network architecture for 5G, the interconnection with LTE, and new features such as network slicing, virtualisation and cloud. The radio interface is also covered in this chapter, mentioning multiple access schemes, spectrum usage including the bands used in 5G, and the types of antennas used. The following section breaks down essential information developed in this thesis, which are capacity, coverage and interference issues. Subsequently, new services and applications provided by 5G are addressed. A radio network planning strategy overview is also performed. The chapter ends with the state of the art on the thesis subject.

In Chapter 3, the parameters that allow an evaluation of the radio network under study are described. This chapter describes the model adopted, which is divided into three distinct sections: coverage, capacity and interference. It equally describes the essential aspects of evaluating a used simulator network, such as the Link Budget, the throughput ratios with Signal Interference plus Noise Ratio (SINR), path loss and cell overload, among others

Chapter 4 presents the used scenarios and parameters and obtained results, as well as their analysis. In this analysis, one can see the impact of different parameters, such as cell radius, influence of frequency, environment, service mix and the deployment analyses. The impact of changing parameters on network operation is described in graphs and tables that are duly analysed.

In Chapter 5, some conclusions are drawn from the topics discussed within the scope of the dissertation project.

Chapter 2

Fundamental Concepts

In this chapter, a technology and architecture summary of both 4G/LTE and 5G/NR is performed focusing primarily on the interfaces that the 5G architecture supports, like coverage, capacity, interference, antennas, and the services and applications that derive from these technologies.

2.1 The Network Architecture

2.1.1 NSA and SA architectures

This subsection is based on [3GPP19]. A characteristic of the 5G architecture is the novel connectivity to the CN by the Access Network (AN). It can be a connection to a 5G Core Network (5GC infrastructure) or an LTE Core Network, called Evolved Packet Core Network (EPC) infrastructure, which means that 5G can still be dependent on the 4G LTE network, being called the non-standalone (NSA) architecture, represented in Figure 2.1.

The NSA architecture, by having a 4G Core and Radio only supports 4G services. The advantages of using a 5G Radio AN is bigger capacity and lower latency. Furthermore, in the NSA architecture, the evolved Node Bs (eNBs – 4G node) are considered master nodes and the en-gNBs (nodes providing NR user and control planes protocol terminations towards the user equipment (UE)) are secondary nodes in the Evolved Universal Terrestrial Radio Access (E-ULTRA) infrastructure. The connection between E-ULTRA nodes is done by the X2 logical interface that interconnects Radio Access Network (RAN) nodes with a E-UTRA-NR Dual Connectivity (EN-DC) function, which provides the capability of an eNB to request an en-gNB for radio resources for a UE. The other type of connections is between the eNB and en-gNB nodes and the EPC core via the S1 interface. This architecture is considered a step to the full deployment of 5G.

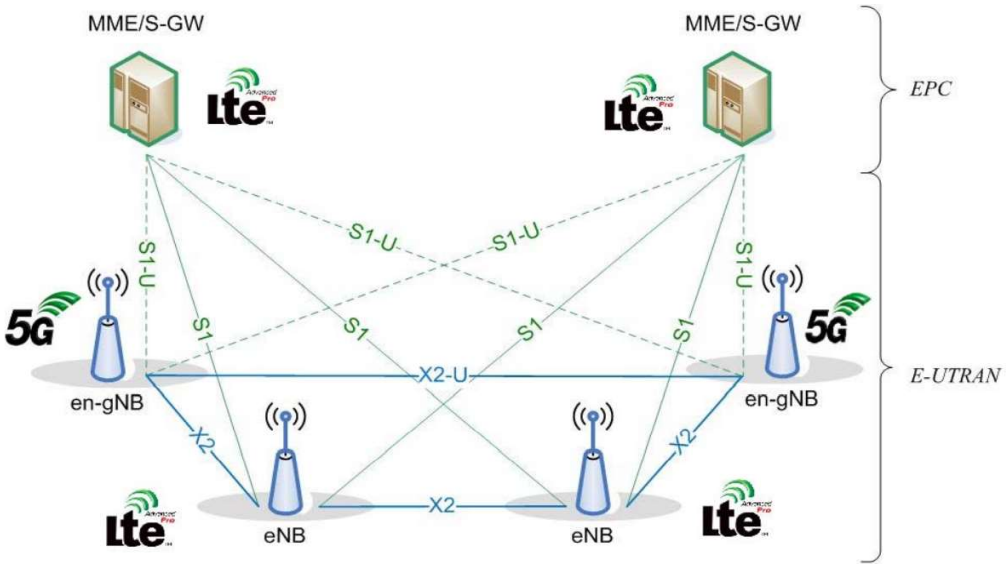

Figure 2.1. NSA architecture (extracted from [3GPP19]).

The full set of 5G, meaning that it does not need any part of a 4G network, is called the standalone (SA) architecture, being based on New Generation Radio Access Network (NG-RAN) that connects to a 5G core network, as represented in Figure 2.2, creating a simplified architecture comparing with NSA and

enabling capabilities such as network-slicing and cloud-native core availability. The connections between NG-RAN nodes are done by Xn, the connections between NG-RAN nodes and the core network are via NG, which are equivalent to the 4G interfaces X2 and S1 respectively.

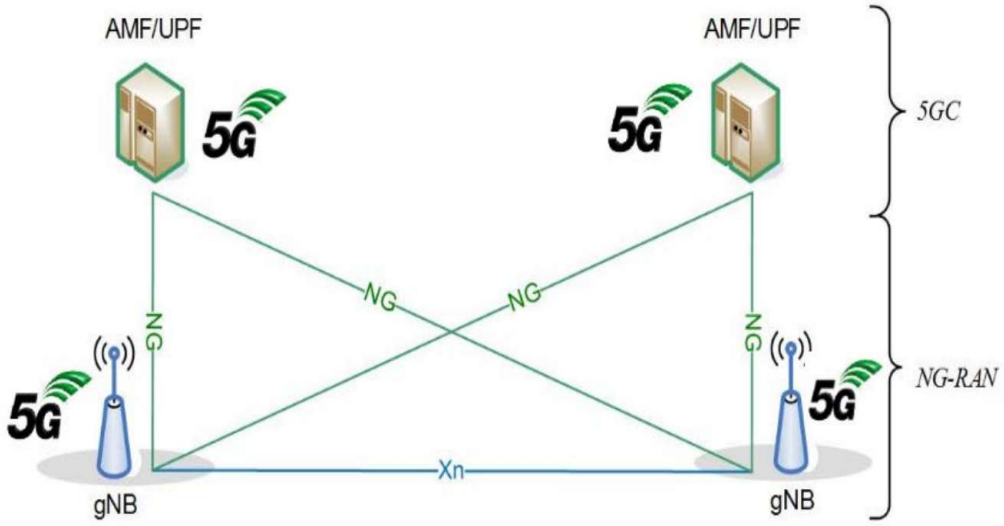

Figure 2.2. SA architecture (extracted from [3GPP19]).

When an operator needs to choose between these two types of architecture, it needs to consider which kind of population they are interacting within the zone where the service will be delivered, more specifically if the studied users are looking mainly for high-speed connectivity, and therefore the NSA architecture should be implemented, or contrarily if it is a community that is looking for new services such as smart cities and smart factories, where the SA architecture should be implemented.

2.1.2 Network architecture

This subsection is based on [3GPP19], [3GPP20a]. The 5G architecture is now on Release 16, the second of the three stages, and its definition is based on the Quality of Service (QoS), interactions between network functions, supporting data connectivity, and services enabling deployments to use techniques such as Network Function Virtualisation and Software Defined Networking. For that purpose, User Plane (UP) functions are separate from Control Plane (CP) ones. The main key functions for the Link Budget, capacity and coverage dimensioning, which are the main purpose of this thesis, are the UE, (R)AN, User Plane Function, Data Network, Access and Mobility Management Function, and Session Management Function, although the network architecture consists of more functions, Figure 2.3.

The New RAN connects the CN to the UE, presenting new functions compared to 4G that are key for supporting new technologies. It supports network slicing that is explained in more detail in Section 2.1.4, a software solution that allows dynamic radio resource allocation and prioritisation for different slices, which means resources can now be allocated by service level. It allows connection to the E-UTRA infrastructure, including dual connectivity and handover between an LTE eNB and a gNB or via the CN. It also has a session management function responsible for creating, updating, and removing Protocol

Data Unit (PDU) sessions and managing sessions related to the User Plane Function (UPF).

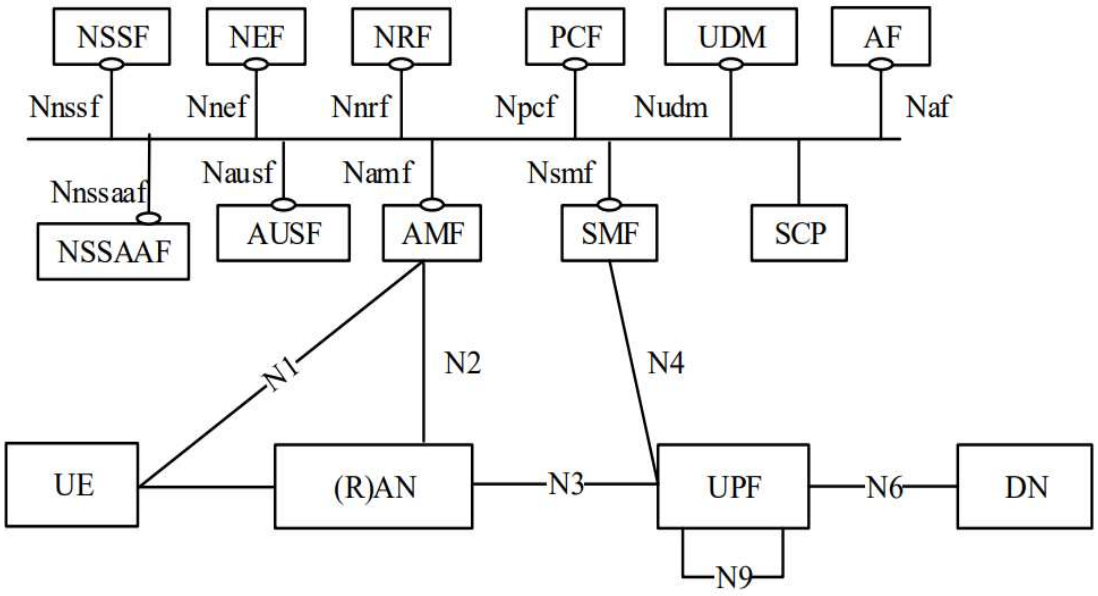

Figure 2.3. 5G system architecture (extracted from [3GPP20a]).

The architecture definition considers that the interface should be based on a logical model and one physical network element can implement multiple logical functions, network architecture functions being:

- Access and Mobility Management Function (AMF) receives all connections and session related information from the UE and RAN, using N1 and N2 respectively, and it is responsible for the registration, connection, reachability and mobility management, access authentication and authorisation, and support for Network Slice-Specific Authentication and Authorisation.
- Data Network (DN) represents the core of the internet or the connection to other services (e.g., operator services, Internet access or 3rd party services).
- Session Management Function (SMF) allocates the IP address to the UE, controls (creates, updates and removes) packet data units, and manages sessions related to the UPF.
- User Plane Function (UPF) is the anchor point for Intra-/Inter-Radio Access Technology (RAT) mobility, when applicable, responsible for packet routing, forwarding, and inspection, traffic usage reporting, QoS handling for the user plane, high latency communication, and downlink (DL) packet buffering and downlink data notification triggering.
- User Equipment (UE) is the physical device, related to the end-user, or a network of devices used for communication that is connected to the RAN and AMF modules.
- (Radio) Access Network ((R)AN) is composed of gNBs (or ng-eNB in E-UTRA), provides the connection to the AMF via N2 or to the UPF via N3, and is used by the UE to connect to the network.
- Network Slice Selection Function (NSSF) selects the Network Slice Instance (NSI) based on information provided during UE attach.
- Network Slice Specific Authentication and Authorisation Function (NSSAAF) supports for Network Slice-Specific Authentication and Authorisation.

- Network Exposure Function (NEF) exposes the overall 5G core network services and capabilities.
- Authentication Server Function (AUSF) supports authentication for 3GPP access and untrusted non-3GPP access and supports unified policy framework to govern network behaviour.
- Network Repository Function (NRF) maintains the network function profile and performs service discovery within a slice.
- Policy Control Function (PCF) provides policy rules to Control Plane function(s) to enforce them.
- Unified Data Management (UDM) gets the UE subscription information.
- Service Communication Proxy (SCP) is a message forwarding and routing to destination NF/NF service, and message forwarding and routing to a next-hop SCP.
- Application Function (AF) is an application influence on traffic routing, Accessing Network Exposure Function, and interacting with the Policy framework for policy control.

2.1.3 LTE interconnection

This subsection is based on [3GPP20a]. The interconnection between LTE and 5G is important for the deployment of 5G, since the latter cannot cover all targeted areas, and therefore LTE is the underlying system. The LTE architecture is divided into four parts: the UE, the E-UTRAN (base station (BS), eNB), the EPC and the services domain that is the access to the internet and 3rd parties' services. EPC functions are:

- Mobility Management Entity (MME) is the main controller in the EPC that operates in the control plane and serves for authentication and security, mobility management, and managing subscription profile and service connectivity.
- Serving Gateway (SGW) manages its own resources, provides to users the routing for data packets, and works as an anchor to the user plane between the connection inter-eNBs.
- Packet Data Network Gateway-User (PGW-U) and Packet Data Network Gateway-Control (PGW-C) provide the connection to the UE to the external network and allow the traffic to enter and exit the network. In addition, they perform traffic filtering regarding Policy and Charging Resource Function (PCRF) rules and policies.
- Home Subscription Server (HSS) is a database that stores users' data, contains user-related and subscription-related data.
- PCRF is a policy tool that defines policy rules, take policy decisions, provides QoS levels, and decides how data flows are handled in the PGW.

Inside the EPC domain there are some functions interconnected with 5G functions. In Figure 2.4, the modules HSS + UDM, PCF + PCRF, PGW-C + SMF and UPF + PGW-U are combined units from the EPC (representing LTE) and 5GS (representing 5G) supporting similar functionality, which are meant to enable interworking between them. This interconnection allows operators to migrate their core infrastructures from EPC to 5GC and permitting the traffic growth caused by the addition of a new BS to their network.

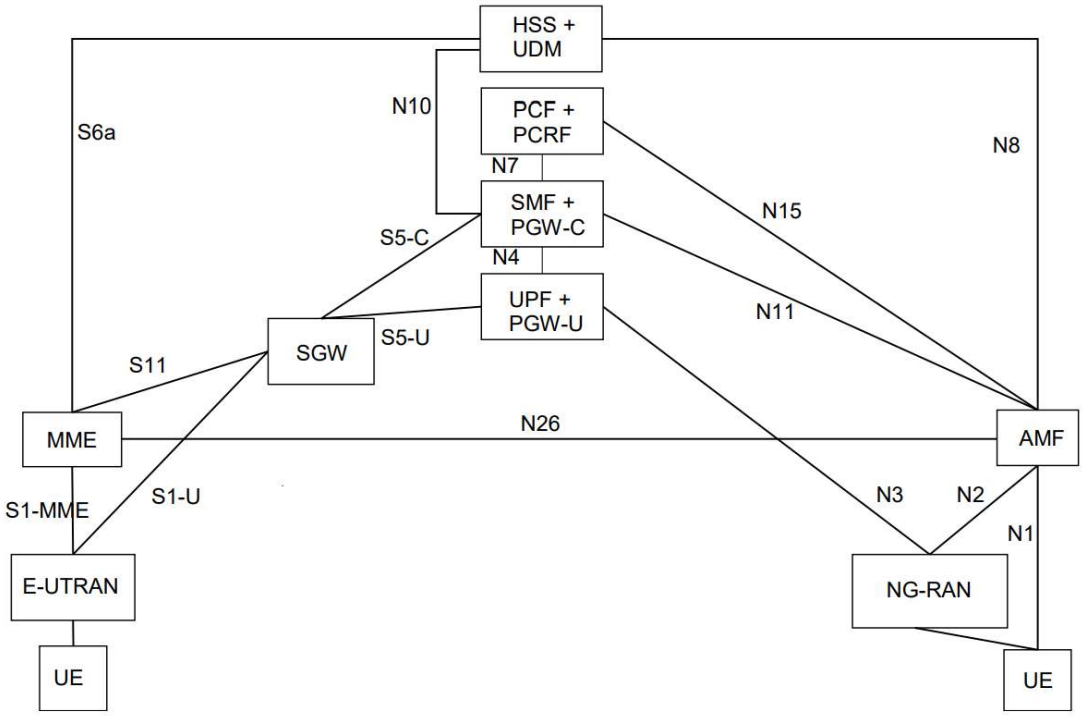

Figure 2.4. LTE interconnection with 5G (extracted from [3GPP20a]).

2.1.4 New network features

This subsection is based on [3GPP19] and [HYW19]. There are two essential orientations of the 5G architecture which are, on the one hand, virtualisation and network slicing, and on the other hand, cloud and edge computing.

5G network slicing is a type of architecture that allows multiple virtualised and independent logical networks to be created on top of a common physical infrastructure. This feature allows each of the network slices to be allocated based on the specific needs of a customer. Each one of the various applications that are enabled by 5G have different requirements in terms of bandwidth, connections, and latency, so it makes sense to have different slices with different needs for different requirements.

The benefit of this architecture is that the network can be divided into multiple parts to create a different slice for each client or a group of clients, which means that resources can be allocated to each slice, turning parameters like throughput, latency, and speed easily managed by the operators. Another benefit of this architecture is that, unlike other elements of 5G, network slicing can be deployed on existing 4G/LTE. With the network division, it becomes unnecessary to mess with the existing services to assess new ones. The changes in slices are also dynamic, meaning that, if the requirements for a specific application change, the operator can change the slice's resources to accommodate the changes needed.

Edge computing is an emerging technology that enables the evolution to 5G by bringing cloud capabilities near to end-users (or user equipment, UEs) to overcome the intrinsic problems of the traditional cloud, such as high latency and lack of security. Edge computing is envisioned to handle

applications and services, such as video streaming, gaming and healthcare services, as seen in Figure 2.5. These services require using edge servers because of their proximity to UEs leading to a significant reduction in latency. For applications and services with a non-real-time requirement, tasks can be offloaded to the cloud for load balancing.

To understand the need for edge computing, consider real-time packet delivery among self-driving cars that require an end-to-end delay of less than 10 ms. The minimum end-to-end delay for cloud access is greater than 80 ms.

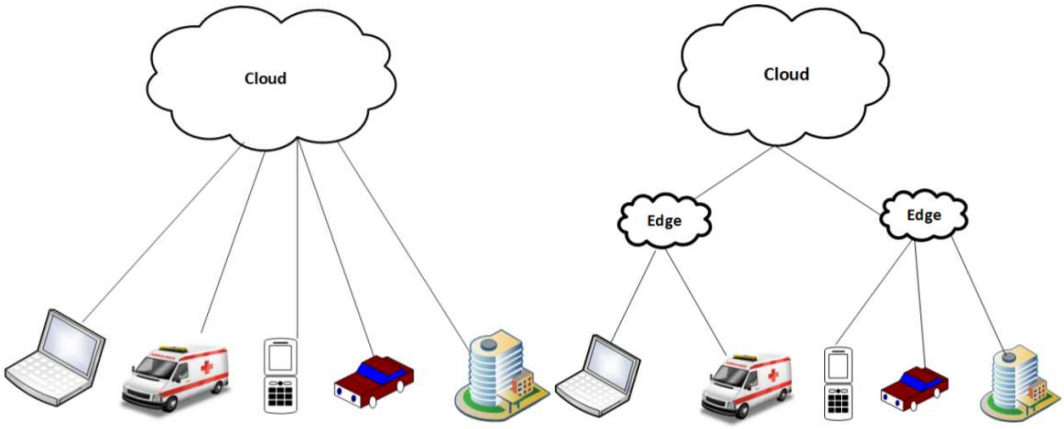

(a) Cloud computing. (b) Edge computing.

Figure 2.5. Comparison between cloud and edge computing models (extracted from [HYW19]).

2.2 Radio interface

2.2.1 Multiple Access

This subsection is based on [3GPP19], [3GPP21], [NAIA14] and [Corr20]. LTE uses Orthogonal Frequency Division Multiple Access (OFDMA) for DL and Single-Carrier Frequency Division Multiple Access (SC-FDMA) for Uplink (UL). OFDMA has been widely used and very successful for 4G and it is used as a 5G multiple access scheme. It requires orthogonality between carriers and the use of a cyclic prefix has some drawbacks.

The 5G radio interface was defined on Release 15 of 3GPP. NR supports OFDMA with cyclic prefix like in LTE as a radio access method, the difference being that this can be used in UL as well, unlike LTE that uses SC-FDMA. 5G also allows multiple OFDM numerologies to provide a variety of services on a wide range of frequencies, which means, unlike LTE that uses a fixed subcarrier spacing of 15 kHz, that NR allows different subcarrier spacing (Δf) based on the numerology (μ). The numerology goes from 0 to 4 and the respective subcarrier spaces (SCS) can be seen in Table 2.1.

A Physical Resource Block (PRB) is divided into 12 subcarriers (channels) like in 4G, subcarriers being seen in Figure 2.6.

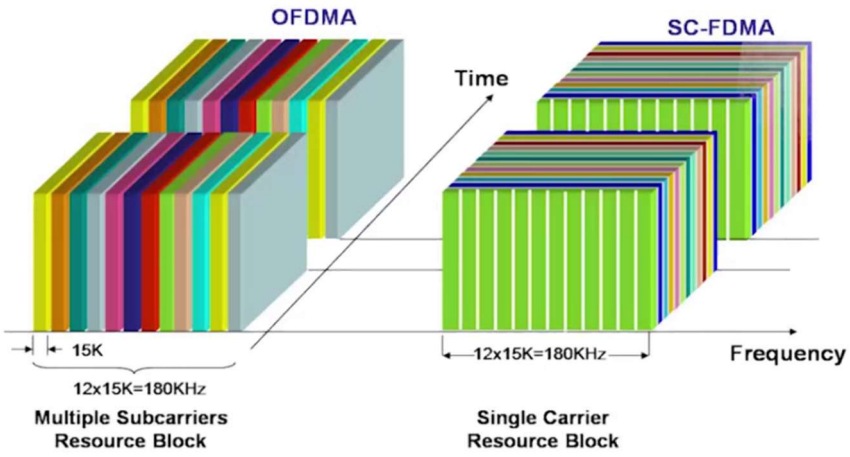

Figure 2.6. Signal structure of OFDMA and SC-FDMA (extracted from [NAIA14]).

When increasing the numerology, the SCSs are going to double and therefore the size of the PRB that is still divided into 12 subcarriers is going to double as well. Numerology has a big effect on the size of the PRB. The numerology is determined by considering the frequency band that the operator is deploying when using a lower frequency band, it should use lower numerology and with millimetre-waves (mm wave), it should use higher numerology. These numerologies are associated with cyclic prefix sizes, as seen in Table 2.1; for a numerology equal to 2, it has a normal and extended cyclic prefixes since that numerology is where the transition from a wide beam antenna to a beamforming one occurs, therefore depending on how it is deployed, and the need for a widebeam antenna implies an extended cyclic prefix.

Table 2.1. Supported transmission numerologies (extracted from [3GPP21]).

μ	$\Delta f = 2^{\mu} \times 15_{[\mathrm{kHz}]}$	1 PRB = 12 subcarriers	Cyclic Prefix
0	15	180 kHz	Normal
1	30	360 kHz	Normal
2	60	720 kHz	Normal, Extended
3	120	1 440 kHz	Normal
4	240	2 880 kHz	Normal

The cell size has a big influence when considering lower latencies. The bigger the cell the bigger the latency, because it has to get to the device and get back again and will take more time if the route is longer, but the numerology will also affect latency, i.e., the larger the symbol the more time is spent until the full symbol reaches the receiver, meaning that higher numerologies that relate to higher frequencies will have lower latencies than lower numerologies. Despite this, even changing the numerology, doubling the symbol size will possess no meaning in terms of latency values, in the matter of this thesis, and so, the latency problem is not a problem related to the transmission time of a symbol.

Higher numerology values lead to lower latencies, with higher binary rates possible when working in the Frequency Range 2 (FR2), so in the 26 GHz band it is possible to transmit more bits, transmitting a

vaster amount of information, being able to accommodate more demanding services.

As highlighted in Table 2.4, the increase in bandwidth leads to greater capacity, the increase in numerology allows to have approximately the equivalent number of RBs, each one carrying more information, which leads to much higher bit rates and allows the possibility to deliver other types of more demanding services. Another key aspect of the 5G interface are the slots and the slot length, again associated with numerologies. Table 2.2 shows the different numerologies and their corresponding number of symbols in a slot (N_{symb}^{slot}), the number of slots in a frame ($N_{slot}^{frame,\mu}$) and the number of slots in a subframe ($N_{slot}^{subframe,\mu}$). Like 4G, the frame lasts 10 ms and a subframe lasts 1 ms, but 5G has several different configurations. For the first configuration with numerology 0, it has 10 subframes each subframe carrying 1 slot and 14 symbols, as seen in Figure 2.7; if one changes the numerology to 1 it doubles the number of slots, and so on. Although there are several numerologies available, they are not implemented in all bands. Higher numerologies are exclusively available for mm waves, which means that it will only be used in the 26 GHz band.

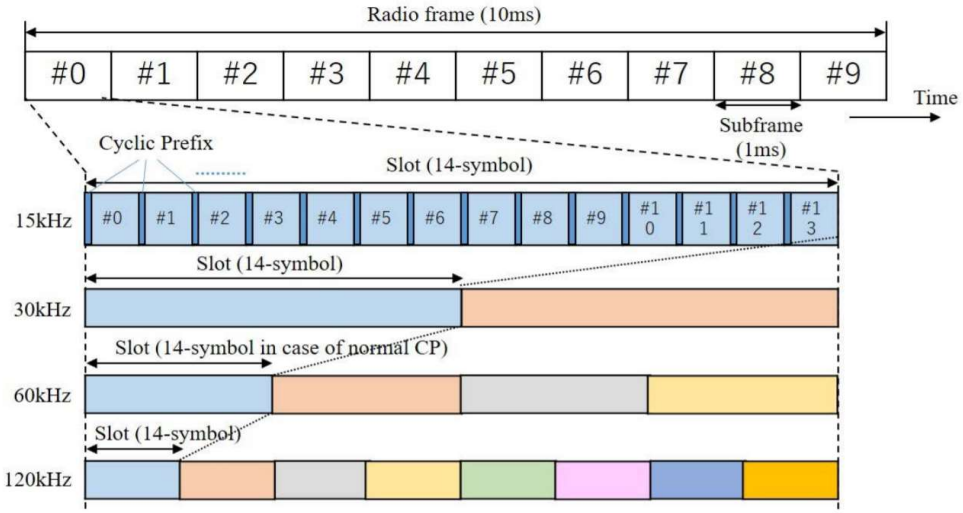

Figure 2.7. Frame structure in NR (extracted from [3GPP19]).

Table 2.2. Number of OFDM symbols per slot, slots per frame, and slots per subframe for normal and extended cyclic prefix (adapted from [3GPP21]).

μ	N_{symb}^{slot}	$N_{slot}^{frame,\mu}$	$N_{slot}^{subframe,\mu}$
0	14	10	1
1	14	20	2
2	12/14	40	4
3	14	80	8
4	14	160	16

By comparing the values of Table 2.1 and Table 2.2, a trade-off between SCS and the number of slots per frame can be seen, with numerology 0 one has fewer symbols per second comparing with the other

numerologies, but one also has a narrower frequency band. As the numerology increases, it has more symbols per second, but this means also the need for a large frequency band.

The supported modulation schemes are Binary Phase Shift Keying (BPSK), Quadrature Phase Shift Keying (2 bits per symbol) (QPSK), Quadrature Amplitude Modulation (4 bits per symbol) (16QAM), 64QAM (6 bits per symbol) and 256QAM (8 bits per symbol), with code rates between 1/3 and 8/9. 5G NR supports all modulation schemes supported by LTE, and in addition it also supports 256 QAM, in DL, and BPSK, π/2-BPSK, in UL. In Table 2.3 one shows the maximum and minimum resource blocks for a given numerology.

Table 2.3. Minimum and maximum number of resource blocks (adapted from [3GPP21]).

μ	$N_{RB,DL}^{min,\mu}$	$N_{RB,DL}^{max,\mu}$	$N_{RB,UL}^{min,\mu}$	$N_{RB,UL}^{max,\mu}$
0	20	275	20	275
1	20	275	20	275
2	20	275	20	275
3	20	275	20	275
4	20	138	20	138

2.2.2 Spectrum

This subsection is based on [3GPP19], [AFZT20], [ANAC20a], [ANAC20b] and [Corr20]. Release 15 defines the frequency bands in low and mid bands, in which 5G will be deployed, each bandwidth can be used in each channel for the two different ranges, Table 2.4. Depending on the chosen bandwidth, a different SCS can be used considering the type of service that is provided to the users.

Table 2.4. NR channel bandwidth (adapted from [3GPP19]).

Frequency range	**Supported channel bandwidth [MHz]**
410 MHz – 7 125 MHz	2, 10, 15, 20, 25, 30, 40, 50, 60, 80, 90, 100
24 250 MHz – 52 600 MHz	50, 100, 200, 400

In Portugal, the frequency bands that are available for the development of NR are the 700 MHz, 2.6 GHz and 3.6 GHz, with two bands that are considered pioneering for 5G: the 700 MHz band, suitable for transitioning to the next generation of mobile networks and coverage in different areas, and the 3.6 GHz one, capable of providing the necessary capacity for services supported by 5G systems. Despite this [5GAm17], the 26 GHz band is also planned, which is the spectrum used for mm waves deployment of 5G, although it will not be implemented soon in Portugal. In this context, a chronological plan was also defined for the development of 5G network/infrastructure in Portugal that started in 2018 and will be deployed until 2025.

Both duplexing techniques, Frequency Division Duplex (FDD) and Time Division Duplex (TDD), are foreseen. In Table 2.5 one shows the techniques used in each band, and the amount of band used for

both UL and DL. Because TDD shares the same spectrum for sent and receiving communications, latencies can be high and variable. FDD systems, however, have an unshared spectrum resulting in much lower and more predictable latencies. TDD, on the other hand, is cheaper than FDD, since in TDD there is no need for a duplexer to isolate transmission and reception.

Table 2.5. Used bands in Portugal (adapted from [ANAC20a], and [ANAC20b]).

Bands	Spectrum usage technique	Uplink	Downlink	Maximum supported channel bandwidth [MHz]
700 MHz	FDD	703-733 MHz	758-788 MHz	10
3.6 GHz	TDD	3 400 – 3 800 MHz		100
26 GHz	TDD	24 250 – 27 500 MHz		100

In 5G, the use of these techniques depends on the geographic location and on the frequency bands used. In the case of TDD, it is used when the UL and DL data rates are asymmetric, since it is possible to dynamically adjust the ratio to match demand, while in the FDD UL/DL capacity is determined by the frequency allocation set out by the regulatory authorities and it is not possible to dynamically change as in TDD. For FDD it is preferable to employ it in dense areas and where nodes are low power, since the increase in the distance from the BS to the UE, the longer the guard period. In the TDD will be worst since the propagation delay increases as the distance increases; this large guard period does not exist in FDD and it has more capacity due to the non-use of these guard periods. In terms of interference, in TDD the BSs need to have the DL and UL transmission times synchronised, since, if they are not synchronised, interference between the cells may occur; this does not apply in FDD since they work at different frequencies. There is also a difference in the frequency bands used, in the case of TDD higher bands are used, and in FDD lower ones are used in the order of 700 MHz.

2.2.3 Antennas

In the development of 5G, two types of antennas are being considered for the BSs, i.e., passive and active antennas. For the 700 MHz band, passive antennas are used and for the 3.6 GHz band active ones are used.

LTE introduced Multiple Input Multiple Output (MIMO) technology, which includes several techniques like transmit diversity, pre-coding and spatial multiplexing. On transmit diversity, the transmitter will send the same data streams in each antenna, creating redundancy in the system; this explores the gains from independent antennas to reduce fading and additionally have a better signal-to-noise ratio (SNR). Another technique that ensures a better SNR is precoding, which weights all signals being transmitted, which means that weights the information stream, thus the transmitter forwards all the information to the receiver preparing the channel for what is coming. Spatial multiplexing consists of sending signals from diverse antennas with different data streams, being possible in the receiver to separate the data streams and therefore increase the peak data rates.

On the other hand, 5G NR introduced an extension of MIMO to Massive MIMO (mMIMO) that will use

more antennas in each BS, which will help to solve some issues. In terms of coverage, the use of more antennas will make a large coverage cell unnecessary, however, there is a counterpart since there is a higher signal attenuation due to the use of higher frequency bands, the higher frequency signals suffer from a signal attenuation 100 times higher than the signals used in LTE usually around 2 - 3 GHz. 5G NR may use transmissions over 24 GHz frequency bands, which "suffer from severe propagation loss leading to small coverage" [GPRC19]. Given this, 5G NR employs a beamforming technique. These techniques increase coverage and minimise interference, thus, the BS can transmit and receive multiple beams from different directions.

Massive MIMO allows BSs to handle a considerable number of antennas per sector (maximum 16 per sector) in this way allowing beamforming. By using beamforming, it is possible to reduce interference, allowing neighbouring nodes to communicate simultaneously. Both examples can be seen in Figure 2.8.

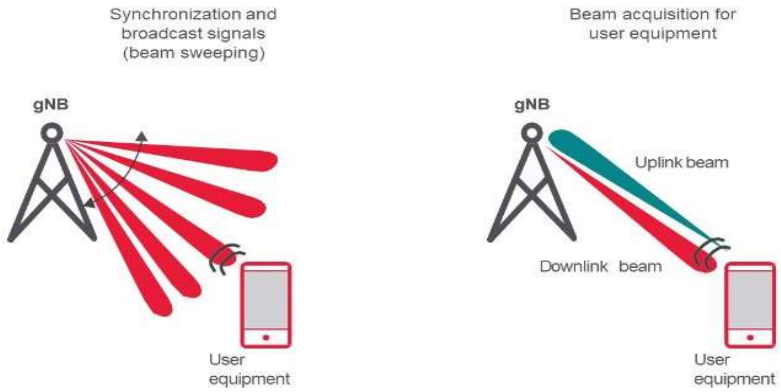

Figure 2.8. Beam sweeping and initial access (extracted from [CJMN20]).

Massive MIMO is used in all frequency bands, although distinctly, due to their specific propagation behaviours and hardware characteristics in various bands. Using MIMO, as the name implies, the transmitter and the receiver both have multiple antennas that allow maximisation in both efficiency and speed. However, MIMO also introduces interference, which as stated earlier led to the use of beamforming. The most used spectrum for 5G is around 3.6 GHz, not only for its critical availability but also for its significant amount of spectrum offered. Despite this band's attractiveness, there is a counterpart, since the cell range is limited in this spectrum range since it covers less than the 2 GHz one (used in LTE networks). To get around this [NOKI18], massive MIMO beamforming antennas are used in the 3.6 GHz band that will achieve a coverage capacity similar to that of the LTE1800 and LTE2100 bands, that is, there is full urban coverage using 5G. When talking about higher-frequency bands, a considerable number of antenna elements are primarily used for beamforming to extend coverage. It is equally recognised that latency and frequency are directly related, since the higher the frequency, the lower the latency. However, as higher frequency bands are used, signal propagation becomes a challenge, since as stated before the attenuation increase is directly proportional to the square of frequency increase.

The antennas are characterised by frequency range, gains, beam range, phase, directivity, radiation intensity, polarisation, among others. In the structure of an antenna pattern, the major lobe is the energy radiated part in direction of maximum radiation, typically being the desired direction for communication.

The electric field for a half-wavelength dipole is given by:

$$E(r,\theta) = \frac{Z_{0\,[\Omega]} I_{max_{[A]}}}{2\pi} \frac{e^{-jk_{[m^{-1}]}\, r_{[m]}}}{r_{[m]}} \frac{\cos[kl\,cos(\theta)] - \cos\left(k_{[m^{-1}]} l_{[m]}\right)}{\sin(\theta)} u_\theta \tag{2.1}$$

where:

- Z_0: free space impedance (120π for free space);
- I_{max}: maximum current in the antenna;
- l: dipole's half length;
- k: free space wave number;
- r: distance between the antenna and the observation point;
- θ: angle between the positive half of the Z-axis and the observation point;
- u_θ: unit vector.

Typically, the length of each dipole is $\lambda/2$, and l is equal or lower than $\lambda/2$ to be resonant. For an array of dipoles, represented in Figure 2.9, the total field radiated by an array with N_a elements is:

$$E = E_a F_{aa} \tag{2.2}$$

where:

- E_a: field radiated by a single element;
- F_{aa}: antenna array factor given by (2.3).

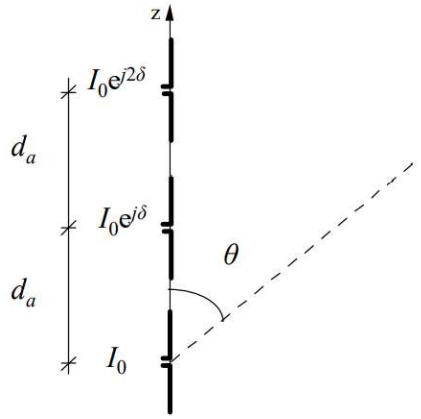

Figure 2.9. Geometry of a uniform colinear array antenna (extracted from [Corr20])

The array factor provides a relation between the radiation pattern and the antenna height

$$F_a = e^{\frac{j(N_a-1)kcos(\theta)}{2}} \frac{sin\left(\frac{N_a k d_a\, cos(\theta) + \delta}{2}\right)}{sin\left(\frac{k\, d_a cos(\theta) + \delta}{2}\right)} \tag{2.3}$$

where:

- d_a: interspacing between elements in an antenna array;

- N_a: number of dipole elements of the array;
- δ: phase difference.

In the majority of the cases d_a is equal to 1 because the array is optimised.

In MIMO technology, planar arrays of antennas are used, taking advantage of different propagation paths to increase the signal transmission speed. Regarding the beamforming technique, the planar array of antennas is used to direct the emitted power to the user terminal.

Each element of the planar array of antennas is constituted by two dipoles orthogonal to each other to implement polarisation diversity. The spacing between array elements influences the size of the sidelobes, which may be non-existent, [COMM21], if the distance between array elements is less than or equal to $\lambda/2$.

The beam's azimuth angle, φ, may vary in [−180°, +180°], which depends on the type of antenna sectoring. In case there are 3 sectors, the beam can vary approximately up to +120º, while its elevation, θ, can vary between [0°, 180°].

Based on [Skol90] , the beamwidth can be related to the number of radiating elements by:

$$\theta_B \cong \frac{100}{\sqrt{N_a}} \tag{2.4}$$

where:

- θ_B: 3 dB beamwidth in degrees.

The number of beams that can actually be generated can be given by:

$$N_{beams} \cong \frac{\pi}{2} N_a \tag{2.5}$$

$$AF(\theta, \varphi) = \sum_{m=-M}^{M} \sum_{p=-P_m}^{P_m} I_{mp} \; e^{j \frac{2\pi}{\lambda} sin\,\theta\,(y_m cos\varphi + z_p\, sin\,\varphi)} \tag{2.6}$$

where:

- I_{mp}: excitation coefficient;
- $(y_m,\ z_p)$: position of the element, where $\sqrt{y_m^2 + z_p^2} \leq r$;
- $\theta \in [0, 90]°$ and $\varphi \in [0, 360]°$.

2.2.4 Coverage

This subsection is based on [Corr20] and [KCFH19]. Cell planning requires the estimation of signals coming from BSs, for both coverage and interference purposes. When looking at the service area, it needs to be defined where to locate the BS and the area that this BS will cover, being required to consider the other BSs in the neighbourhood that can be using the same frequency and therefore will

cause interference on the user equipment. Cell planning uses propagation models to estimate both coverage and interference, and a good estimation is needed, since a bad estimation will cause costs in the end-user such as dropped calls caused by the interference. The cell type is determined with its characteristics in terms of size and Effective Isotropic Radiated Power (EIRP), Table 2.6.

Table 2.6. Cell types and characteristics (adapted from [Corr20]).

Cell Type		**Radius [km]**	**P_{EIRP} [dBm]**
Macro	Large	> 3	[50, 60]
	Small	1 – 3	[47, 50]
Micro		0.1 - 1	[30, 47]
Pico		< 0.1	[22, 33]
Femto		< 0.05	[10, 25]

Spectrum management represents the crucial issue when talking about cell dimensioning. A balance in the frequency band used by the BSs and the distances they have to the neighbours BS is necessary, and for that when doing the estimation of the signal, which includes path loss, gains and power of the antennas since these are the parameters that influence the radius of the cell. As mentioned before, this thesis focuses on the 0.7 and 3.6 GHz frequency bands, for outdoors coverage estimation each one of these frequency bands will have a different propagation model, as seen in Table 2.7.

Table 2.7. Propagation Models for Outdoors Coverage Estimation (adapted from [KMHZ08]).

Propagation	**Frequency Band [GHz]**	
Scenario	**0.7**	**3.6**
Urban	Okumura-Hata	WINNER II
Suburban		
Rural		

The Okumura-Hata model is employed for considerable large distances, usually greater than 5 km and it is valid for urban, suburban, and rural environments. With this model, good results based on measurements are obtained up to 2 GHz, for values higher being necessary to adopt another model. This model considers a standard environment that is urban and flat terrain. Therefore, the result of this model represents the median value for the path loss, and if necessary, the average can be extracted. Despite this, by including corrective factors to the model, it adapts to other environments.

The Winner II model is used in 3G, 4G, and 5G technologies since they use frequencies above 2 GHz. This model is an extension of some models, such as Okumura-Hata and Walfisch-Ikegami, to the band [2, 6] GHz with up to 100 MHz bandwidth [KMHZ08]. This model is valid for macro-cells in urban, suburban and rural areas.

Despite the coverage parameters previously discussed, there are more critical issues, for example, if is it a greenfield or brownfield environment. Greenfield and brownfield are concepts used in the most varied industries besides mobile communications, however, in almost all areas they have the same meaning. Greenfield refers to a project established from scratch; in this case, it will be the implementation of the 5G network placing the necessary BSs in the desired locations. A brownfield refers to a project in which the existing architecture is used, in this case, it will be the use of LTE BSs for the implementation of 5G, taking advantage of their location. This thesis will use the brownfield concept, implementing 5G over the existing LTE architecture.

The cell radius depends on multiple parameters that were mentioned previously, such as the path loss, the propagation model chosen for the specific scenario and the frequency band, among others. All parameters collectively generate a radius distance for a cell, which can be defined by:

$$d_{max_{[\mathrm{km}]}} = 10^{\frac{L_{p,max_{[\mathrm{dB}]}} - L_{p,ref_{[\mathrm{dB}]}}}{10\ \alpha_{pd}}} \tag{2.7}$$

where:

- $L_{p,max}$: maximum path loss (MAPL) given by the Link Budget;
- $L_{p,ref}$: reference path loss, reference for 1 km distance;
- α_{pd}: average power decay.

2.2.5 Capacity

Another significant topic when talking about cell planning is the user traffic in the area where the BS is located and signal modulations. This is designated as capacity, and it is important to ensure a minimum level of QoS. The total capacity is calculated by knowing the size of each cell, the number of combined resources and the throughput for each UE [Belc18]. It is possible to know the theoretical throughput for each UE, being needed to calculate the total resources available per UE (N_{RB}^{u}) since one knows that the total throughput is divided equally by all UEs connected to a given BS. In this manner, the total resources available per UE is given by:

$$N_{RB}^{u} = \frac{N_{RB}}{N_u} \tag{2.8}$$

where N_{RB} is the total number of Resource Block (RBs) available and N_u is the total number of users in the system. The theoretical throughput is given by:

$$R_{b,teo_{[\mathrm{Mbps}]}} = \frac{N_{SC}^{RB}\ N_{RB}^{u}\ N_{symb\ [\mathrm{symbol}]}^{SF}\ \log_2(m)_{[\mathrm{bit\ per\ symbol}]}\ N_{streams}}{10^{-6}\ T_{SF_{[\mathrm{s}]}}} \tag{2.9}$$

where:

- N_{SC}^{RB}: number of subcarriers per RB, in 5G it is 12 for all numerologies;

- N_{RB}^{u}: number of RB per user;
- N_{symb}^{SF}: number of symbols per sub-frame (for one slot: 14 for normal CP or 12 for extended CP);
- m: order of modulation;
- $N_{streams}$: number of streams, in case of MIMO (2x2 MIMO means the number of streams is 2);
- T_{SF}: sub-frame period, 1ms.

This formula does not represent the throughput at which data can be sent. Since the bits used in the header, signalling, among others are being considered. 5G QoS management mechanism is supported by Network Function Virtualisation (NFV) software solutions. The radio spectrum is virtually all allocated to wireless communications systems [WJSW17], bearing this in perspective, the technologies used in 5G needed to improve spectrum efficiency, the improvement is possible using advanced Radio Frequency (RF) domain processing, network architectures, and breakthroughs that have happened concerning RF architecture. [WJSW17] identifies three key aspects to improve spectrum efficiency through multiple access schemes, channel coding, and waveform.

2.2.6 Interference

Interference refers to the process of disruptive modification of a communication signal as it travels between its source and the receiver. Like so, the consequence of interference is a degradation of the signal at the reception, by reducing the throughput level. Interference also can cause a reduction of the capacity that is essential when referring to the cell planning and the radius cover by the BS. Interference presents a severe problem since it reduces the QoS given by providers to costumers.

This interference may occur due to many reasons and there are various types, such as:

- Self-interference due to the interference induced among signals that come from the same transmitter.
- Multiple access interference, which refers to the interference induced among the transmission from multiple transmitters using the same frequency resource to a single receiver.
- Co-channel interference between links that reuse the same frequency band.
- Adjacent channel interference represents the interference induce between links that communicate in the same location using neighbouring frequency bands.

In addition, in 5G-NR due to the introduction of numerologies, there are situations in FDD where resources of adjacent frequencies are used simultaneously causing inter-numerologies interference. The same does not apply in TDD because there is only one numerology in each Transmission Time Interval.

“A large number of small BSs can be expected to provide up to 1 000 times more capacity than today” [Rodr15]. Despite this, inter-cell interference is increasing as it is reducing the size of the cell, which will imply the need for signalling control. Therefore, inter-cell interference management techniques are needed at the BS level along with complementary interference cancellation techniques at the UEs.

Interference is responsible for decreasing the Signal-to-Interference-plus-Noise Ratio (SINR), which

decreases along the path, which means when the longer the distance the lower the SINR. The SINR combined with the spectrum efficiency is crucial to define an appropriate modulation coding scheme. The smaller the number of useful bits that can be carried by a symbol, the more robust and tolerant to higher values of interference at the cost of lower transmission throughput.

2.3 Services and Applications

Since 3G emerged, different generations of mobile communications have been associated with IMT technologies defined by International Telecommunication Union - Radiocommunication (ITU-R). The process of defining IMT technologies goes through the ITU-R to specify the necessary technological resources and requirements that the technology needs to fulfil [DAPS16]. The primary motivation and drive for 5G is the use cases and, therefore, ITU-R has defined three use scenarios that are part of the IMT recommendation:

- **eMBB**: This scenario is considered to be the most important since it is a continuous problem, the need is always increasing and new areas of application appear every day. To note the abruptness of this scenario, one can think of two different use cases, for example, the need for a BS for a high user density zone and, on the other hand, the need to cover a considerable area. In the case of BSs, the importance will be high data rates and a large capacity while covering large areas the importance will be mobility and continuity of coverage. The enhanced mobile broadband scenario is considered to represent a constantly evolving scenario to improve human communication.
- **uRLLC**: This scenario is characterised by use cases with strict latency requirements, such as wireless control of industrial equipment or remote medical surgery. It is additionally used in communications between vehicles (V2V), being usually described by small packets.
- **mMTC**: As the name implies, it is a use case where there are a large number of connected devices and whose transmissions are limited volumes of data that are usually not sensitive to delays. The significant adversities in this case study are the considerable total number of connected devices, which lead to a low-cost need.

The three described scenarios do not cover all possible use cases, but represent the majority of the cases, which makes it possible to identify most of the necessary resources, which can be seen in Figure 1.2. In Figure 2.10 one can see the importance of key capabilities in the three different scenarios.

The services provided by 5G, as in previous generations, will have different transmission rates due to the requirements of each one. It is expected that voice services, despite being the most sensitive to delay, only require transmission rates in the order of 8 to 64 kbps to have a minimum QoS guaranteed [Belc18], while web browsing, file transfer, streaming, email and Peer-to-Peer (P2P) services will require higher transmission rates to obtain minimum QoS, these transmission rates will have to reach Mbps.

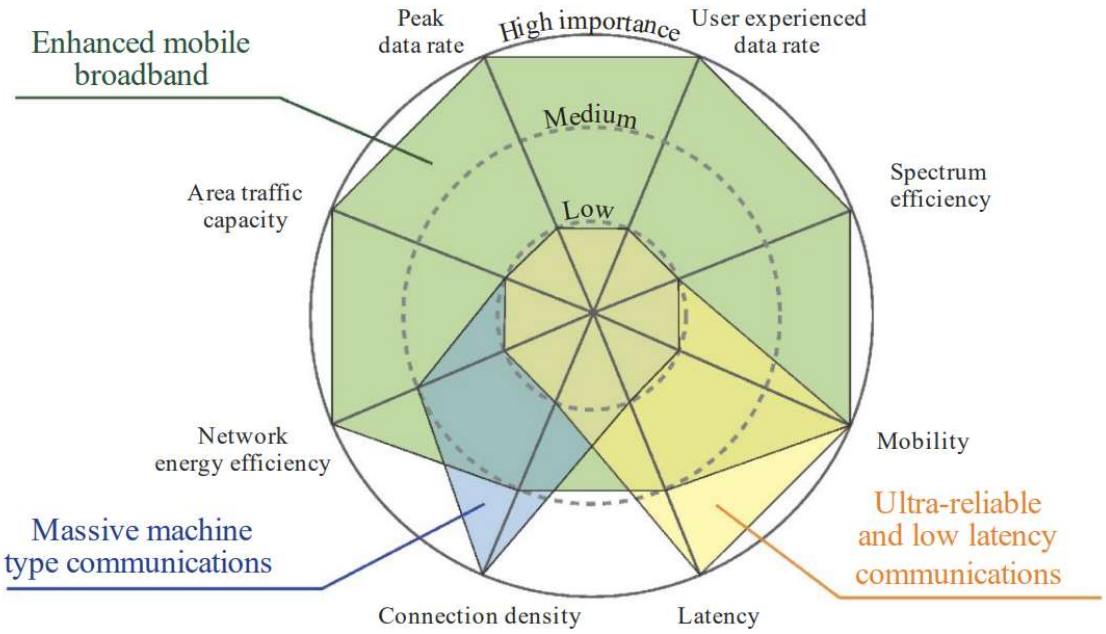

Figure 2.10. Capabilities in different usage scenarios (extracted from [ITUR15a]).

Table 2.8. 5G Services - Requirements per use-case (extracted from [Viei18]).

Class	Service	Throughput DL [Mbps]	Throughput UL [Mbps]	Latency [ms]	Number of devices per km^2
eMBB	Ultra-high broadband access (VR & AR)	1000	500	10	75 000
	Broadband access in dense areas	300	50	10	[200; 2 500]
	Broadband access in a crowd	25	50	10	150 000
	50 Mbps in suburban scenario	50	25	50	400
	50 Mbps in rural scenario	50	25	50	100
mMTC	Massive low-cost, long-range, low-power MTC	< 0.1	< 0.1	Seconds to hours	200 000
uRLLC	Ultra-low latency	50	25	< 1	-
	Ultra-high reliability, ultra-low latency	0.005 to 10	< 10	1	-

2.4 Radio Network Planning

The dimensioning of the network should be done by analysing the resources and the number of cells needed to cover the desired area for a traffic load profile. The sheer number of cells needed depends on the lowest requirements to provide a given service, and this minimum QoS is guaranteed by the coverage provided by the BS and its respective capacity. The dimensioning of a network should not purely be focused on the service levels achieved, but also on their efficiency, both in terms of cost and in terms of optimisation.

The purpose of planning a radio network is to achieve good levels of signal quality and maintain that

quality over time, cover the desired area, and maximise the use of resources to increase the capacity of the radio network. Since in this thesis a brownfield scenario is used, that is, the network is implemented over an existing architecture, it is necessary to perceive the numerous problems that may occur with its location, since it is necessary to take advantage of the existing hardware. It is necessary to understand the size of the area to be covered and its definition (such as its relief), from the location of the antenna (either on a tower or a rooftop) it is necessary to understand its height, the azimuths, the number of necessary sectors and their orientations as well as the tilts that the antennas will need (both electrical and mechanical). As stated earlier, it is equally necessary to recognise the diverse levels of propagation for the various frequencies that can be used. Good planning is necessary due to the limitations of spectrum allocation, the efficient use of existing resources and architecture, and, of course, optimise the quality-cost ratio [Tabb19].

Network dimensioning can be divided into 2 planes: coverage and capacity planning. However, before executing these plans, it is necessary to obtain the necessary inputs received from the user, the network and the scenario. The two plans will then be executed sequentially, therefore obtaining the necessary outputs. As stated before, the first scheme is to determine the coverage limit planning, which limits the maximum radius that the cell coverage reaches when connecting to a UE. In this plan, the minimum QoS required is yet not taken into account. Coverage planning is defined by the evaluation of the radio Link Budget for DL and UL. From this assessment, the maximum allowed path loss (MAPL) is computed from the required SNR values, from which it will then be possible to compute the radius and cell area and finally, the number of cells needed [Viei18]. If the previously planning complies with the limits imposed by the network, the outputs will be extracted directly from the coverage planning, otherwise, a capacity plan will be used. One that considers the total traffic imposed by the users' activity and adjusts the size of cells according to it and the resources present on the network.

In addition, adaptive antennas were introduced in 5G networks in the 3.6 GHz band, which makes it necessary to take a different approach concerning network planning. Since adaptive antennas are capable, as the name implies, of adjusting their radiation pattern to adapt to noise, interference, and multipath fading [ITUR04], these systems identify all relevant signals and interferences to maximise the signals of interest and decrease the interference dynamically, the antennas are used to improve the SINR for a specific network.

Only adaptive systems can provide gain while mitigating interference [ITUR04]. These generally discriminate and identify transmitters based on the relative phases and amplitudes. These values are known as the "spatial signature" of a transmitter [ITUR04]. There are differences between the calculation of spatial signature values for UL and DL. For UL, the signature is measured directly by the BS, however, in DL the signature is estimated since it is not possible to measure it directly. It is then necessary to establish the differences between the use of TDD and FDD systems due to the way spatial signature is calculated. The increase in capacity and the DL gain provided by the adaptive antennas in FDD systems are less than those of TDD, since in TDD the UL and DL channels are considered more reciprocal.

2.5 State of Art

This section refers to an overview of research done related to the subject of this thesis. For each of them, one explains the methodologies and their results.

Two theses were considered that focus on essential points of coverage and capacity. The work in [Viei18] addressed 5G technology taking cellular network design for 0.7 and 3.5 GHz bands, in different Link Budget parameters and different traffic profile configurations into account. In this thesis, multiple scenarios were developed and so they will be used as a key element for the development and proof of the models in terms of capacity and coverage aspects. Despite this, essential aspects such as throughput and the SNIR relationship were addressed in a simplified way. It was also considered that all numerologies can be used regardless of the maximum coverage. Other essential points like interference were not considered.

When using the same propagation model, it was noticed that by increasing the frequency the areas with higher density of devices will have less increase in the number of cells comparing with areas with lower density of devices. In terms of throughput, it was proved that the throughput value per frequency and bandwidth configuration is proportional to the share percentage of bandwidth allocated to the cell edge. Then it was noticed that the global cell capacity has a deviation compared to the literature, caused by the maximum bandwidth per cell currently defined as valid by 3GPP (100 MHz) without carrier aggregation and the fact that it was considered that the majority of devices do not support a MIMO configuration higher than 2x2.

In another thesis [Belc18], the topic of coverage and capacity in DL for the 3.5 GHz and UL 700 MHz and 1.2 GHz band (LTE) was also studied. Several input parameters were considered, which implies the system must adapt to these parameters. That causes different traffic models and different radio configurations in the model deployed.

It is expected that 4G cellular networks are able to provide the necessary coverage for reliable communications since it uses a lower frequency band [YUKI13]. In this paper, it was equally employed the brownfield concept, in which the transition to 5G is made using a hybrid network with 4G and mm wave system structures. The 4G network is used for management information and low-rate applications, such as voice and text, among others. The mm wave structure is used for high-rate applications, namely multimedia services. The transmission-reception of mm waves is based on high directional antennas, which can cause a massive reduction in the interference between BSs.

Radio planning represents an imperative task in a cellular network. This includes the calculation of the number, locations and configuration of the radio nodes in the network. Only the number of BSs and their locations were considered in the first generations since there was no existing infrastructure. In the context of 5G, its deployment is done through overlay architectures, meaning mm wave cells placed on top of the existing infrastructure in the form of hierarchical or mixed cell structures. The use of overlay architectures allows mm wave cells the ability to increase the capacity of the system due to much wider bandwidth and the use of beamforming and MIMO [AFZT20]; there is yet another identified advantage

that is the separation of control signals and transmission messages, that is, control signalling is supported by the existing network and high transmission rates are supported by the mm wave network. "5G radio planning is now of utmost importance since not only does it require cost-optimised deployments capable of handling a variety of demand constraints, but also since it then affects the optimal placement of the core network elements, e.g., for achieving low latency values." [AFZT20].

A study was conducted by [FCDY20] to evaluate the 5G NR against the Key Performance Indicators (KPIs) provided in 2020 by IMT. In this work, each KPI is evaluated based on the three scenarios previously described, i.e., eMBB, URLLC, or mMTC. In these scenarios the one that will occupy more resources in terms of data rate, spectral efficiency or traffic capacity, will be eMBB and this was the case investigated in this study.

The KPIs evaluated in this work were bandwidth, peak data rate, peak spectral efficiency, user plane latency, control plane latency, energy efficiency, 5^{th} percentile user spectral efficiency, user experienced data rate, average spectral efficiency and mobility.

The conclusions reached from this study, identify that 5G NR fulfils the IMT-2020 requirements under specific conditions. Interesting values were achieved in this study, for example, 6.4 GHz of bandwidth were reached, therefore enabling a peak data rate of 78.05 Gbps employing the FDD mode, 8 layers, and one numerology among other values.

In another KPI measurement study of the implementation of a 5G network in a non-standalone architecture [SFVS20], the results were compared with those measured in a current 4G network. The compared KPIs were throughput, latency and packet error rate. It was expected by the authors that the 5G network will have a higher data transmission rate due to the increase in bandwidth, different coding, and the improved modulation used, the results achieved showing that the tested 5G network reached peak rates for DL and UL significantly higher than 4G (a difference of approximately 100 Mbps in the case of DL, and minimum differences around 5 Mbps). It was also expected that the latency will be drastically reduced concerning 4G, and it was proven that the latency of the data transmission is significant (difference of 8 to 10 ms), the Packet Error Rate (PER) was expected to be detected only in lower layers, where it is not possible to restore the packages, and the results confirmed this view.

In the paper [KGE20] an innovative approach to the dimensioning of a radio network called Heuristic Radio Network Dimensioning (HRND) is proposed, which uses concrete data in the network dimensioning activity. This provides the dimensioning target area by means of network data selection and visualisation from the existing infrastructure. It considers the necessary parameters like numerology and bandwidth parts (BWP) supported by New Radio (NR) to a sound design mediating amid the requirements of coverage, capacity, Quality of Experience (QoE) and cost.

The dimensioning of the network was divided into two aspects, capacity and coverage dimensioning. These represent necessary phases of the network planning process to determine the number of radio sites that satisfy the coverage and capacity requirements. Coverage dimensioning consists of computing the coverage cell range in the target area to determine which service provides the most restrictive coverage cell range and then computing the required number of sites based on this range. Capacity

dimensioning determines the capacity cell range based on the effective capacity of the gNB, subscriber's density, and the market share. These two stages can guarantee that the network design is balanced, i.e., the variation of cell ranges and cell loads from coverage and capacity scaling are under some given thresholds.

In [KGE20], it was concluded that inferring about the existing infrastructure can lead to information to the mobile network dimensioning. It was also demonstrated that the model used ensures the availability of the peak data rates for greater than 50% of the time for all services, as a use case. Furthermore, dimensioning outcomes indicate that up to 32% cost savings as contrasted with conventional dimensioning can be obtained.

In the paper [WLY20] an optimisation problem for the location and selection of macro and micro base stations is presented. This problem optimally intends to reduce the cost of deployment in addition to strengthening the coverage of the radio signal with the deployment of 5G base stations. In the paper, a mathematical model was presented to optimise the base station selection process. A series of numerical examples were then concluded and presented in the paper to demonstrate the proposed coverage-based location approach. In addition, the cost-benefit analysis was conducted to determine the optimal deployment plan for the number of macro and micro base stations, which can optimally reduce the deployment cost and strengthen the signal coverage.

Chapter 3

Methodologies and Expected Results

In this chapter, methodologies are presented, along with the models to be taken in the thesis, the necessary performance parameters and some expected results.

3.1 Model Overview

This section provides a description and explanation of the models used in this thesis along with thier mathematical formulation. The global model to be developed is based on the concepts studied and consolidated in Chapter 2. An overview of the model is shown in Figure 3.1.

Regarding the model's input parameters, three components were considered:

- Users, which include the density of users, what types of services they use, and what areas these services are used on.
- Services, i.e., users can utilise various types of services such as voice, video, among others, when using each service, their requirements are added, such as minimum transmission rate, among others.
- Network, which are defined by the operators, are related to the position of the antennas, the frequencies used, the available bandwidth, the number of channels available and the priorities assigned to the different users, among other parameters.

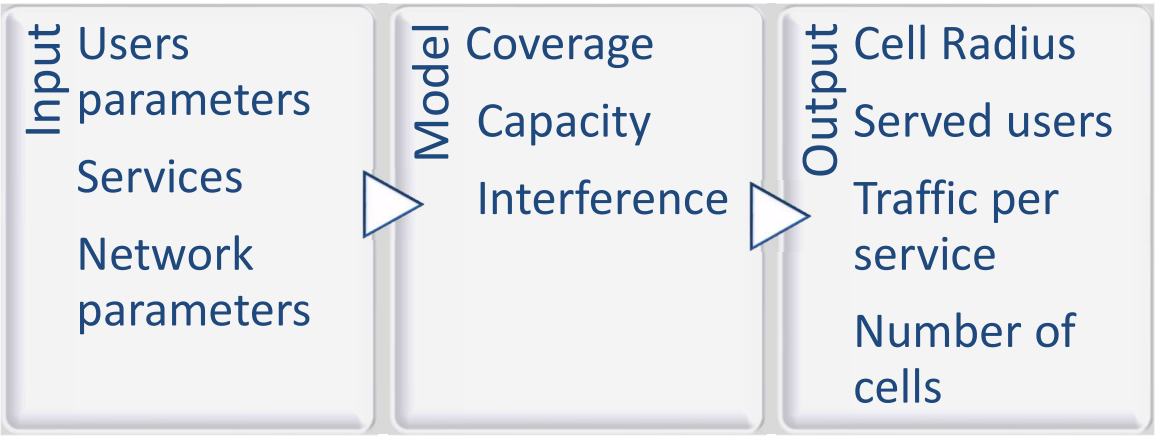

Figure 3.1. Model configuration.

Regarding the model itself, it is equally divided into three parts:

- Coverage model, which consists of placing the cells in a certain area, including the Link Budget and path loss among others.
- Capacity model, which is based on the occupancy rate in the cells by the users and the reassessment of the coverage model considering the QoS, including cell load calculation and cell load adjustment.
- Interference model, which is composed of a model proportional to the traffic, meaning that, as the traffic increases, the interference also increases, this will be added as a margin to the power balance.

As output parameters for the model, it is expected to obtain results in the three areas of coverage, capacity and interference. For coverage, it is expected to obtain parameters such as cell radius. For the capacity, it is expected to obtain parameters like the number of users per cell, which depends on the services. And finally, for the interference, the carrier to interference ratio is obtained. The referred

parameters, among others, are then used for the evaluation of various scenarios. In addition to the Link Budget, 5G is also studied, including the diverse parts of the spectrum. It additionally includes the study of antennas, as the 32T32R as opposed to the 8T8R in terms of MIMO technology. It also includes the KPIs that may emerge as an evaluation of this model, such as some referenced in other works in the state of the art, as it is the case of throughput, peak data rate and latency, among others.

More specifically, the model is divided into two, where the first is the coverage model and the second the capacity model. The interference model is involved in both. To obtain more specific inputs and outputs, more specific configurations were designed for both models in Figure 3.2 and Figure 3.3.

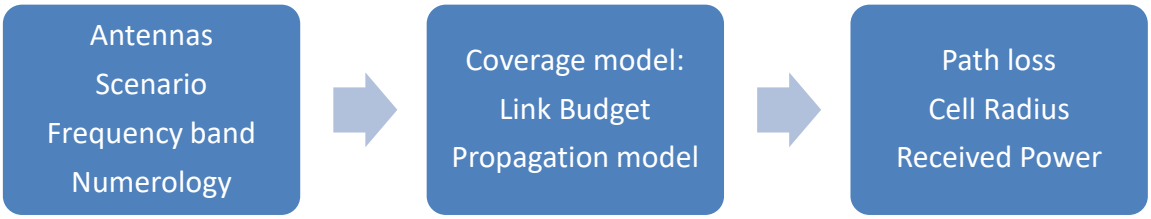

Figure 3.2. Coverage model configuration.

In the configuration shown in Figure 3.2, coverage configuration, the antenna gain and the transmission power both depend on the antenna type, the number of sectors, regarding the BS and also the type of connected device.

The type of scenario (urban, suburban or rural) influences path loss. Regarding the numerology used, the higher it is, the greater is the bandwidth of each RB and also the higher the output power value. A higher numerology also slightly decreases the SNR obtained for the same distance with a smaller numerology. However, when using a smaller numerology, the throughput is the double than with higher numerologies, thus, it achieves higher quality requirements.

Finally, regarding the frequency band used, it directly influences the propagation model used.

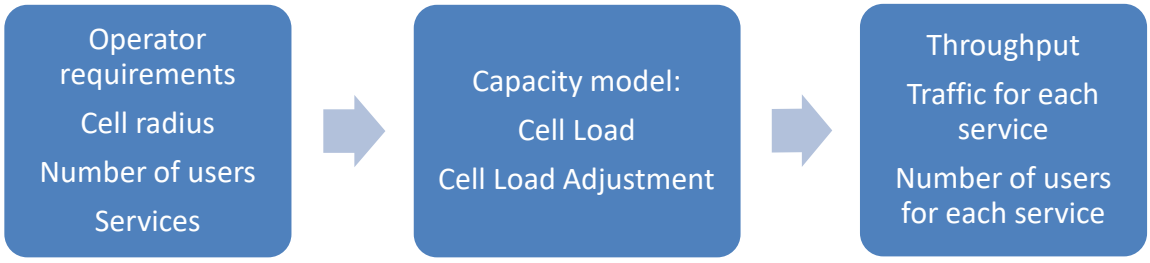

Figure 3.3. Capacity model configuration.

Considering the capacity model configuration, Figure 3.3, the operator requirements like service requirements e.g., throughput, latency and others are used as an input, as well as the cell radius which represents a result of the previous model (the coverage model) and finally the number of users per cell and what kind of services are used also represents an input. Using the capacity model and parameters previously described, it is possible to calculate parameters like SNR, transfer rate, traffic for each service among others for each modulation used.

Figure 3.4. Interference model configuration.

The interference model, Figure 3.4, takes into account the input parameters of the BS donor antennas, which are considered the same for the neighbouring BS, and it is also necessary to take into account in the scenario, as it influences path loss exponent. With these parameters, the interference model calculates the SINR available for each connection.

Considering that the propagation models influence the developed model, it is necessary to establish in which circumstances they are valid, Table 3.1.

Table 3.1. Generic description of the considered propagation models.

<table>
<tr><th rowspan="4">Distance between the base station and the mobile terminal</th><th colspan="6">Frequency bands [GHz]</th></tr>
<tr><td colspan="3">0.7</td><td colspan="3">3.6</td></tr>
<tr><td colspan="3">Scenarios</td><td colspan="3">Scenarios</td></tr>
<tr><td>Urban</td><td>Suburban</td><td>Rural</td><td>Urban</td><td>Suburban</td><td>Rural</td></tr>
<tr><td>> 100 m</td><td colspan="2">Walfisch-Ikegami</td><td>-</td><td colspan="3" rowspan="2">Winner II</td></tr>
<tr><td>> 1 km</td><td colspan="3" rowspan="3">Okumura-Hata</td></tr>
<tr><td>< 10 km</td><td colspan="3" rowspan="2">Winner II</td></tr>
<tr><td>< 20 km</td><td colspan="3">-</td></tr>
</table>

Regarding the Walfisch-Ikegami model [Corr20] used in the 0.7 GHz band, it is restricted in terms of frequency between 0.8 to 2 GHz, so using the model under 0.8 GHz introduces some error in the calculations. Despite this, a model approximation can be made, comparing with the Okumura-Hata model [Corr20] between 1 to 5 km, as both models are valid in this interval, as seen in Table 3.2.

Table 3.2. Propagation models and respective requirements.

Parameters	Walfisch-Ikegami	Okumura-Hata	Winner II
Frequency [GHz]	0.7 – 2	0.15 – 2	2 – 6
Base Station Height [m]	4 – 50	30 – 200	1 – 32
Mobile Height [m]	1 – 3	1 – 10	1 – 5
Distance [km]	0.02 – 5	5 – 20	0.03 – 10

For environments where the UE is indoors and the BS is outdoors, two propagation models are considered, one being more generic and possible to use in both bands under study as it is valid in the range 0.7 to 3.8 GHz, and another propagation model is the Winner II [KMHZ08] which is valid from 2 to 6 GHz, so it is only used for the 3.6 GHz band.

3.2 Dimensioning Process

3.2.1 Coverage Planning

This section describes the planning in terms of coverage, the objective being to calculate the output parameters of Figure 3.2, having as main purpose the cell radius calculation, which is defined by the maximum distance between the BS and the UE so that a connection can be established in UL and DL. Coverage planning is divided into the Link Budget calculation and the use of an appropriated propagation model to calculate maximum distance between the BS and the UE, this way the cell radius is defined.

Link Budget [Corr20] is a calculation of all power gains and losses that a signal experiences while establishing a communication between receiver and transmitter, including cable and user losses.

The received power for coverage estimation is mainly defined by the receiver sensitivity power, which varies with the RB bandwidth defined in Table 2.5 and the reference throughput defined for a cell:

$$P_{r,min_{[\mathrm{dBm}]}} = -174 + 10\log\left(B_{RB_{[\mathrm{Hz}]}}\right) + F_{N_{[\mathrm{dB}]}} + \rho_{N,\min\,[\mathrm{dB}]} + M_{SF_{[\mathrm{dB}]}} \tag{3.1}$$

where:

- B_{RB}: bandwidth per RB, which depends on SCS (10 MHz for NR700 and100 MHz for NR3600);
- F_N: noise figure of the receiver;
- $\rho_{N,min}$: SNR requirement for a given throughput;
- M_{SF}: Slow-fading margin.

The B_{RB} values that correspond to the bandwidth of each channel are the values in Table 2.1, that is, it can take the following values 15 kHz, 30 kHz, 60 kHz, 120 kHz or 240 kHz. As mentioned above, the higher numerology will be used for the 26 GHz band, and for that, as they will not be addressed in this thesis, this model will exclusively be used for B_{RB} equal to 15 kHz, 30 kHz and 60 kHz. The noise figure usually varies between 5 to 8 dB, this being dependent on whether the connection is UL or DL.

The throughput values required for a given SNR level, Figure 3.5, depend on the modulation order, M. For M=4, QPSK with coding rate of 1/3 and MIMO 2x2, for M=16, 16-QAM with coding rate of 1/2 and MIMO 2x2, for M=64, 64-QAM with coding rate of 3/4 and MIMO 2x2, and for M=256 256-QAM considering MIMO 2x2. the throughput per RB and the corresponding SNR can be given by [Belc18]:

$$R_b = 2^{\mu}\frac{N_{MIMO}}{2}\begin{cases}\dfrac{2.34201\times 10^6}{14.0051 + e^{-0.577897\ \rho_{IN}}} & M = 4\\ \dfrac{47613.1}{0.0926275 + e^{-0.295838\ \rho_{IN}}} & M = 16\\ \dfrac{26405.8}{0.0220186 + e^{-0.24491\ \rho_{IN}}} & M = 64\\ \dfrac{26407.1}{0.0178868 + e^{-0.198952\ \rho_{IN}}} & M = 256\end{cases} \tag{3.2}$$

where:

- N_{MIMO}: MIMO order.

For a connection using MIMO 4x4, the throughput is 2 times the referenced one [Mour21].

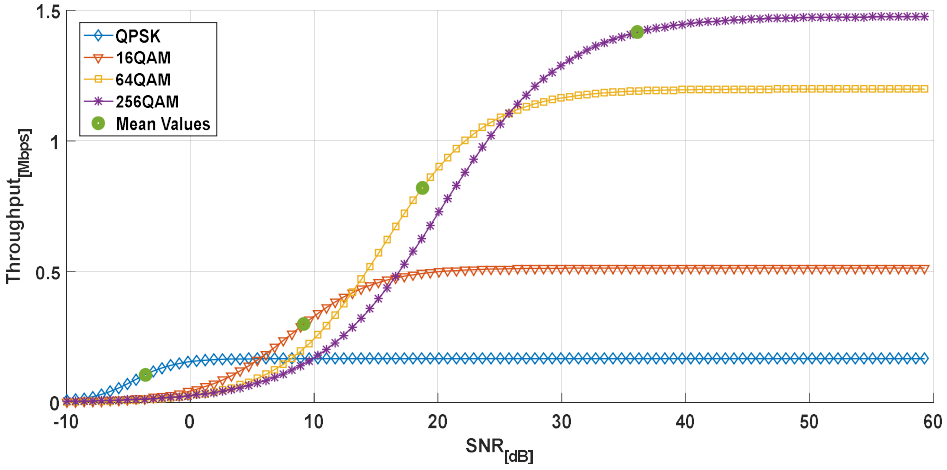

Figure 3.5. Throughput as a function of the SNR, considering MIMO 2x2.

Table 3.3. Mean Values of SNR and the correspondent throughput.

Modulation	Throughput [Mbps]	SNR [dB]
QPSK	0.107	-3.5
16-QAM	0.300	9.2
64-QAM	0.823	18.8
256-QAM	1.414	35.9

As seen in Table 3.3, for QPSK the mean value of SNR is lower than 0, which in practical terms is not possible, since the signal value will not be lower or equal to the noise value, and because of this, 2 dB was used for this modulation.

The maximum path loss is given by the system along with the antenna gains, (3.3). These gains depend on the equipment, at the BS it depends essentially on the antenna type and the number of sectors, while the UE depends on the type of device, essential for the computation of the power feed to the antenna DL and UL, (3.4) and (3.5) respectively. The maximum path loss also depends on the transmitted power and the receiver sensitivity power, and can be computed from:

$$L_{p,max_{[\mathrm{dB}]}} = P_{t_{[\mathrm{dBm}]}} + G_{r_{[\mathrm{dBi}]}} + G_{t_{[\mathrm{dBi}]}} - P_{r,min_{[\mathrm{dBm}]}} \quad (3.3)$$

where:

- P_t: power fed to the transmitting antenna;
- $L_{p,max}$: maximum path loss;
- G_r: gain of the receiving antenna;
- G_t: gain of the transmitting antenna.

When calculating the transmission power, it is necessary to determine whether it is being calculated in UL or DL which influences the type of transmitter losses, given that in the case of UL the element that causes losses is the user, otherwise, it is the cables as well as the base station antenna.

$$P_t^{DL}{}_{[\mathrm{dBm}]} = P_{Tx}{}_{[\mathrm{dBm}]} - L_c{}_{[\mathrm{dB}]} \tag{3.4}$$

where:

- P_t^{DL}: power feed to the antenna in the DL;
- P_{Tx}: transmitter output power;
- L_c: losses in the cable between the transmitter and the antenna.

$$P_t^{UL}{}_{[\mathrm{dBm}]} = P_{Tx}{}_{[\mathrm{dBm}]} - L_u{}_{[\mathrm{dB}]} \tag{3.5}$$

where:

- P_t^{UL}: power feed to the antenna in the UL;
- L_u: losses due to the user's body.

As for the transmission power, the receiver power will suffer losses due to the user in the DL case and losses due to the BS antenna in the UL case, which are respectively (3.6) and (3.7).

$$P_{Rx}^{DL}{}_{[\mathrm{dBm}]} = P_r{}_{[\mathrm{dBm}]} - L_c{}_{[\mathrm{dB}]} \tag{3.6}$$

where:

- P_{Rx}^{DL}: receiver input power at DL.

$$P_{Rx}^{UL}{}_{[\mathrm{dBm}]} = P_r{}_{[\mathrm{dBm}]} - L_u{}_{[\mathrm{dB}]} \tag{3.7}$$

where:

- P_{Rx}^{UL}: receiver input power at UL.

In addition to the user's losses and also the ones caused by the cable at the BS between the transmitter and the antenna, the fact that MIMO technology is used in the receiving antenna must also be taken into account and, for this, its gain must be taken into account. A correlation value between coverage and capacity, the interference margin, which depends on the cell structure, number of active users, and their services, and can take values between 2 dB and 4 dB for coverage limited cells, and between 4 dB and 7 dB for capacity limited ones [Belc18] and finally, there is a gain that reduces the BS noise figure and improves sensitivity, but introduces insertion loss in DL, the Tower Mounted Amplifier (TMA) gain. The path loss can be summarised by:

$$L_{p,max} = P_t{}_{[\mathrm{dBm}]} + G_r{}_{[\mathrm{dBi}]} + G_t{}_{[\mathrm{dBi}]} - P_{r,min}{}_{[\mathrm{dBm}]} - L_c{}_{[\mathrm{dB}]} - L_u{}_{[\mathrm{dB}]} - I_m{}_{[\mathrm{dB}]} + G_{div}{}_{[\mathrm{dB}]} + G_{TMA}{}_{[\mathrm{dB}]} \tag{3.8}$$

where:

- I_m: interference margin;

- G_{div}: diversity gain;
- G_{TMA}: TMA gain.

By calculating the Link Budget and using the propagation models mentioned above in the Table 3.2 and detailed in Annex A the maximum distance that the user can be from the BS is calculated so that communication can exist between them using the 0.7 GHz band by using this band the most suitable models are the Okumura-Hata and the Walfisch-Ikegami depending on the user's distance from the base station. The Okumura-Hata model is adopted for long distances between 5 to 20 km while the Walfisch-Ikegami model is used for short distances between 0.1 to 5 km.

$$d_{max\,[\mathrm{km}]} = 10^{\frac{L_{p,max\,[\mathrm{dB}]} - L_{A\,[\mathrm{dB}]} - L_{C\,[\mathrm{dB}]}}{L_{B\,[\mathrm{dB}]}}} \tag{3.9}$$

where:

- L_A: correction factor related to the frequency, BS and UE antenna height, dependent on the propagation scenario;
- L_B: correction factor related to the BS antenna height;
- L_C: propagation scenario correction factor.

For outdoor to indoor environments, the generic model is characterised by the sum of the outdoor path loss plus the indoor one, which, for the outdoor case, is calculated using the propagation models adapted to the scenario, contained in Annex A. For the indoor case, the following model is used:

$$\overline{\overline{L_{p_{ind}}}} = \begin{cases} 6.6 + 2.1\, f_{[\mathrm{GHz}]} - 1.5\, N_f & , N_f \leq N_{f\,th} \\ 0 & , N_f > N_{f\,th} \end{cases} \tag{3.10}$$

where:

- N_f: number of floors;
- $N_{f\,th}$: number of floors theoretical given by (3.11).

$$N_{f\,th} = \frac{6.6 + 2{,}1\, f_{[\mathrm{GHz}]}}{1.5} \tag{3.11}$$

This model assumes a Log-Normal distribution and determines the penetration attenuation.

In the case of the Winner II model adapted for outdoor to indoor environments, this is explained in Annex A together with the outdoor environments.

Within the 3.6 GHz band, active antennas are used, given this it must be used an array of antennas for a given sector. There are several possible configurations. These are classified by the amount of transmission and reception channels, being possible, in mMIMO, to use the 16T16R, 32T32R, and 64T64R configurations characterised in Figure 3.6.

The case of the 64T64R is characterised by being used in urban areas with the distribution of users, mainly in high-rise buildings, small subarrays with high-gain beams that can be steered in an extensive

range of angles are applied. The case of the 32T32R is characterised by being used in urban areas with the distribution of users, mainly in low-rise buildings. Large antenna areas are applied to deliver the required cell data rates - but the vertical coverage range can be decreased. The last case, 16T16R, is characterised by small vertical user distribution.

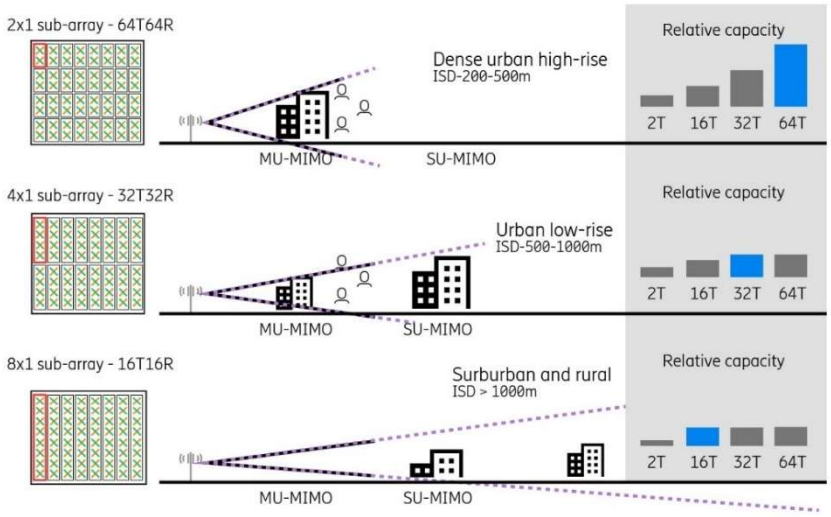

Figure 3.6. Active antennas configurations for a range of network deployment scenarios (extracted from[ERIC18]).

3.2.2 Capacity Planning

This section describes planning in terms of capacity, based on [Belc18] and [Corr20]. In this sense, the objective is to calculate the output parameters of Figure 3.3, having as purpose to calculate the number of users that a cell can accommodate for each service. The capacity model takes advantage of the cell area that is the subject of the coverage model's response to calculate the number of users within each cell. This can be calculated with the following expression:

$$N_{users,cell} = \eta_{[\text{users/km}^2]} \; A_{cell}{}_{[\text{km}^2]} \tag{3.12}$$

where:

- η: load factor;
- A_{cell}: area of a cell.

The area of a cell depends on the configuration of each site, and for a tri-sectorised site, the area is given by:

$$A_{cell}{}_{[\text{km}^2]} = \pi \; {d_{max}}^2 \tag{3.13}$$

In the use of active antennas, in terms of available throughput levels to users, this depends on the occupation of each beam, that is, if the UEs are in the same restricted area they can be covered by the same beam and its level throughput is lower because of having to share resources with other users, otherwise, each UE is entitled to one beam and the available throughput level is higher. It is possible to

calculate the maximum throughput for DL and UL, defined by 3GPP from:

$$R_{b\,[\mathrm{Mbps}]} = 10^{-6} \sum_{j=1}^{J} v_{Layers}^{j}\ Q_m^j\ f^j\ R_{max}\ \cdot \frac{N_{PRB}^{BW\,j,\mu} \cdot N_{SC}^{RB}}{T_s^{\mu}}\ \cdot (1\ -\ O^j) \tag{3.14}$$

where:

- J: number of aggregated component carriers in a band or band combination;
- v_{Layers}^{j}: maximum number of supported layers;
- Q_m^j: maximum supported modulation order (2, 4, 6 or 8 respectively QPSK, 16-QAM, 64-QAM or 256-QAM);
- f^j: scaling factor, can take the values 1, 0.8, 0.75, and 0.4;
- R_{max}: maximum code rate (948/1024);
- $N_{PRB}^{BW^j,\mu}$: maximum RB allocation in bandwidth BW^j with numerology μ, where BW^j is the UE supported maximum bandwidth in the given band or band combination;
- T_s^{μ}: average OFDM symbol duration in a subframe for numerology μ, i.e., $T_s^{\mu} = \frac{10^{-3}}{14 \times 2^{\mu}}$;
- O^j: overhead (0.14 for DL and 0.08 for UL).

The number of layers depends on the number of transmission channels, that is, 64T64R corresponds to 64 layers, although current algorithms cannot reduce co-channel interference of such a large number of transmission layers, so the maximum value supported is 16 layers.

Having access to the number of users that is accommodated in a cell, it is relevant to perceive how they are distributed throughout the service area, since that the closer to the base station, the greater the modulation used is:

$$N_{u,cell\,[\mathrm{users}]}^{M} = \sum_{M} N_u^M\ [\mathrm{users}] \tag{3.15}$$

where:

- M: are the modulations served in the cell: 4 QPSK, 16 QAM, 64 QAM and 256 QAM;
- N_u^M: is the number of users served by the modulation M given by:

$$N_{u,cell}^{M} = \begin{cases} \frac{R_Q^2 - R_{16}^2}{R_Q^2}\ N_{u,cell} & M = 4 \\ \frac{R_{16}^2 - R_{64}^2}{R_Q^2}\ N_{u,cell} & M = 16 \\ \frac{R_{64}^2 - R_{256}^2}{R_Q^2}\ N_{u,cell} & M = 64 \\ \frac{R_{256}^2}{R_Q^2}\ N_{u,cell} & M = 256 \end{cases} \tag{3.16}$$

where:

- R_Q: cell QPSK radius;
- R_{16}: cell 16-QAM radius.
- R_{64}: cell 64-QAM radius.
- R_{256}: cell 256-QAM radius.

It is essential to take into account the available bandwidth, as the greater the bandwidth available by the BS, the greater the traffic capacity accommodated by it. For this, the number of RBs allocated in the BS for a user for a specific service will be calculated and rounded up to the closest intiger:

$$\overline{N_{RB,users,s}} = \frac{\overline{R_{b,users,s}}_{[\text{Mbps}]}}{\overline{R_{b,RB}^{M}}_{[\text{Mbps}]}} \tag{3.17}$$

where:

- $\overline{R_{b,users,s}}$: average throughput per user of a service s;
- $\overline{R_{b,RB}^{M}}$: average throughput per RB of each modulation M.

The average throughput per RB of each modulation M, (3.2), was calculated previously in Section 3.2.1 to measure the sensitivity of the receiver.

Therefore, having the number of RBs per user, it is possible to allocate them in a cell, dividing them by the different modulations, thus calculating the total number of RBs for a modulation and the total number of RBs in a single cell, which are respectively (3.18) and (3.19).

$$\overline{N_{RB}^{M}} = \sum_{service} \overline{N_{RB,users,s}}\, N_{u,cell}^{M}\, P_{u,s_{[\%]}} \tag{3.18}$$

where:

- $N_{u,cell}^{M}$: number of served users by modulation M;
- $P_{u,s}$: subscriber usage percentage of a service s.

$$\overline{N_{RB,required}^{M}} = \sum_{M} \overline{N_{RB}^{M}} \tag{3.19}$$

where:

- $\overline{N_{RB}^{M}}$: number of RBs required in modulation M.

With the calculations presented above, it is possible to determine if the system is limited in terms of coverage or capacity. In case it is limited in terms of coverage, the value of $\overline{N_{RB,required}^{M}}$ will be inferior than the total value of RBs accommodated in a single cell, and in this case, there is an overuse of the available resources which it is considered good in terms of QoS but bad in terms of costs for the service provider. In the case of being limited in terms of capacity, users will have lower throughput levels, which implies that each user has less RB to use a service than what would be expected, $N_{RB,users,s}$. It will be possible to evaluate the overload of a cell in the following equation:

$$\eta_{cell_{[\%]}} = \frac{\overline{N_{RB,required}}}{N_{RB,cell}} 100 \quad (3.20)$$

where:

- $\overline{N_{RB,required}}$: total number of required RBs in the respective cell;
- $N_{RB,cell}$: total number of RBs in the respective cell.

To continue the cell capacity study, the average user consumption in all services can be determined, meaning the total average throughput of a cell, through the sum of the average throughput per user for each service multiplied by the number of users who enjoy this same service.

$$\overline{R_{b,cell_{[\text{Mbps}]}}} = \sum_{services} \overline{R_{b,users,s_{[\text{Mbps}]}}} N_{u,s_{[\text{users}]}} \quad (3.21)$$

where:

- $N_{u,s}$: number of active users in the service s.

To obtain more detailed information about the services that are used in the cells, that is, what type of traffic exists and what percentage of cell users use a particular service, it is possible to calculate the percentage of traffic for each service, as well as the fraction of active served users, which are respectively (3.22) and (3.23).

$$p_{traffic,s_{[\%]}} = \frac{\overline{R_{b,user,s}} N_{u,s} \eta_{cell}}{\overline{R_{b,cell_{[\text{Mbps}]}}}} \quad (3.22)$$

$$\eta_{u,cell_{[\%]}} = \frac{N_{u,cell_{[\text{users}]}}}{N^{M}_{u,cell_{[\text{users}]}}} \quad (3.23)$$

where:

- $N_{u,cell}$: number of active users in the cell.

3.2.3 Interference Planning

Interference may lead to deterioration of the received signal and for this reason cause throughput reduction. In this way, interference limits network capacity and makes the throughput received by the users not enough for the services desired. As a result, the increase in interference leads to cell radius degradation, which necessarily leads to data rates reduction.

Taking into account the information on the number of resource blocks distributed by users and the SNRs accessible to each one, it is also necessary to include the interference in the global performance of the system in this way, the SINR possible to reach the i^{th} link on each subcarrier (k) is given by, [Alco17]:

$$\rho_{IN_{i,k}[\mathrm{dB}]} = 10\ \log\left(\frac{P_{i_{[\mathrm{mW}]}}\left|B_{i,k}\right|^2}{N_{[\mathrm{mW}]} + \sum_{j=0}^{N_{n,cell}} P_{j_{[\mathrm{mW}]}}\left|B_{j,k}\right|^2}\right) \quad (3.24)$$

where:

- P_{i} and P_j:transmit power of donor and neighbouring BS, respectively;
- $B_{i,k}$ and $B_{j,k}$: fading channel gain for donor and neighbouring cell, respectively;
- N: noise power;
- $N_{n,cell}$: number of neighbouring cells.

In a severely interference limited scenario, the noise power can be ignored to simplify the calculations and the above expression can be written as:

$$\rho_{IN_{i,k}[\mathrm{dB}]} = 10log\left(\frac{P_{i_{[\mathrm{mW}]}}\ LD_{i,k}{}^{-\beta}_{[\mathrm{m}]}}{\sum_{j=1}^{N_{n,cell}} P_{j_{[\mathrm{mW}]}}\ L_j d_{j,k}{}^{-\beta}_{[\mathrm{m}]}}\right) \quad (3.25)$$

where:

- B: function of path loss leads to $|B|^2 = LD^{-\beta}$;
- L: constant, $L = G_t G_r$ depending on the infrastructure of sender and receiver;
- β: path loss exponent explained in Annex A;
- $D_{i,k}$, and$d_{j,k}$: distances from user to donor BS and neighbouring cells respectively as shown Figure 3.7.

For this model, two situations are considered, using a BS and a reference radius obtained from the previous models, from which the interference is calculated for a given user. In the first case, the user is at the extreme of the area covered by the BS, that is, the user is at a distance from the reference radius, which is the worst case, being subject to greater interference from the surrounding BS. In the second case, the user is in the same position as the BS, this being the best case, because the user is as far away as possible from the surrounding BS. It will also be considered that all neighbouring BS are positioned at twice the coverage radius of the owner and that they have the same powers and gains as the owner. Although both cases are not physically realistic, they are the worst and the best interference estimate.

For these two cases, the expression can be simplified using the radius of coverage of the BS, thus, for the best-case scenario:

$$\rho_{IN_{best}[\mathrm{dB}]} = 10\ \log\left(\frac{100^{-\beta}_{[\mathrm{m}]}}{6\ (2r)^{-\beta}_{[\mathrm{m}]}}\right) \quad (3.26)$$

where:

- r: coverage radius of the donor BS.

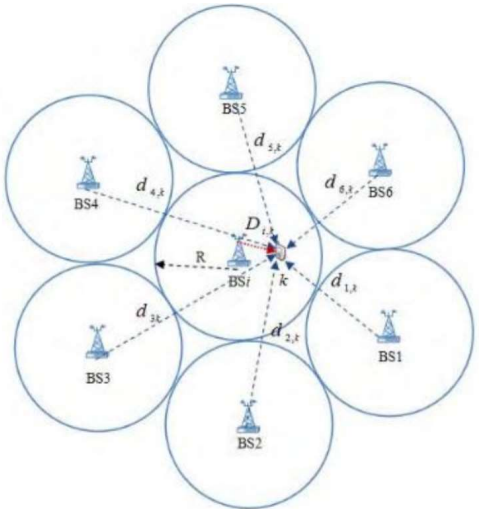

Figure 3.7. Example of interference scenario (extracted from [Alco17]).

To prevent $\rho_{IN_{best}}$ from producing a value that tends to infinity, it is considered that instead of the user being in the equivalent position as the BS donor the user will be at a distance of 100 m. Using this value, the interference for the best case will be approximately $+\infty$, the same is not true for the worst case being defined as follows:

$$\rho_{IN_{worst}[\mathrm{dB}]} = 10\ \log\left(\frac{1}{P_{t_{[\mathrm{mW}]}}\ G_t\ G_r\ r_{[\mathrm{m}]}^{-\beta}\left(2\left(\sqrt{3}^{-\beta}+\sqrt{7}^{-\beta}\right)+3^{-\beta}\right)}\right) \tag{3.27}$$

To the worst case calculation, it was considered the same conditions to the donor and neighbours BS and the user is located at a r distance from the donor BS and one of the neighbours BS. Through this, it is possible to calculate the others neighbours' BS distance to the user and apply it in (3.25).

3.3 Model Implementation

This section describes the model implementation as well as the flowchart. The model was implemented in MATLAB.

Figure 3.8 illustrates the flowchart of the model. The program is based on several functions dependent on each other. It starts by choosing a scenario, in this case where the BS is located as well as its surrounding environment, which will define, among others, the most suitable propagation model. In addition, other parameters inherent to the users' profile and the services they use must also be defined. Once the scenarios are defined, the program moves to coverage planning. The steps developed for this excerpt of the program are explained in Section 3.2.1 and Annex A, which involve the Link Budget and the propagation models, this block that has the purpose of calculating the maximum distance that the user can be situated from the BS, this being also influenced by the modulation in use. Subsequently, the capacity planning is followed, this was also detailed previously in Section 3.2.2, this model has the

particularity of making a readjustment to the dimensioning of the cell resources in case the system is limited.

The Print Results block aims to collect all the results obtained in the previous blocks and create a results file as well as a set of graphs which subsequently is used in the results analysis phase in order to simplify it.

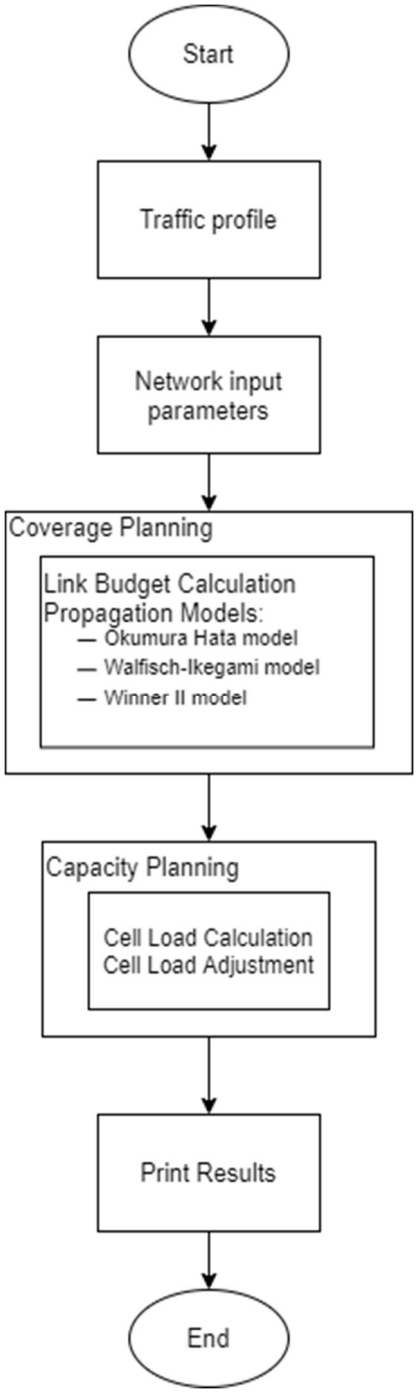

Figure 3.8. Model flowchart.

In order to have a better understanding of the model, for the Coverage Planning and Capacity Planning blocks of Figure 3.8, explanatory flowcharts were made in Figure 3.9 and Figure 3.10 respectively.

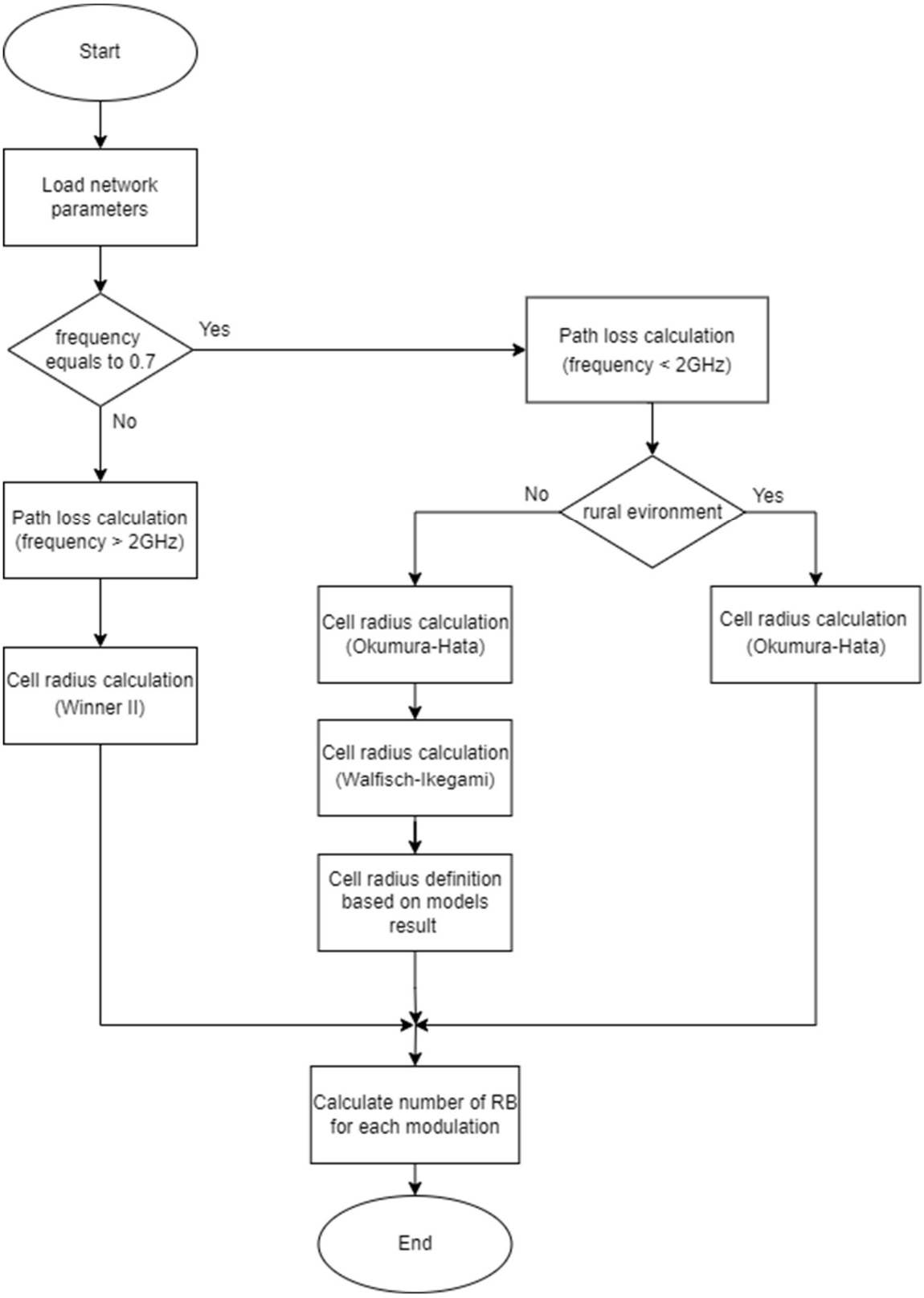

Figure 3.9. Coverage planning.

In the implementation of the coverage model, the network parameters are taken into account, and in this way, the working frequency of the cell is chosen, in the case where the frequency is different from 0.7 GHz the model adopted is Winner II and hence in this way, the radius of the cell is calculated and how many RBs are needed so that it is possible to guarantee a certain transmission rate at the end of

the cell, as well as for the remaining modulations. If the frequency is equal to 0.7 GHz, the environment is checked and in case it is rural, only the Okumura-Hata model is used to calculate the cell radius, otherwise, the Okumura-Hata and Walfisch-Ikegami models are used and a choice is made based on the results obtained since for one of the cases the results were outside the predicted distance for this model. After obtaining the result of the cell radius, the number of RBs for a given transmission rate is calculated.

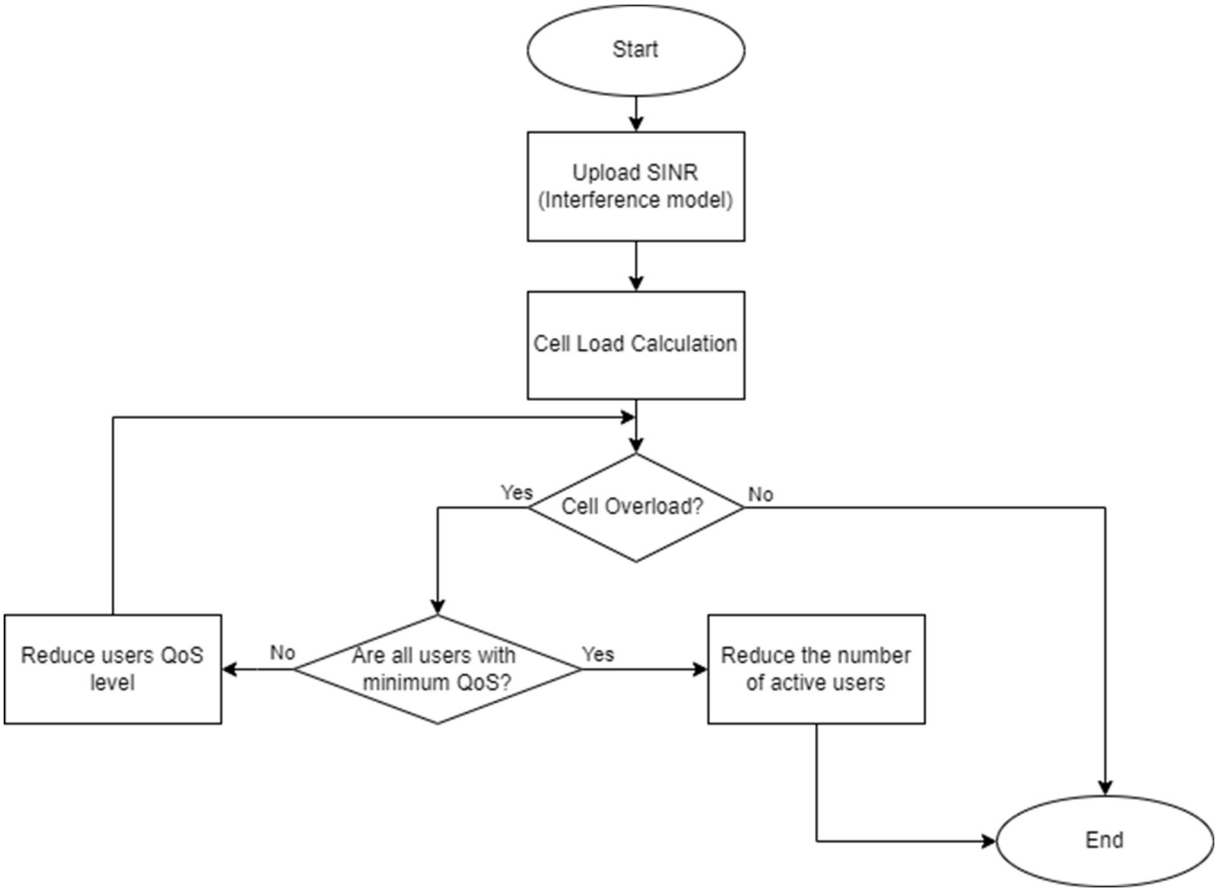

Figure 3.10. Capacity planning.

In the coverage planning block implementation with respect to the Walfisch-Ikegami propagation model and in the case of the urban Micro cell scenario of Winner II, they were used, as an alternative to calculating the maximum distance from the mobile terminal to the BS using the Path Loss, a numerical solution due to the algorithm complexity.

As explained above in Section 3.2.2 the system may be limited in terms of capacity and in that case, adjustments must be made to the cell load. Starting by removing RB from users who are using values higher than the minimum QoS value required to utilise the service, which can solve the system problem. If the reduction in the number of RB is not enough, the following step is to remove users, thus reducing the number of active users in the cell, with the objective of achieving the maximum capacity of the cell. The algorithm is properly explained in Figure 3.10.

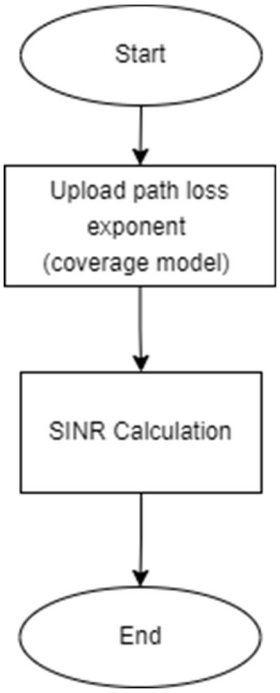

Figure 3.11. Interference planning.

3.4 Model Assessment

In order to validate the model described in Section 3.2, this section is based on a series of tests that validate all model blocks. For the model to become valid, theoretical values are used so that a comparison can be made with the results obtained and, if necessary, the appropriate adjustment is performed.

In this sense, the main building blocks of the model were evaluated, starting with the verification of the input parameters and proceeding with the evaluation of the coverage, capacity, and interference blocks. Consequently, for the coverage model to become valid, the following tests in Table 3.4 were performed and as a result of these, the graphs found below were created.

Table 3.4. Empirical tests performed to validate the implementation of the coverage model.

Test ID	Element Validation
1	Link Budget and propagation models (compare with values obtained from simulator, generate figures).
2	Cell radius changes in the 2 frequency bands and from different input parameters (e.g., required throughput at cell edge, BS/Mobile Terminal (MT) height).
3	Verify if the cell radius is decreasing with the increase of modulation order.
4	Verify if the cell radius is decreasing with the increase of frequency band.
5	Verify if the cell radius decreases with the increase of numerology.

As expected in Figure 3.12, the test id number 4 was corroborated, when increasing frequency, the cell radius decreases. It is equally possible to verify the variation of the cell radius according to the propagation model used.

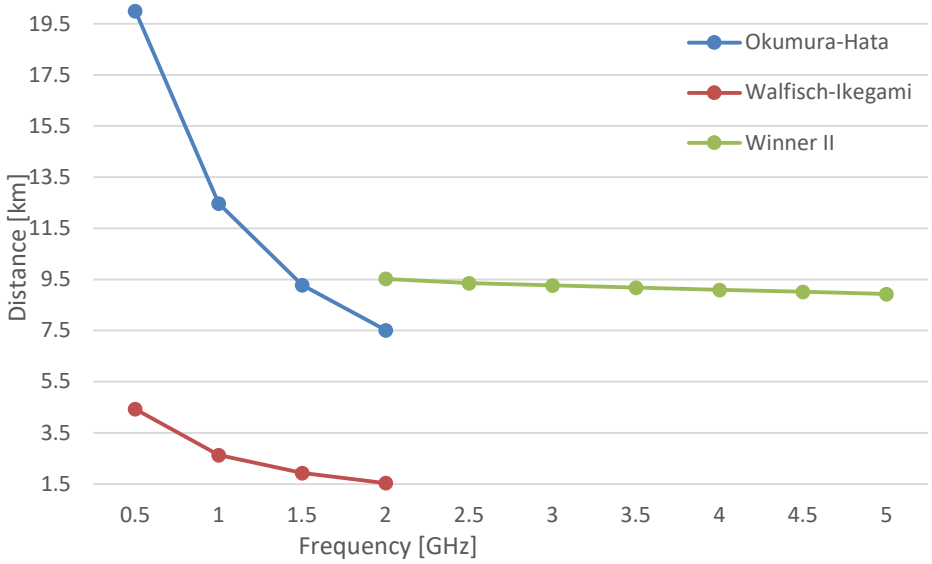

Figure 3.12. Distance in function of the frequency for multiple propagation models

For the capacity model to become valid, the following tests in Table 3.5 were performed.

Table 3.5. Empirical tests performed to validate the implementation of the capacity model.

Test ID	Element Validation
1	Check with a calculator the distribution of users across the various cell areas associated with the modulation in question (uniformly distributed).
2	Verify if the cell is overloaded if the QoS value is reduced to the minimum QoS determined for the service.
3	Verify if the QoS values are the minimum possible for each user. In this way, users will have to be removed until they correspond to the full capacity of the cell.

In addition to verifying that the cell load increases with the increase in the number of users, Figure 3.13, it is equally important to verify that users are served according to the priority assigned to them, as the cell load increases, Figure 3.14.

As expected, as the number of users increases, the percentage of active users per service decreases, Figure 3.14. Despite this, when the density of 200 users is achieved, Real Time Gaming (RTG) service returns to a percentage of users served at 100%. This is justified by the fact that the algorithm, after removing users, checks if some services with less priority require fewer resources and that these are equivalent to the load that was available in the cell. This is intended to take advantage of all the available capacity in the cell.

For the interference model to become valid, the following tests in Table 3.6 were performed.

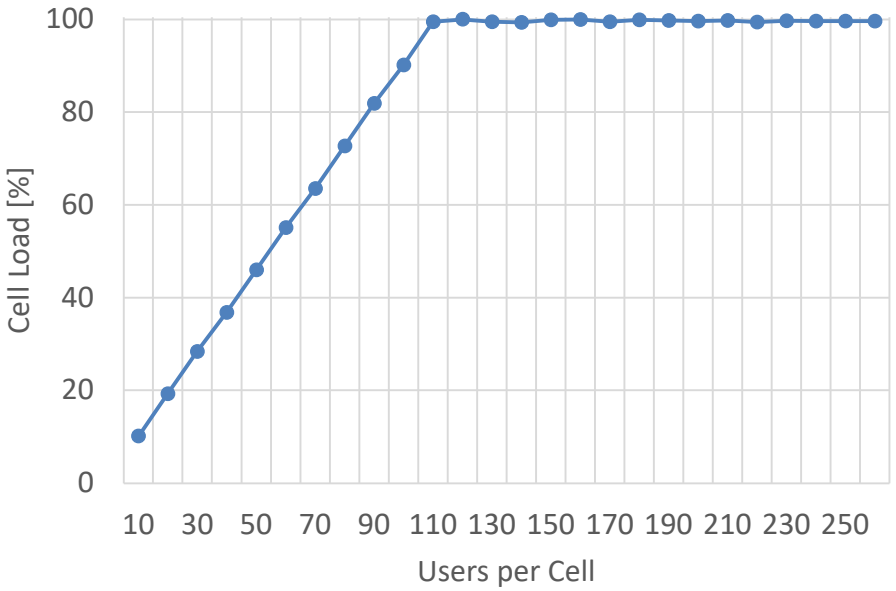

Figure 3.13. Cell Load in function of the user density.

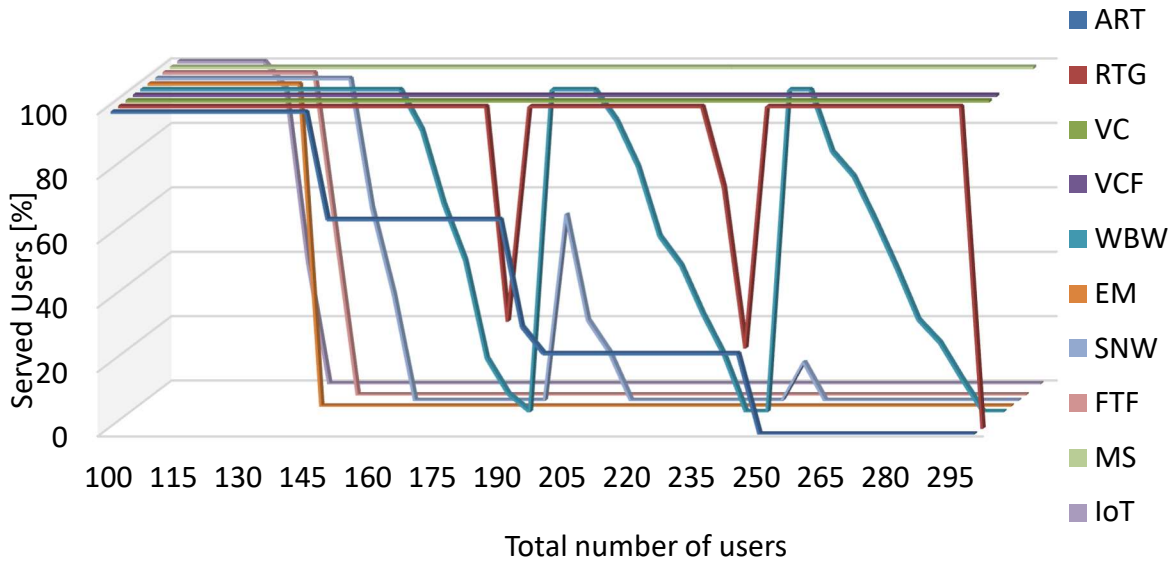

Figure 3.14. Served users in function of user density for multiple services.

Table 3.6. Empirical tests performed to validate the implementation of the interference model.

Test ID	Element Validation
1	Check with a calculator the SNR values for the worst and best cases.
2	Verify if the SNR value is making exchanges on the capacity module (the cell has more capacity when the user is near the BS donor).

Although the interference model is simplistic, it also needs to be tested since when it is combined with the other two models, it is producing correct differences in the model. Therefore, the objective of this model is to change the available cell capacity.

Chapter 4

Results Analysis

This chapter provides a description of the simulated scenarios and the results obtained after applying the model described in the previous chapter to the described scenarios.

4.1 Scenario Description

As previously described in the model overview, parameters that describe the users are required, such as their geographic spread, the used services description, and also the network description. This is the focus of this subsection.

The chosen scenario represents a case study with multiple users dividing the resources of a cell, each of the resources used will be characterised by a service level agreement (SLA), this SLA is accompanied by a certain priority level. In terms of services performed by the UE, four classes are considered for both UL and DL, Table 4.1. Services are classified by their type, eMBB, URLLC or mMTC, that is already mentioned in Chapter 2, their data rate, in Mbps, and their class can be: chat services, such as voice calls and multimedia communications, demand lower latencies due to the bidirectional flow of data; Streaming Services, which represent an alternative to downloading data, consist of performing activities that require real-time data transfer, like listening to music or watching videos; Interactive Services comprise services where the user can directly interact with the application, such as online games and web browsing; Background services are typically distinguished as the process of sending and receiving data in the background, requiring no user interface, some instances of this class of resources being Short Message Service (SMS) and email.

Regarding the Remote Surgery (RSU), Intelligent Transport System (ITS) and Factory Automation (FAU) services, these are composed of a set of sub-services, that is, only when they work simultaneously is it possible to perform these three services. The RSU service is possible behind 4 sub-services, each with their respective data rates:

- Internal Control Manipulation with a data rate of 0.512 Mbps;
- Video streaming with an average data rate of 15 Mbps and a minimum of 5 Mbps;
- Haptic feedback with a data rate of 0.400 Mbps;
- External Control Manipulations with a data rate of 0.512 Mbps.

The ITS service is possible through 3 sub-services, each with their respective data rates:

- Traffic information with an average data rate of 2 Mbps and a minimum of 0.384 Mbps;
- Remote driving with an average data rate of 25 Mbps and a minimum of 7 Mbps;
- Network based sensor sharing with an average data rate of 20 Mbps and a minimum of 5Mbps.

The FAU service is possible through 3 sub-services, each with their respective data rates:

- Machine tools with a data rate of 1 Mbps;
- Printing machines with a data rate of 1 Mbps;
- Packaging machines with a data rate of 1 Mbps.

Table 4.2 shows the reference values that were used to calculate the Link Budget, which is necessary to obtain the maximum path loss that is used in propagation models to obtain the maximum cell radius. In the table, it is possible to check the gain and loss values that are based on [Belc18] and [Patr21]. The frequency bands are the ones that have been used in this thesis, 0.7 GHz and the 3.5 GHz that belongs to NR and, in addition, the 0.8 GHz,1.8 MHz and 2.6 GHz bands that belongs to LTE.

Table 4.1. Services classes and demanded data rates (extracted from [Carv21])

Service	Service Class and Type	Data Rate [Mbps]		Priority	References
		Average	Minimum		
Remote Surgery (RSU)	Conversational URLLC	16.424	6.424	1	[JMJL02] [JMJL02] [IAIH18] [QJGZ18]
Intelligent Transport System (ITS)	Conversational URLLC eMBB	47	12.384	2	[ALTI20] [3GPP18a]
Factory Automation (FAU)	Conversational URLLC	3	3	3	[PSMM17] [IAIH18]
Voice (VOI)	Conversational	0.032	0.005	4	[SeDo19]
Music (MUS)	Streaming	0.32	0.016	5	[Mari21]
Video Conference (VCF)	Conversational	1.8	0.064	6	[SeDo19]
Video Streaming (VST)	Streaming URLLC	15	5	7	[JMJL02]
Augmented Reality (ART)	Streaming URLLC	200	50	8	[Qual18]
Real-time Gaming (RTG)	Streaming eMBB	20	0.5	9	[Mari21]
Web Browsing (WBW)	Interactive	0.5	0.031	10	[SeDo19]
Social Networking (SNW)	Interactive	2	0.500	11	[SeDo19]
File Transfer (FTF)	Interactive	1.024	0.384	12	[SeDo19]
Email (EMA)	Background	0.512	0.010	13	[SeDo19]
IoT	Background	0.512	0.081	14	[Mari21]

One of the study scenarios includes 3 clusters, Figure 4.1, that covers 3 different environments, urban environment composed by 5 sites, suburban environments composed by 9 sites and rural environment composed by 7 sites. For these three clusters, an analysis is performed of how this area can be covered including the 5 bands.

Table 4.2. Reference values for the Link Budget parameters.

Parameter	NR700 L800	L1800 L2600	NR3600
Slow-Fading Margin [dB]	5	6	7
Interference Margin [dB]	2	4	6
Cable Losses [dB]	2	2	0
SCS [kHz]	15	15	30
Number of RBs	50	100	273
Bandwidth [MHz]	10	20	100
MT Height [m]	1.5		
BS Height [m]	42.0		
MT Antenna Gain [dBi]	3.0		
MT Losses [dB]	3.0		
MT Noise Figure [dB]	7.0		
Coverage Probability [%]	90.0		
Output Power per Carrier/MIMO Element [W]	40	42	5
Maximum Antenna Gain [dBi]	15.2	17.8	23.8
Number of MIMO Elements	2	2	32

Table 4.3 enables studying different percentages of use of services depending on usage scenarios. The reference scenario is used to assess the model and review any problems that may exist after the model creation. Throughout this chapter, multiple service mix scenarios are used, which will vary according to the scenario under study, the expected evolution of the population over the years and a greater use of new technologies.

(a) Urban

(b) Suburban

(c) Rural

Figure 4.1. BS location for the different scenarios Clusters.

In contrast to Table 4.3, which aims to investigate the various urban, suburban and rural scenarios,

Table 4.4 aims to investigate the behaviour of the system when there is an underload of RSU, ITS and FAU services, which are the highest priority services and with different data rates between them, which may affect the number of active users in the cell.

Table 4.3. Reference, urban, suburban and rural scenarios service mix.

Service	Mix Reference [%]	Urban Service mix [%]	Suburban Service mix [%]	Rural Service mix [%]
RSU	0	12	0	0
ITS	0	9	12	17
FAU	0	3	6	0
VOI	20	39	38	37
MUS	5	1	2	2
VCF	35	4	2	0
VST	0	5	2	1
ART	2	1	2	2
RTG	2	2	1	1
WBW	10	5	11	17
SNW	10	10	10	10
FTF	3	4	2	2
EMA	3	3	10	10
IoT	10	2	2	1

Table 4.4. Urban scenario service mix variation.

Service	Urban Service mix 1 [%]	Urban Service mix 2 [%]	Urban Service mix 3 [%]
RSU	12	4	4
ITS	9	18	4
FAU	3	2	16
VOI	39	39	39
MUS	1	1	1
VCF	4	4	4
VST	5	5	5
ART	1	1	1
RTG	2	2	2
WBW	5	5	5
SNW	10	10	10
FTF	4	4	4
EMA	3	3	3
IoT	2	2	2

In order for the model to involve realistic values for the areas being studied, real values are used, taken from the census for the load of inhabitants in the study areas, as seen in Table 4.5. Although the values are realistic, many users are using private networks, networks of other operators and not all of them are active at the same time, so one only considered that 30% of users are active.

Table 4.5. Scenarios and users' density in the respective location.

Scenario	Area [km^2]	Number of habitants per km^2	30 percent of number of habitants per km^2
Urban	0.5	6420	1926
Suburban	2.0	910	273
Rural	10.0	18	5

Table 4.6 aims to study the evolution over the years of mobile networks and the various transitions in the use of different bands and technologies, for that, two scenarios were built, one that aims to include LTE and NR bands without refarming and the other one with refarming. It was considered that the current traffic is equal to 40% and with the years the number of users increase according to [ERIC21]. It was also considered the remaining bandwidth for each site type, which is represented in Table 4.7, and is divided per each technology bandwidth.

Table 4.6. Evolutive urban scenarios

Year	Total number of users	LTE traffic [%]	NR traffic [%]	Scenario 1 (without Refarming)	Scenario 2 (with Refarming)
2022	500	20	20	NR7 + L8 + L18 + L26 + NR35	NR7 + L8 + L18 + L26 + NR35
2023	500	35	30	NR7 + L8 + L18 + L26 + NR35	NR7 + L8 + L18 + L26 + NR35
2024	500	40	40	NR7 + L8 + L18 + L26 + NR35	NR7 + L8 + L18 + NR26 + NR35
2025	725	55	90	NR7 + L8 + L18 + L26 + NR35	NR7 + L8 + L18 + NR26 + NR35
2026	900	60	120	NR7 + L8 + L18 + L26 + NR35	NR7 + L8 + NR18 + NR26 + NR35
2027	1300	80	180	NR7 + L8 + L18 + L26 + NR35	NR7 + L8 + NR18 + NR26 + NR35

Table 4.7. Total bandwidth per site types and 5G and 4G technologies.

Site Type	BW 4G	BW 5G
NR7 + L8 + L18 + L26 + NR35	50	110
NR7 + L8 + L18 + NR26 + NR35	30	130
NR7 + L8 + NR18 + NR26 + NR35	10	150

4.2 Cell Radius

In this section, results regarding the cell radius are presented, taking into account the parameters in Table 4.2. In these figures, there are variations of the urban, suburban, and rural scenarios, of the propagation models, Okumura-Hata (OH), Walfisch-Ikegami (WI), and Winner II (Win II), and of the 0.7 GHz, 1.8 GHz, 2.6 GHz, and 3.6 GHz. Figure 4.2, Figure 4.3, and Figure 4.4 show the cell radius for the throughput levels of 1 Mbps, 5 Mbps, and 10 Mbps, respectively.

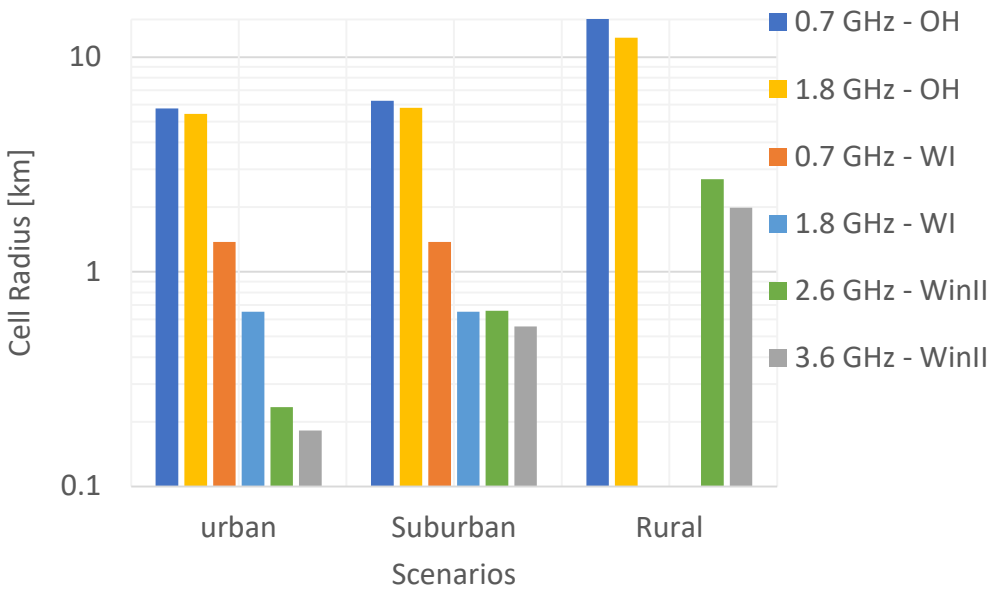

Figure 4.2. Cell radius for different scenarios and models for 1 Mbps.

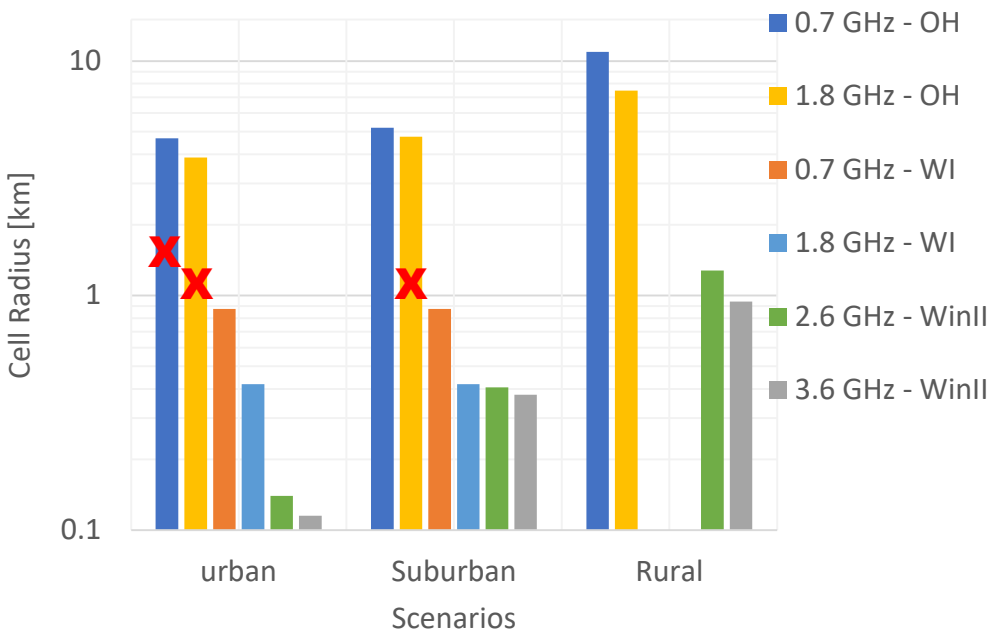

Figure 4.3. Cell radius for different scenarios and models for 5 Mbps.

With the required value at the cell end increased, to 5Mbps, some of the models become invalid according to Table 3.2, in this case, the Okumura-Hata model is not valid for distances less than 5 km, and therefore these are found marked with “X” the columns for which this happens, that is, for urban environments with frequencies 0.7 GHz and 1.8 GHz and for suburban environments with frequencies 1.8 GHz.

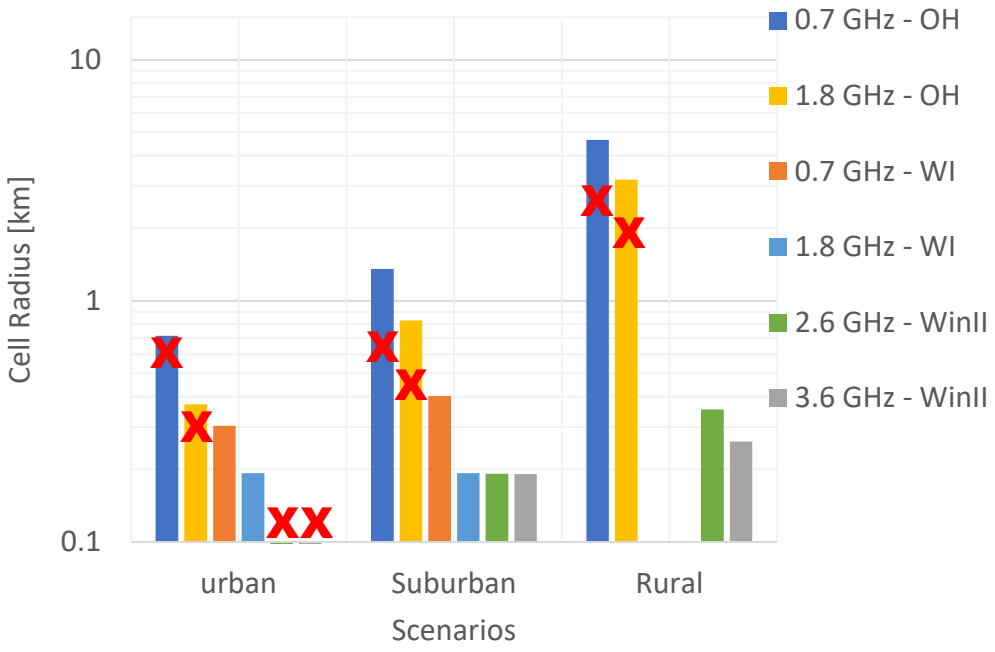

Figure 4.4. Cell radius for different scenarios and models for 10 Mbps.

As for 5 Mbps, for 10 Mbps the cell radius distances decrease again. Hence, the Okumura-Hata model is not valid for any of the environments and the Winner II model is not valid for the urban scenario, for frequencies 2.6 GHz and 3.6 GHz.

In the figures, it is possible to verify that the radius of the cell increases, with the change of the scenario from urban to suburban and from suburban to rural, it can also be confirmed that the radius decreases with increasing frequency, as already seen in Figure 3.12, and finally, by comparing the three graphs, it can be seen that with the increase of the required throughput at the end of the cell, the radius of the cell decreases and for cases where the required throughput is high, the cell radius saturates, as can be seen for the urban scenario for 3.6 GHz frequency.

In the event that the services that are to be performed have throughputs higher than the levels available at the end of the cell, they can use more RB, that is, in case the throughput available at the end of the cell is 1 Mbps, it is possible to perform a service that requires 2 Mbps using 2 RB.

4.3 Influence of Frequency

In this section, the analysis of results is presented regarding the influence of the frequency used, depending on the number of users in the cell, between 100 and 300 users, taking into account the urban service mix in Table 4.3. The frequencies used for this evaluation will be 2.6 GHz for 4G technology and 0.7 GHz and 3.6 GHz for 5G technology.

The results are presented taking into account the various services in Table 4.1. As the service mix and the total number of users in the cell are introduced into the programme, the programme calculates for each service the number of users taking into account the percentages of the service mix and, consequently, the load on the network, later, if the necessary load is higher than the available load, users are deactivated according to priority and finally the percentage of active users is calculated. In the figures, each row represents a service and is ordered by priority level.

When the cell load increases, there is a deterioration of the users' throughput level, and even, its deactivation. This deactivation happens after reaching the minimum throughput value and also exceeding the cell load limit. For this purpose,

Figure 4.5, Figure 4.6, and Figure 4.7 were used to evaluate the increase in the number of users in the cell.

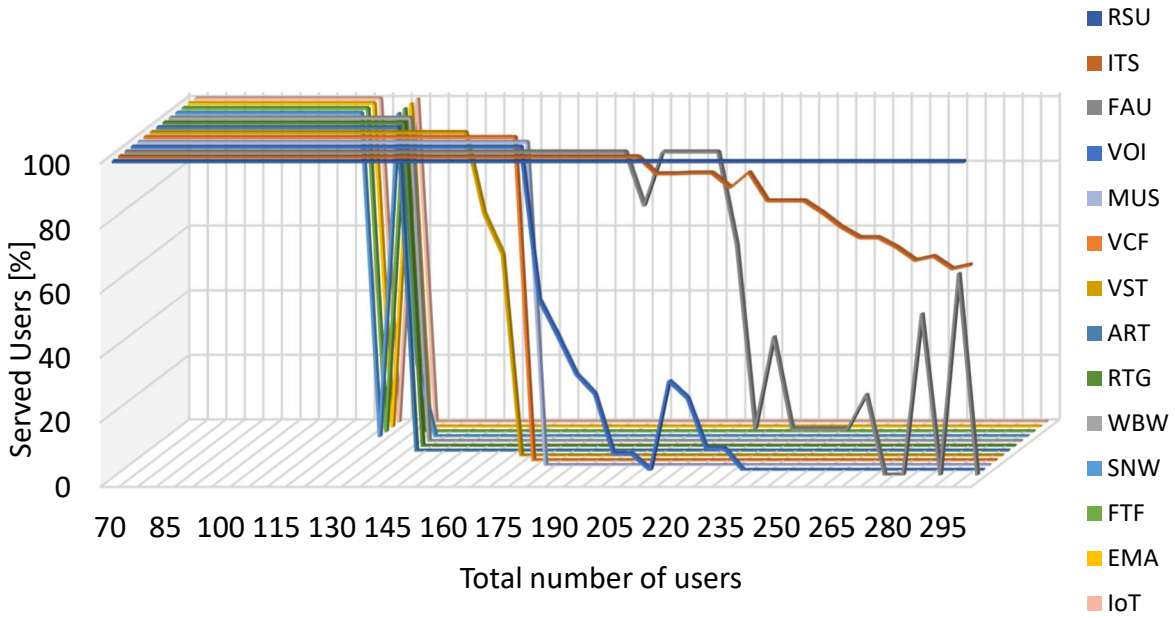

Figure 4.5. Percentage of served users per number of users for 0.7 GHz.

Comparing Figure 4.6 with Figure 4.5 it can be seen that due to the increase in bandwidth from 10 to 20 MHz the system can guarantee capacity for more users until the maximum load of the cell is reached, for 0.7 GHz it is up to 120 users and for 2.6 GHz 125 users. It is equally possible to verify that with 2.6 GHz up to 300 users is possible to ensure that users performing the two highest priority services always remain active.

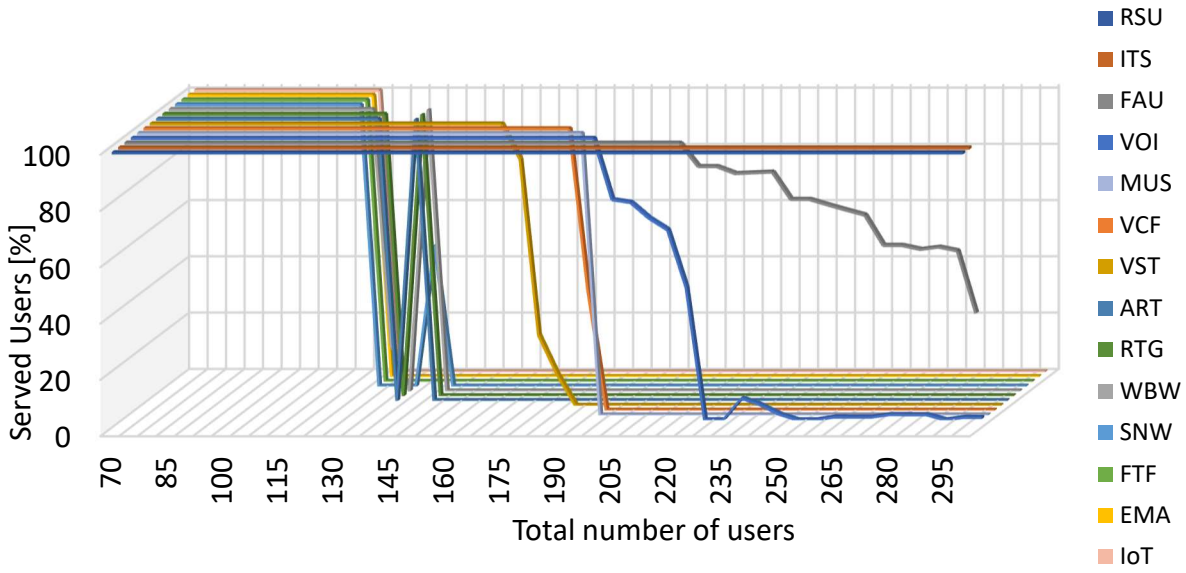

Figure 4.6. Percentage of served users per number of users for 2.6 GHz.

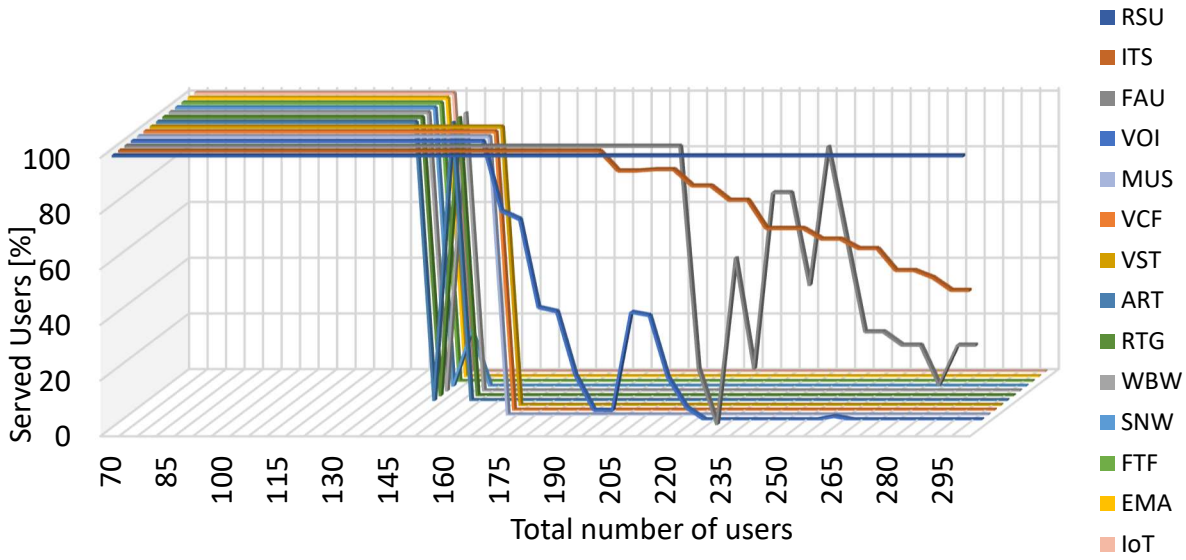

Figure 4.7. Percentage of served users per number of users for 3.6 GHz.

Analysing Figure 4.7, it is possible to conclude that up to a combined number of users equal to 145, it is possible to guarantee that all services are served at 100%, that is, with the increase in bandwidth, the cell capacity also increased, as it would be expected.

4.4 Influence of the Scenario

This section analyses the percentage of traffic per service, taking into account the aggregate number of users in the cell, as well as the number of users served in terms of the total number of users in the cell. This result analysis is performed by varying the scenarios according to Table 4.3, excluding the

reference service mix and keeping the frequency of 3.6 GHz. The same load of users in the cell was used as in the previous section, between 70 users and 300 users. The figures are grouped in pairs, each referring to the urban setting, subsequently suburban and rural.

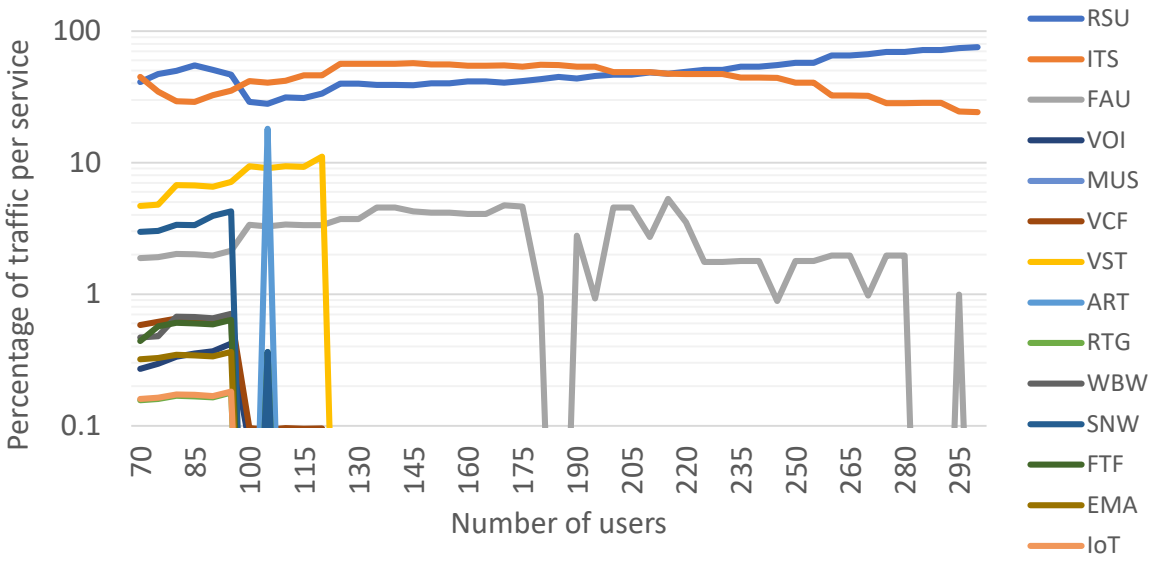

Figure 4.8. Percentage of traffic per service for urban scenario.

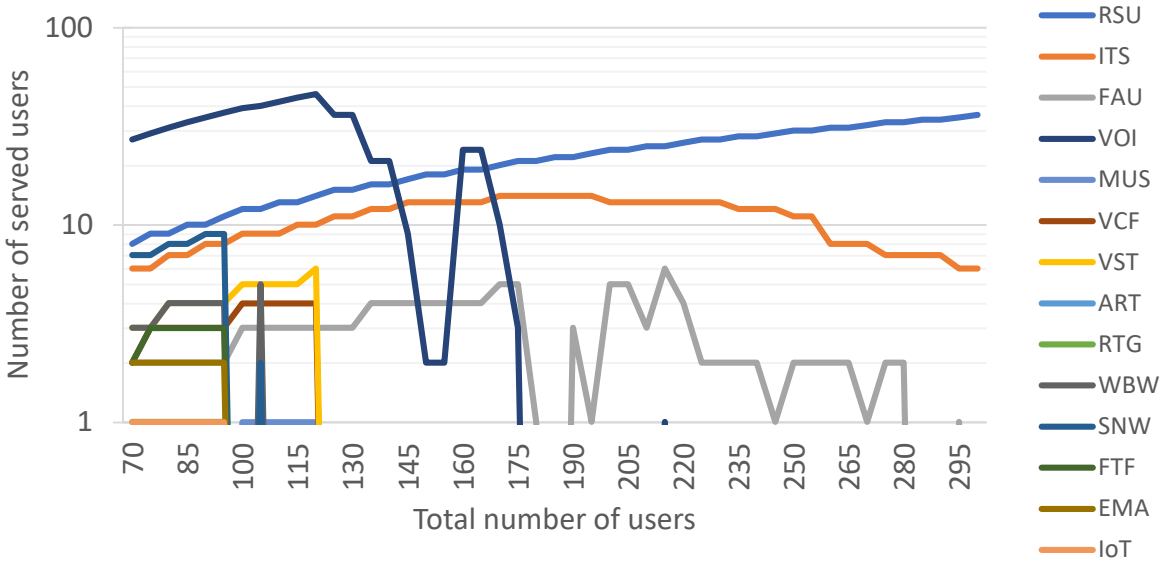

Figure 4.9. Number of users served per service for urban scenario.

By evaluating Figure 4.8 and Figure 4.9, regarding the urban scenario, it is possible to verify that the percentage of traffic from all services increases until achieving a total of 90 users in the cell. It can still be verified that the VOI service, despite the considerable number of users corresponding to 39% of the total cell load, it is not the service with the highest percentage of traffic due to its data rate. For the total load of 75 users in the cell, 29 utilise the VOI service. This service represents 0.3% of traffic, on the other hand the RSU service, which for the equivalent total number of users in the cell, only 9 use the RSU, represents 47% of the percentage of traffic generated.

When the aggregate number of users reaches 220, the combined number of served users no longer

varies greatly, being always between 41 and 43 users, justified by the fact that most services are no longer being served by the cell, leaving only 3, which require higher levels of data rate.

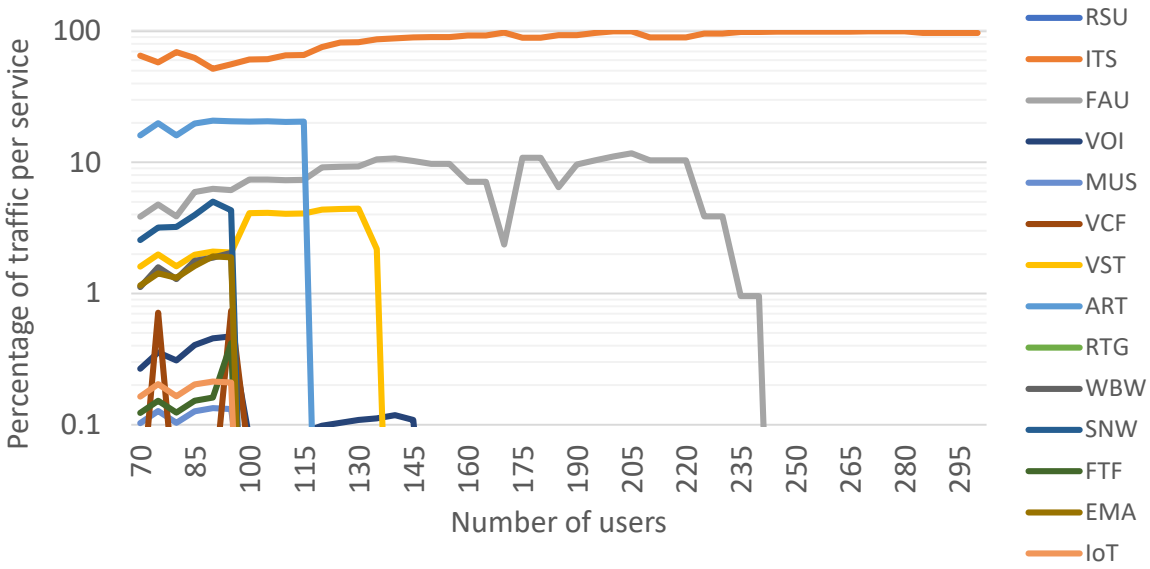

Figure 4.10. Percentage of traffic per service for suburban scenario.

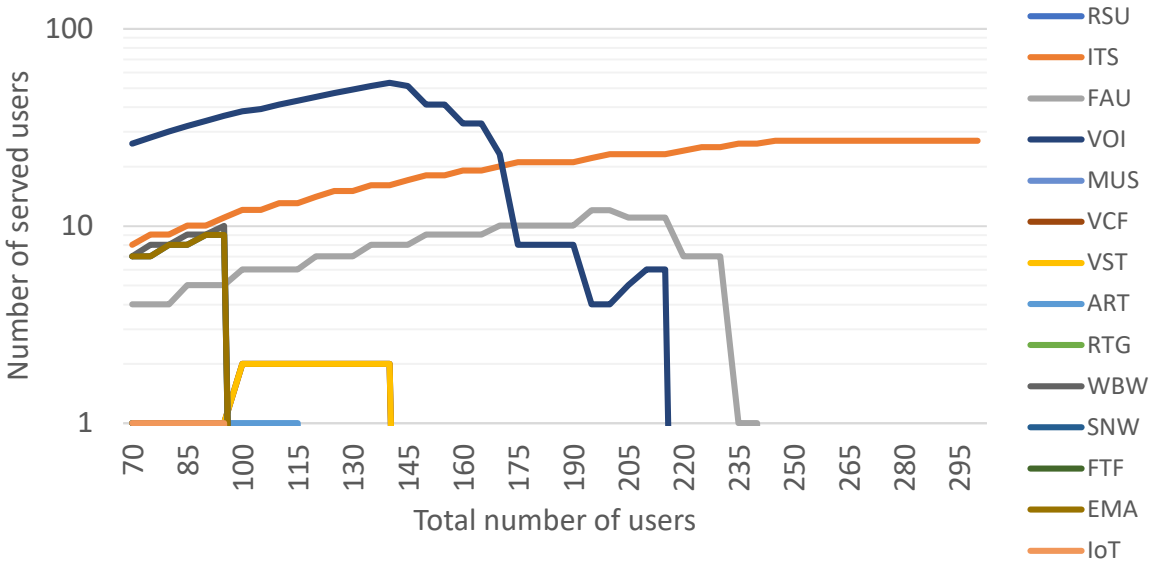

Figure 4.11. Number of users served per service for suburban scenario.

By analysing Figure 4.10 and Figure 4.11, regarding the suburban environment, it is possible to verify that the RSU resource is no longer included in both figures due to having 0% in the suburban service mix, with its percentage being distributed among the remaining services. It is equally possible to verify that due to the increase in the percentage of the ITS service in the transition from the urban to the suburban environment (9% and 12% respectively) and the fact that this service has a data rate at least 4 times higher than the other services, which from the total value of 150 users in the cell the ITS service represents more than 90% of the traffic generated. It is also verified that, as for the urban environment, the number of users served increases until achieving a total value of 90 users.

From the total value of 245 users, the number of users served becomes constant and equal to 27, and

these users are performing the ITS service. In comparison with the result obtained for the urban scenario, of about 42 users served, this is justified by the fact that the service data rate with the highest priority in use, in this case, ITS, has a minimum data rate almost double that of the service of highest priority in the urban scenario.

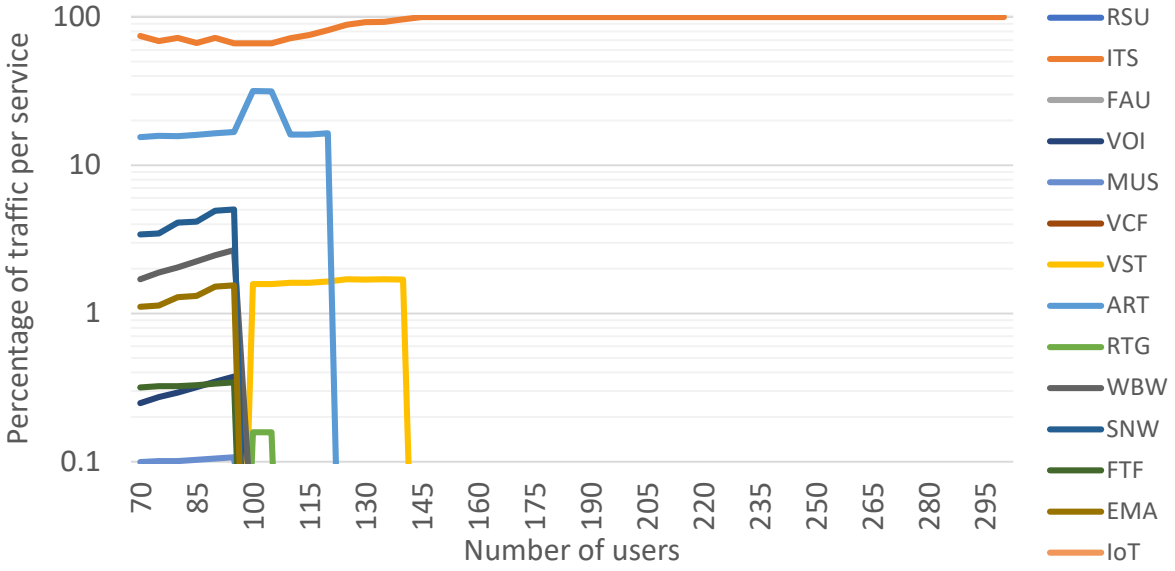

Figure 4.12. Percentage of traffic per service for rural scenario.

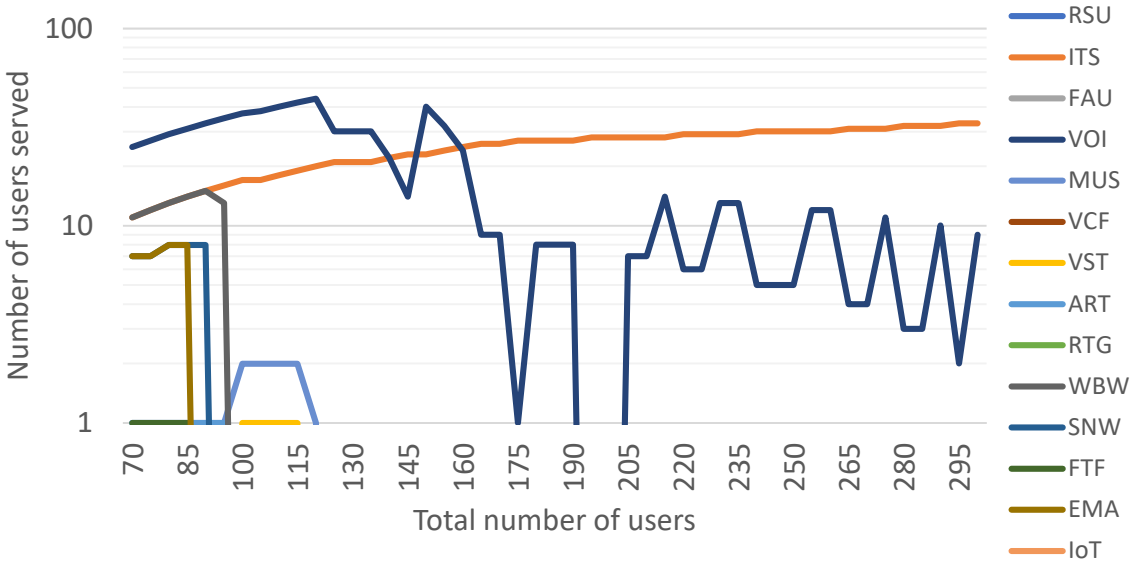

Figure 4.13. Number of users served per service for rural scenario.

From the evaluation of Figures 4.12 and 4.13, it is possible to verify the RSU and FAU services are not represented, as it would be expected and that due to the absence of these services, the VOI service has a vaster number of active users as the total number of users in the cell.

Regarding the number of users served, from the total value of 210 users, it varies between 35 and 42, which is higher than the suburban environment (27 users served) and when at most it fits the values of the urban environment (between 41 and 43 active users). It is possible to verify that from the total value of 120 users it is only possible to carry out ITS and VOI services.

4.5 Influence of the Service Mix

In this section, an analysis will be developed of the number of users served according to the total number of users of the cell, maintaining the urban scenario and the frequency of 3.6 GHz and only varying the service mix for 3 services, RSU, ITS and FAU according to Table 4.4.

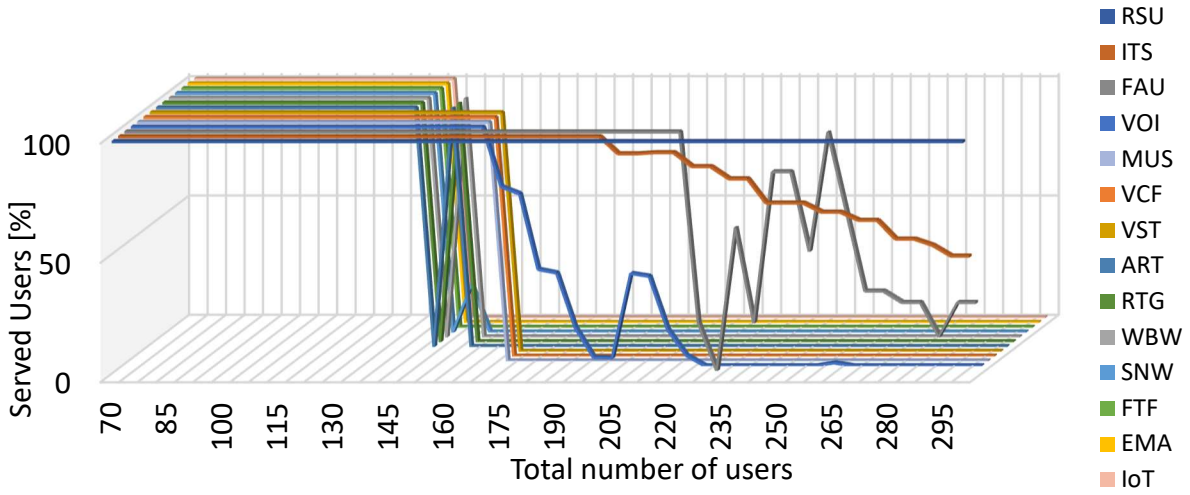

Figure 4.14. Number of users served per service to urban service mix 1.

In Figure 4.14, there is an increase in the percentage of the RSU service in the service mix, and it can be seen that the number of users served remains at 100% up to 145 total network users. It is also possible to see that despite the ITS service being more prioritised than the FAU service, the users who perform this service are no longer 100% when 205 users are reached, while the FAU service is no longer 100% served at 220 users that is, due to the fact that the ITS service has a high data rate and when users of this service are deactivated, it will be possible to occupy the vacant bandwidth with a less priority service with a data rate lower than the ITS service and that does not exceed the cell capacity.

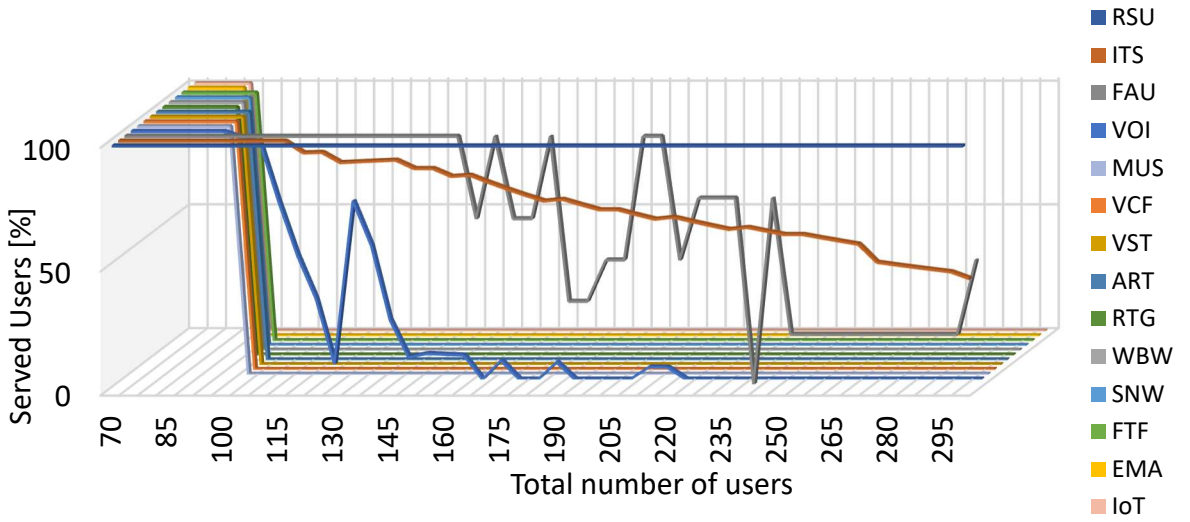

Figure 4.15. Number of users served per service to urban service mix 2.

In Figure 4.15, there is an increase in the percentage of the ITS service in the service mix, which, as

seen in the variation of scenarios, leads to the deactivation of most users who perform services of lesser priority when it achieves the total value of 95 users in the cell, not returning these services to have active users unlike service mix 1.

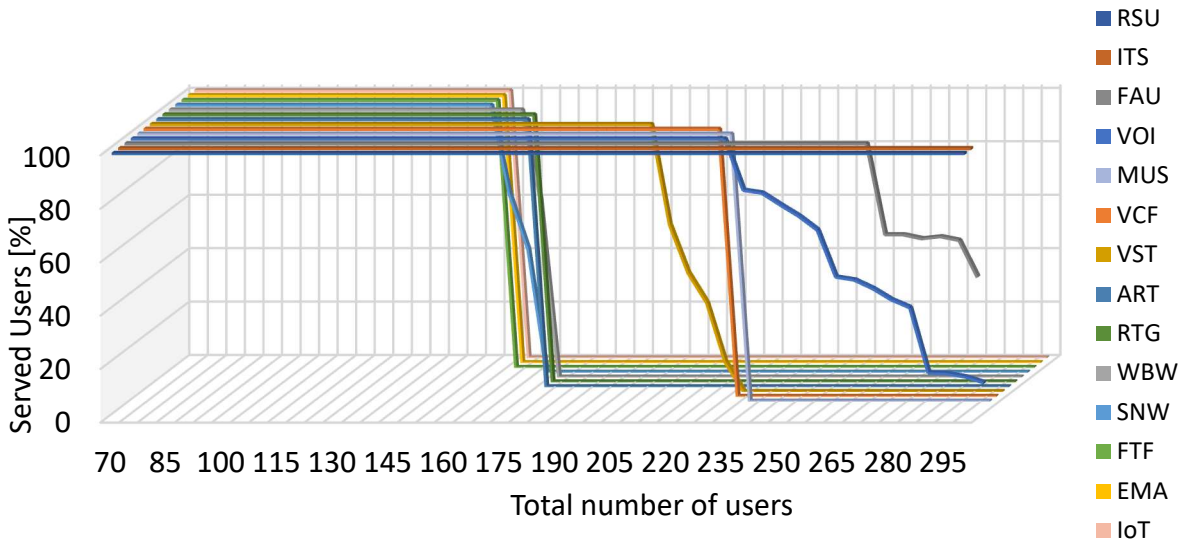

Figure 4.16. Number of users served per service to urban service mix 3.

In Figure 4.16, there is an increase in the percentage of the FAU service in the service mix as this service has a lower data rate than the other two, it can be perceived that the number of users served per service remains at 100 % for a greater total number of users than in the other two service mix. It can equally be noted that for urban service mix 3, the three highest priority services remain with 100% active users, up to a total of 270 users.

With this, it can be concluded that if the services with the highest percentage of users are services with lower data rates, it will allow more users to be active when the total number of users increases.

4.6 Deployment Analysis

Taking into account all the analysis carried out previously in terms of cell radius, as well as the number of users served and traffic generated, it is possible to develop an analysis regarding the three clusters represented in Figure 4.1, on how the three different scenarios can be covered.

Considering the probability of coverage is 90%, the cluster with urban scenario would need to cover 866 users in 0.5 km^2 the cluster with suburban scenario would need to cover 491 users in 2 km^2 and the cluster with rural scenario would need to cover 45 users in 10 km^2.

To obtain the results in Table 4.8, the cell radius was calculated for the various scenarios and for the different frequency bands through the Link Budget. Subsequently, the maximum capacity in which the cell guarantees that all cell users are served was calculated. Then, with the maximum value obtained, the number of cells necessary to guarantee that users for the various environments are covered by the

radio network was calculated.

Table 4.8. Number of cells to cover different scenarios.

Scenario	Area [km^2]	Number of users (90% of coverage)	Number of cells		
			Frequency band [GHz]		
			0.7	2.6	3.6
Urban	0.5	866	8	7	6
Suburban	2	491	7	6	3
Rural	10	45	2	2	4

For the urban scenario, eight cells of the 0.7 GHz frequency are necessary so that it is possible to cover the entire area and to have capacity for 866 users, for the case of the 2.6 GHz band, seven cells would be necessary to have capacity for 866 users and for 3.6 GHz, 6 cells would be needed. Aiming at the analysis made previously, this considerable number of cells would be caused by the traffic exerted on the network and not by the area that it is necessary to cover.

For the suburban scenario, due to the intensification of the ITS service traffic, a service with the most demanding data rate, the system continues to require a significant number of cells due to the traffic exerted.

As for the rural scenario, as the number of users is reduced and consequently the traffic generated is also reduced, the limitation in this scenario is caused by the 10 km^2 area that needs to be covered.

For the analysis over the years, it will be considered that in 2022 the total traffic will represent 500 users and that the services will be distributed by the bands as follows:

- the FAU, VST and RTG services will merely be carried out in the 0.7 GHz frequency band using NR technology;
- the VOI, MUS, VCF, WBW, SNW, FTF, EMA and IoT services will be carried out in the 0.8 GHz, 1.8 GHz and 2.6 GHz bands with identical percentages using LTE technology;
- the RSU, ITS and ART services will only take place in the 3.5 GHz frequency band using NR technology.

Table 4.9, Table 4.10, Table 4.11 and aim at a sounder understanding of how the traffic was assigned to the different bands, considering the three different conjugations of the bands with and without refarming, taking into account the urban service mix of Table 4.3, the sum of the percentages of the entire table is equal to 100%.

Table 4.9. Deployment service mix 1 (without refarming).

NR0.7 + L0.8 + L1.8 + L2.6 + NR3.6 Service mix [%]														
Freq [GHz]	RSU	ITS	FAU	VOI	MUS	VCF	VST	ART	RTG	WBW	SNW	FTF	EMA	IoT
0.7	0	0	3	0	0	0	5	0	2	0	0	0	0	0
0.8	0	0	0	13	0.3	1.3	0	0	0	1.6	3.3	1.3	1	0.6
1.8	0	0	0	13	0.3	1.3	0	0	0	1.7	3.3	1.3	1	0.7
2.6	0	0	0	13	0.4	1.4	0	0	0	1.7	3.4	1.4	1	0.7
3.5	12	9	0	0	0	0	0	1	0	0	0	0	0	0

Table 4.10. Deployment service mix 2 (with refarming of 2.6 GHz band).

NR0.7 + L0.8 + L1.8 + NR2.6 + NR3.6 Service mix [%]														
Freq [GHz]	RSU	ITS	FAU	VOI	MUS	VCF	VST	ART	RTG	WBW	SNW	FTF	EMA	IoT
0.7	0	0	1.5	0	0	0	2.5	0	1	0	0	0	0	0
0.8	0	0	0	19.5	5	2.5	0	0	0	2.5	5	2	1.5	1
1.8	0	0	0	19.5	5	2.5	0	0	0	2.5	5	2	1.5	1
2.6	0	0	1.5	0	0	0	2.5	0	1	0	0	0	0	0
3.5	12	9	0	0	0	0	0	1	0	0	0	0	0	0

Table 4.11. Deployment service mix 2 (with refarming of 1.8 and 2.6 GHz band).

NR0.7 + L0.8 + NR1.8 + NR2.6 + NR3.6 Service mix [%]														
Freq [GHz]	RSU	ITS	FAU	VOI	MUS	VCF	VST	ART	RTG	WBW	SNW	FTF	EMA	IoT
0.7	0	0	1	0	0	0	1.6	0	0.6	0	0	0	0	0
0.8	0	0	0	39	1	4	0	0	0	5	10	4	3	2
1.8	0	0	1	0	0	0	1.7	0	0.7	0	0	0	0	0
2.6	0	0	1	0	0	0	1.7	0	0.7	0	0	0	0	0
3.5	12	9	0	0	0	0	0	1	0	0	0	0	0	0

In addition to the distribution of services by the various bands as shown in the tables, the capacity over the years is also dependent on the type of traffic carried on the distinct bands, that is, the data rates of the services will influence the Cell load as can be seen in Figure 4.17, Figure 4.18 and Figure 4.19.

Figure 4.20 was built with the service mix of Table 4.9 and Figure 4.21 was built with the service mix of Table 4.9 for 2022 and 2023, the service mix of Table 4.10 for 2024 and 2025, and the service mix of Table 4.11 for 2026 and 2027.

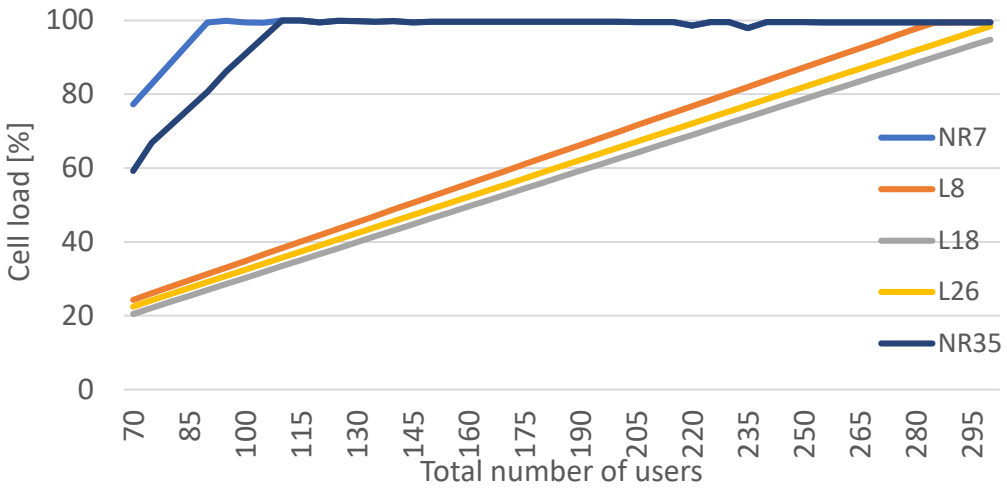

Figure 4.17. Cell load (without refarming).

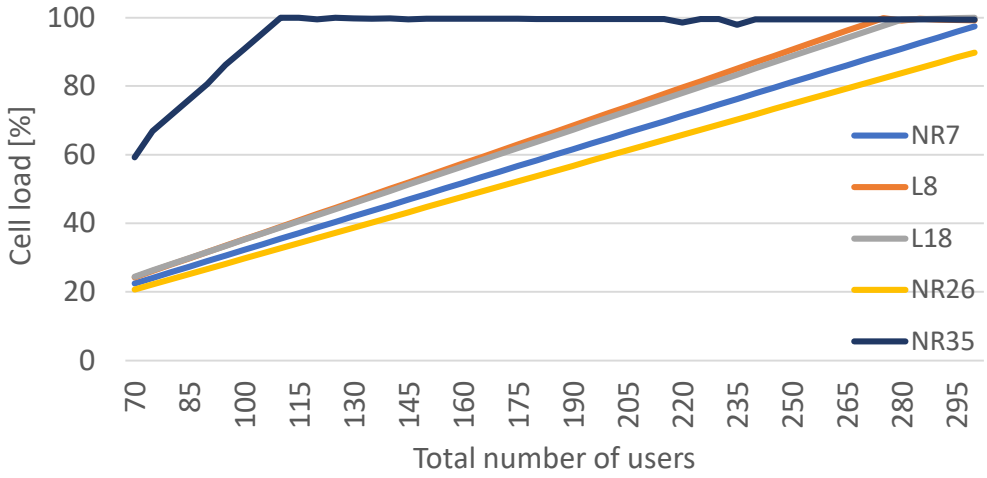

Figure 4.18. Cell load (with refarming of 2.6 GHz band).

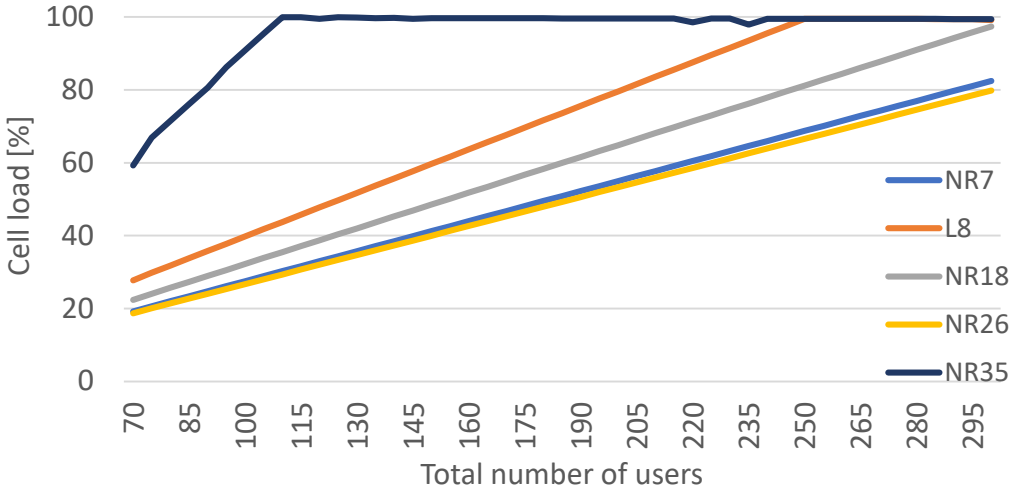

Figure 4.19. Cell load (with refarming of 1.8 and 2.6 GHz band).

In Figure 4.20, the same frequency bands and bandwidths are consistently used over the years, only

suffering changes due to the increase in traffic. The increase in traffic is not uniform for all services, taking into account Table 4.6. Although the 3.5 GHz band is only occupied by three services, these are services with high data rates, which leads to users who perform the ART service being unable to be served by the same cell from 2023 onwards, due to having exceeded the capacity thereof. The same occurs for the IT service from 2025 onwards.

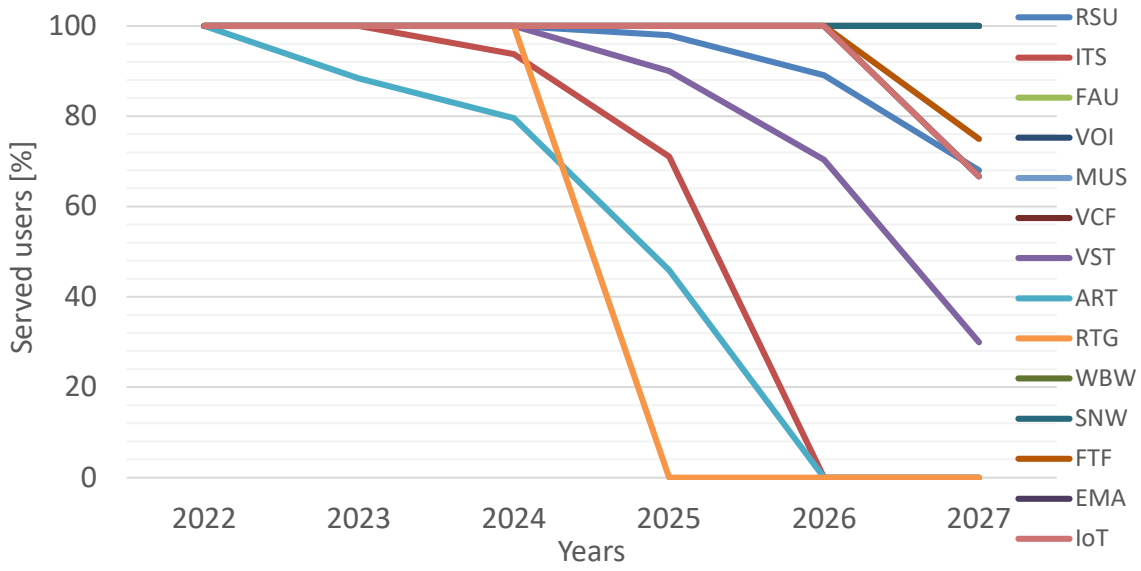

Figure 4.20. Percentage of users served during the years for scenario 1 (without refarming).

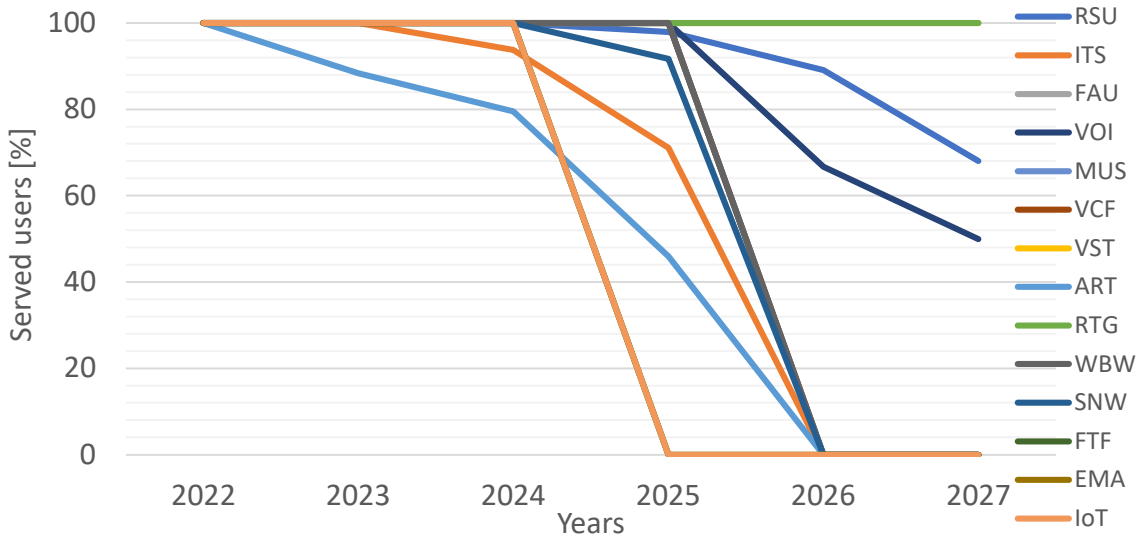

Figure 4.21. Percentage of users served during the years for scenario 2 (with refarming).

With the use of 2.6 GHz band refarming in 2024 and the 1.8 GHz band in 2026, the traffic of VOI, MUS, VCF, WBW, SNW, FTF, EMA and IoT services became limited to only two bands and subsequently to one band, limiting the available capacity for this type of service. Since there was no transition of traffic to the NR bands, and traffic from these services continues to increase, in 2025 users who perform the IoT service will be deactivated and in 2026 the WBW and SNW services will be deactivated. The

refarming of the two bands was carried out in such a way that the traffic of services carried out in the 0.7 GHz band would be executed in 3 bands, concluding users who perform these services can always be served 100% over the years.

Chapter 5

Conclusions

This chapter summarises all the information in the thesis as well as the main conclusions of each chapter.

The primary objective of this thesis was to study a 5G network implementation in a brownfield scenario, that is, on an existing network. This implementation helps to grasp the advantages and disadvantages in terms of coverage and capacity that this network offers. In order to achieve this, there was the need to develop a model that can be used to analyse the coverage and capacity variations by varying the input parameters according to the kind of scenario in question. As the name implies, the input parameters operated are deemed to simulate the regular behaviour of a 5G network. This model additionally allows to understand the importance of user density, traffic profiles among others on the network's coverage and capacity. As the name indicates, the input parameters are deemed to simulate the regular behaviour of a 5G network insert in a brownfield.

Chapter 1 presents a brief summary of the current state of mobile communications, establishing the transition and differences between LTE and 5G, such as the upgrades in terms of capacity that 5G provides. Also, in this chapter, the motivation for the development of this thesis is established, as well its structure.

Chapter 2 presents the fundamental information about the thesis, focusing on the architecture and presenting the standalone and non-standalone 5G perspectives, the network architecture for 5G and its interconnection with LTE and recent features such as network slicing, virtualisation and cloud. The radio interface is also discussed, mentioning multiple access schemes, spectrum usage including the bands used in 5G and the types of antennas use. This chapter is also focused on the fundamental characteristics of the study, issues of capacity, coverage, interference and a radio network planning is carried out. To conclude, the state of the art on the subject of this thesis is presented, which helped in the creation of the model, and in obtaining and analysing the results.

In Chapter 3, the parameters that allow the evaluation of the radio network, which is the object of study of this thesis, are exposed, as well as in which sub-model they are framed, between coverage, capacity, and interference. Subsequently, the description of the models used in the simulation, that allows the results achieved in this thesis. Annex A contains information utilised in relation to propagation models that are equally essential in creating the coverage model. The model functioning is briefly described as well, having been separated into 3 sections: coverage, capacity, and interference. It is equally necessary to describe the critical aspects of the use of the simulation model such as the Link Budget calculation, throughput ratios with Signal Interference plus Noise Ratio (SINR), path loss, cell overload, and others. Then, one presents how the model was implemented in a simulator, having been again divided into the three models. To conclude, the model assessment was carried out, which included a set of tests carried out on the three models, to ensure the veracity of the results and to make the necessary adjustments.

Chapter 4 describes the different scenarios that are used in the following sections, such as description of services, parameters for executing the Link Budget that include antenna power and gain, bandwidth, among others, different service mixes including the reference used. In order to assess the model, the number of users was varied for the urban, suburban and rural scenarios and, finally, information regarding the various bands are implemented at the same time so later it can be evaluated. The results described in the chapter are computed with the 0.7, 0.8, 1.8, 2.6 and 3.5 GHz bands. For Sections 4.4 and 4.5, the analysis of results is performed taking into account only the 3.5 GHz band. The focus of

this chapter is to carry out a three-dimensional evaluation of the frequency band parameters, scenarios (urban, suburban and rural) and service mix, that is, by fixing two of the factors, evaluate the parameters referring to the third factor. In addition to the three-dimensional evaluation, an evaluation is also carried out in terms of coverage and, finally, the use of the various bands at the same time, producing a variation over the years of the traffic.

In Section 4.2, the maximum distances at which a BS user can be found in order to carry out cell traffic with 1 Mbps, 5 Mbps, and 10 Mbps were analysed for the frequency bands 0.7, 1.8, 2.6, and 3.6 GHz. The Link Budget calculation and the use of propagation models allowed the calculation of the cell radius and it can be concluded that the Okumura-Hata model is invalid for 5 Mbps, in the urban setting with frequencies 0.7 and 1.8 GHz and for the suburban environment with the frequency 1.8 GHz. With the increase in the required rate to 10 Mbps, the Okumura-Hata model becomes invalid for all frequencies studied and for all environments, and the Winner II model is invalid for urban environments with frequencies 2.6 and 3.6 GHz. The results obtained in the section show that with increasing frequency there is a decrease in the maximum distance at which the user can be found, which for suburban environments the maximum distance at which the user is located is higher than in the suburban environment, and the same happens between the suburban and rural environment and finally with the increase of the required pace there is a decrease in the maximum distance at which the user can be found, causing some of the models invalid.

In Section 4.3, the frequency bands of 0.7, 2.6, and 3.6 GHz are analysed, using the same service mix and a similar scenario, in this case, the urban scenario is used. The results obtained are presented in terms of users served by service in function of the total number of users in the cell, and it is possible to verify that the system guarantees that 100% of the users are served for a total number of users of 120, 125 and 145 for the bandwidth of 0.7, 2.6 and 3.6 GHz respectively. The increase in the number of users served is primarily due to the rise in the bandwidth used for the different frequencies, 10 MHz for the 0.7 GHz band, 20 MHz for the 2.6 GHz band, and 100 MHz for the 3.6 GHz band.

In Section 4.4, the influence of urban, suburban, and rural scenarios analysis is carried out, maintaining the 3.6GHz band and adapting the service mix to the scenarios, as the type of traffic used varies depending on the scenario. Data are analysed in terms of traffic percentage and number of users served. The results show that the ITS service is one of the services that exerts the highest percentage of traffic in the cell due to its high data rate. Although this service is not the highest priority, nor does it have the highest percentage in the urban service mix, when the number of users is between 95 and 210, this is the service with the highest percentage of traffic generated. In the suburban environment, the deactivation of users of the RSU service further intensifies the percentage of traffic from users of the ITS service and has also increased the percentage of traffic from the FAU service, the third-highest priority service. Finally, in the rural environment, with the elimination of the service mix of MSW and FAU services, there is once again an increase in the percentage of traffic from users of the ITS service. For a certain level of users, the remaining traffic from other services is less than 0.1%, it should additionally be noted that in this scenario there is a densification of the number of users who use the VOI service, but even so, it has a traffic percentage below 0.1%.

In Section 4.5, the analysis of different service mixes kept the frequency band at 3.6 GHz and the urban scenario constant. The service mixes used to study the services of Remote Surgery, Intelligent transportation systems, and Factory automation, considered the highest priority services, having been made for each mix the intensification of the traffic generated by these services. It is a constant load in this study. The results obtained show that for services with more demanding data rates such as the Intelligent transportation system, the radio network saturates with fewer users compared to the other two services that have fewer demanding data rates. It is equally possible to verify that when using the Factory Automation Service, which has a lower data rate required, the highest priority services are able to maintain 100% of the users served, even when the total load of users in the cell is high, up to 270 users.

In Section 4.6, an analysis is performed of the conjunction of all the studies carried out in the previous sections, the urban, suburban and rural scenarios is evaluated for the frequencies 0.7, 2.6, and 3.6 GHz and the capacity, using an evolutionary increase in traffic over 6 years from 2022 to 2027, using 5 frequency bands, 0.7 and 3.5 GHz relative to NR; 0.8, 1.8 and 2.6 GHz relative to LTE. In one of the scenarios, two of the bands are refarmed, changing the NR frequency bands to 0.7, 0.8, 1.8, 2.6, and 3.6 GHz, with LTE traffic limited to the 0.8 GHz band.

The results obtained for this study are not the desired ones as it would not be expected in a radio network to be unable to perform a service due to excess load in a set of cells, this is justified by the fact that the traffic is not distributed correctly over the numerous bands and the traffic has been divided, assigning traffic from specific services to specific bands. A solution to solve the problem would be to assign different user deactivation loads according to the cell capacity being exceeded, preventing the total deactivation of users and distributing the traffic differently across the frequency bands.

In the future it would be interesting to consider and improve the interference among cells of this network, since in this simulator the interference is equal both for users in the centre of the cell and at the edge and that is not a realistic assumption, also other considerations about carrier aggregation can be accessed in the future since that could produce results with the greater bandwidths accessible for the 3.5 GHz band.

It would be useful for future work to consider a percentage deactivation of users, that is, due to the priority levels, the system completely deactivates the users of lower priority, as soon as the capacity saturates due to the underload of users. If the lowest priority service has a high data rate, these users will never be able to perform the same again, unless the number of cell users decreases. For this, a percentage deactivation in accordance with the priority would be more suitable.

It is a real complex issue to implement a realistic network of mobile communications. In practice, the terrain conditions are not consistently the same nor are they helpful for the solution, whereas in the simulator it is assumed that all buildings are equal with the same height. Furthermore, one aspect was briefly discussed in the thesis, given that the user distribution is even in all cell areas. In the future it would be interesting to adopt models that determine a more realistic user distribution, in order to produce more realistic results.

Annex A

Propagation Model

This Annex presents the Propagation Models used in this thesis are described in this annex.

A.1 Walfisch-Ikegami

Walfisch-Ikegami is developed for urban areas and it takes into consideration obstructing building height and street width, as well as other factors related to the urban environment. Walfisch-Ikegami considers distances greater than 100 m and less than 5 km

$$L_p = 42.6 + 26\log\left(d_{[\mathrm{km}]}\right) + 20\log\left(f_{[\mathrm{MHz}]}\right) \quad \text{(A.1)}$$

For: $\phi = 0$

Other cases:

$$L_p = \begin{cases} L_{0[\mathrm{dB}]} + L_{rt[\mathrm{dB}]} + L_{rm[\mathrm{dB}]}, L_{rt} + L_{rm} > 0 \\ L_{0[\mathrm{dB}]} \qquad\qquad\qquad\qquad , L_{rt} + L_{rm} \leq 0 \end{cases} \quad \text{(A.2)}$$

where:

- L_0: free space path loss;
- L_{rt}: Loss due the multi-screen diffraction;
- L_{rm}: Loss by diffraction and scattering from rooftop to street.

$$L_0 = 32.44 + 20\log\left(d_{[\mathrm{km}]}\right) + 20\log\left(f_{[\mathrm{MHz}]}\right) \quad \text{(A.3)}$$

$$L_{rm} = -16.9 - 10\log\left(w_{s[\mathrm{m}]}\right) + 10\log\left(f_{[\mathrm{MHz}]}\right) + 20\log\left(H_{B[\mathrm{m}]} - h_{m[\mathrm{m}]}\right) + L_{ori[\mathrm{m}]} \quad \text{(A.4)}$$

where:

- w_s: street width;
- H_B: building height;
- h_m: height of MT antenna;
- L_{ori}: orientation factor.

$$L_{ori} = \begin{cases} -10 + 0.354\phi_{[^\circ]} & ,0^\circ < \phi < 35^\circ \\ 2.5 + 0.075\left(\phi_{[^\circ]} - 35\right), & 35^\circ \leq \phi < 55^\circ \\ 4.0 + 0.114\left(\phi_{[^\circ]} - 55\right), & 55^\circ \leq \phi \leq 90^\circ \end{cases} \quad \text{(A.5)}$$

$$L_{rt} = L_{bsh[\mathrm{dB}]} + k_a + k_d\log\left(d_{[\mathrm{km}]}\right) + k_f\log\left(f_{[\mathrm{MHz}]}\right) - 9\log\left(w_{B[\mathrm{m}]}\right) \quad \text{(A.6)}$$

where:

- L_{bsh}: shadowing gain that occurs when the base station antenna is higher than rooftops;
- k_a: attenuation factor;
- k_d: distance factor;

- k_f: scenario factor;
- w_B: building separation.

$$k_d = \begin{cases} 18 & , h_b > H_B \\ 18 - 15\dfrac{h_b - H_B}{H_B} & , h_b \le H_B \end{cases} \quad \text{(A.7)}$$

where:

- h_b: height of BS antenna.

$$L_{bs} = \begin{cases} -18\log\left(h_{b\,[\mathrm{m}]} - H_{B\,[\mathrm{m}]} + 1\right) & , h_b > H_B \\ 0 & , h_b \le H_B \end{cases} \quad \text{(A.8)}$$

$$k_a = \begin{cases} 54 & , h_b > H_B \\ k_a' & , h_b \le H_B \end{cases} \quad \text{(A.9)}$$

$$k'_a = \begin{cases} 54 - 0.8(h_{b\,[\mathrm{m}]} - H_{B\,[\mathrm{m}]}) & , d \ge 0.5km \\ 54 - 1.6\left(h_{b\,[\mathrm{m}]} - H_{B\,[\mathrm{m}]}\right) d_{[\mathrm{km}]} & , d < 0.5km \end{cases} \quad \text{(A.10)}$$

$$k_f = \begin{cases} -4 + 0.7\left(\dfrac{f_{[\mathrm{MHz}]}}{925} - 1\right) & , urban\ and\ suburban \\ -4 + 1.5\left(\dfrac{f_{[\mathrm{MHz}]}}{925} - 1\right) & , dense\ urban \end{cases} \quad \text{(A.11)}$$

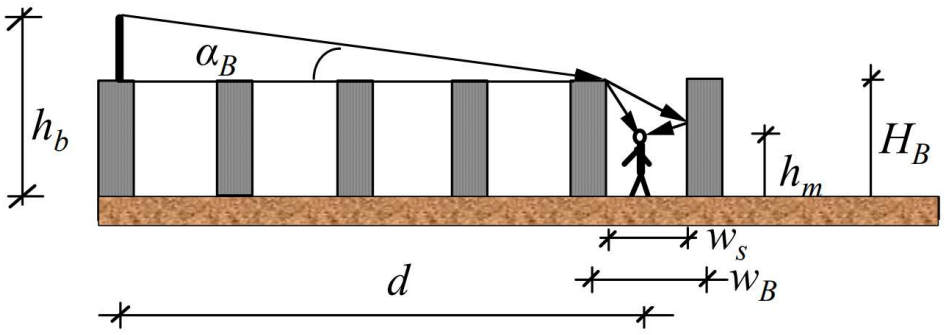

Figure A.6.1. Model parameters definition

The predicted path loss from the COST 231 Walfisch Ikegami model varies according to the parameters described above (i.e., street orientation, street width, building separation, base station height, and roof height).

The value for the path loss exponent for the interference model mention in (3.25) is given by:

$$\beta = \begin{cases} 26, & \phi = 0 \\ 20, & \phi \neq 0 \end{cases} \quad \text{(A.12)}$$

A.2 Okumura-Hata Model

This section aims to allow the path loss estimation between the BS and the UE for various environments used during this thesis. From the Okumura-Hata model that assesses frequencies between 0.7 GHz and 2 GHz for distances greater than 5 km and less than 10 km

$$L_{p_{[dB]}} = L_{A_{[\mathrm{dB}]}} + L_{B\,[\mathrm{dB}]} \log\left(d_{[\mathrm{km}]}\right) + L_{C_{[\mathrm{dB}]}} \quad \text{(A.13)}$$

where:

- L_A : correction factor related to the frequency, BS and UE antenna height, dependent on the propagation scenario;
- L_B : correction factor related to the BS antenna height;
- L_C : propagation scenario correction factor;

$$L_{A_{[\mathrm{dB}]}} = 69.55 + 26.16\, log\left(f_{[\mathrm{MHz}]}\right) - 13.82\, log\left(h_{be\,[\mathrm{m}]}\right) - \alpha\left(h_{mt\,[\mathrm{m}]}\right) \quad \text{(A.14)}$$

$$L_{B\,[\mathrm{dB}]} = 44.90 - 6.55 \log\left(h_{be\,[\mathrm{m}]}\right) \quad \text{(A.15)}$$

Urban	$\alpha\left(h_{mt\,[\mathrm{m}]}\right) = \left[1.1\, log\left(f_{[\mathrm{MHz}]}\right) - 0.7\right] h_{m\,[\mathrm{m}]} - \left[1.56\, log\left(f_{[\mathrm{MHz}]}\right) - 0.8\right]$	(A.16)
	$L_{C_{[dB]}} = 0$	(A.17)
Suburban	$\alpha\left(h_{mt\,[\mathrm{m}]}\right) = 8.29\ log\left(1.54 h_{m\,[\mathrm{m}]}\right)^2 - 1.1$	(A.18)
	$L_{C\,[\mathrm{dB}]} = -2 \log\left(\frac{f_{[\mathrm{MHz}]}}{28}\right)^2 - 5.4$	(A.19)
Rural	$\alpha\left(h_{mt\,[\mathrm{m}]}\right) = 3.2\ log\left(11.75\ h_{m\,[\mathrm{m}]}\right)^2 - 4.97$	(A.20)
	$L_{C\,[\mathrm{dB}]} = -4.78\, log\left(f_{[\mathrm{MHz}]}\right)^2 + 18.33\, log\left(f_{[\mathrm{MHz}]}\right) - 40.98$	(A.21)

The value for the path loss exponent for the interference model mention in (3.25) is given by:

$$\beta = L_B \quad \text{(A.22)}$$

A.3 Winner II

The WINNER II model aims to calculate the path loss between the BS and the UE, with distances between 100 m and 20 km using four different scenarios, B1 Urban Micro-cell scenario, C1 Suburban, C2 Urban Macro-cell, and finally D1 Rural Macro-cell.

$$L_{p_{[dB]}} = A\log(d_{[\mathrm{m}]}) + B + C\log\left(\frac{f_{c[\mathrm{GHz}]}}{5}\right) \quad \text{(A.23)}$$

$$d_{BP} = 4 \times h_{BS_{[\mathrm{m}]}} \times h_{m_{[\mathrm{m}]}} \times \frac{f_{[\mathrm{GHz}]}}{c_{[\mathrm{m/s}]}} \quad \text{(A.24)}$$

$$d'_{BP} = 4 \times h'_{BS_{[\mathrm{m}]}} \times h'_{m_{[\mathrm{m}]}} \times \frac{f_{[\mathrm{GHz}]}}{c_{[\mathrm{m/s}]}} \quad \text{(A.25)}$$

$$h'_{BS_{[\mathrm{m}]}} = h_{BS_{[\mathrm{m}]}} - 1 \quad \text{(A.26)}$$

$$h'_{m_{[\mathrm{m}]}} = h_{m_{[\mathrm{m}]}} - 1 \quad \text{(A.27)}$$

Table A.6.1. Path loss calculation Winner II model.

<table>
<tr><th colspan="2">Scenario</th><th>Path Loss [dB]</th><th>$\sigma_{[dB]}$</th><th>Applicability range/antenna height default value</th></tr>
<tr><td rowspan="5">B1</td><td>LOS</td><td>$A = 22.7,\ B = 41.0,\ C = 20$</td><td>3</td><td>$10\ \mathrm{m} < d_{1_{[\mathrm{m}]}} < d'_{BP_{[\mathrm{m}]}}$</td></tr>
<tr><td rowspan="2">LOS</td><td rowspan="2">$L_{p_{[\mathrm{dB}]}} = 40\,log(d_{1_{[\mathrm{m}]}}) + 9.45 - 17.3\,log\left(h'_{BS_{[\mathrm{m}]}}\right) - 17.3\,log\left(h'_{m_{[\mathrm{m}]}}\right) + 2.7\,log\left(\frac{f_{[\mathrm{GHz}]}}{5}\right)$</td><td rowspan="2">3</td><td>$d'_{BP_{[\mathrm{m}]}} < d_{1_{[\mathrm{m}]}} < 5\ \mathrm{km}$</td></tr>
<tr><td>$h_{BS} = 10\ \mathrm{m},\ h_m = 1.5\ \mathrm{m}$</td></tr>
<tr><td rowspan="4">NLOS</td><td rowspan="4">$L_{p_{[\mathrm{dB}]}} = \min\left(L_{p_{[\mathrm{dB}]}}(d1, d2), L_{p_{[\mathrm{dB}]}}(d2, d1)\right)$
Where:
$L_{p_{[\mathrm{dB}]}}(d_k, d_l) = L_{p_{LOS_{[\mathrm{dB}]}}}(d_k) + 20 - 12.5n_j + 10n_j\,log(d_l) + 30\,log\left(\frac{f_{[\mathrm{GHz}]}}{5}\right)$
And $n_j = max(2.8 - 0.0024d_k, 1.84)$,
$L_{p_{LOS}}$ is the path loss of B1 LOS scenario and $k, l \in \{1,2\}$</td><td rowspan="4">4</td><td>$10\ \mathrm{m} < d_{1_{[\mathrm{m}]}} < 5\ \mathrm{km}$</td></tr>
<tr><td>$w/2 < d_{2_{[\mathrm{m}]}} < 2\ \mathrm{km}$</td></tr>
<tr><td>$w = 20\ \mathrm{m}$(Street width)</td></tr>
<tr><td>$h_{BS} = 10\ \mathrm{m},\ h_m = 1.5\ \mathrm{m}$</td></tr>
</table>

C1	LOS	$A = 23.5,\ B = 41.2,\ C = 20$	4	$30\ \text{m} < d_{[\text{m}]} < d_{BP[\text{m}]}$
		$L_{p_{[\text{dB}]}} = 40\,log(d_{[\text{m}]}) + 11.65 - 16.2\,log\left(h_{BS[\text{m}]}\right) - 16.2\,log\left(h_{m[\text{m}]}\right) + 3.8\,log\left(\frac{f_{[\text{GHz}]}}{5}\right)$	6	$d_{BP[\text{m}]} < d_{[\text{m}]} < 5\ \text{km}$
				$h_{BS} = 25\ \text{m},\ h_m = 1.5\ \text{m}$
	NLOS	$L_{p_{[dB]}} = \left[44.9 - 6.55\,log\left(h_{BS[\text{m}]}\right)\right] log(d_{[\text{m}]}) + 31.46 + 5.83\,log\left(h_{BS[\text{m}]}\right) + 23\,log\left(\frac{f_{[\text{GHz}]}}{5}\right)$	8	$50\ \text{m} < d_{[\text{m}]} < 5\ \text{km}$
				$h_{BS} = 25\ \text{m},\ h_m = 1.5\ \text{m}$
C2	LOS	$A = 26,\ B = 39,\ C = 20$	4	$10\ m < d_{[m]} < d'_{BP[m]}$
		$L_{p_{[dB]}} = 40\,log(d_{[m]}) + 13.47 - 14\,log\left(h_{BS[m]}\right) - 14\,log\left(h_{m[m]}\right) + 6\,log\left(\frac{f_{[GHz]}}{5}\right)$	6	$d'_{BP[m]} < d_{[m]} < 5\ km$
				$h_{BS} = 25\ m,\ h_m = 1.5\ m$
	NLOS	$L_{p_{[\text{dB}]}} = \left[44.9 - 6.55\,log\left(h_{BS[\text{m}]}\right)\right] log(d_{[\text{m}]}) + 34.46 + 5.83\,log\left(h_{BS[\text{m}]}\right) + 23\,log\left(\frac{f_{[\text{GHz}]}}{5}\right)$	8	$50\ m < d_{[m]} < 5\ km$
				$h_{BS} = 25\ m,\ h_m = 1.5\ m$
D1	LOS	$A = 21.5,\ B = 44.2,\ C = 20$	4	$10\ \text{m} < d_{[\text{m}]} < d_{BP[\text{m}]}$
		$L_{p_{[\text{dB}]}} = 40\,log(d_{[\text{m}]}) + 10.5 - 18.5\,log\left(h_{BS[\text{m}]}\right) - 18.5\,log\left(h_{m[\text{m}]}\right) + 1.5\,log\left(\frac{f_{[\text{GHz}]}}{5}\right)$	6	$d_{BP[\text{m}]} < d_{[\text{m}]} < 10\ \text{km}$
				$h_{BS} = 32\ \text{m},\ h_m = 1.5\ \text{m}$
	NLOS	$L_{p_{[\text{dB}]}} = 25.11\,log(d_{[\text{m}]}) + 55.4 - 0.13\left(h_{BS[\text{m}]} - 25\right) log\left(\frac{d_{[\text{m}]}}{100}\right) - 0.9(h_{m[\text{m}]} - 1.5) + 21.3\,log\left(\frac{f_{[\text{GHz}]}}{5}\right)$	8	$50\ \text{m} < d_{[\text{m}]} < 5\ \text{km}$
				$h_{BS} = 32\ \text{m},\ h_m = 1.5\ \text{m}$

The value for the path loss exponent for the interference model mention in (3.25) is given by:

$$\beta = \begin{cases} 22.7\ , B1\ scenario \\ 23.5\ , C1\ scenario \\ 26.0\ , C2\ scenario \\ 21.0\ , D1\ scenario \end{cases} \quad \text{(A.28)}$$

References

[3GPP18a] 3GPP, *Technical Specification Group Services and System Aspects: Study on enhancement of 3GPP Support for 5G V2X Services (Release 16),* Report TR 22.886, V16.2.0, Dec.2018. Available: https://www.tech-invite.com/3m22/tinv-3gpp-22-886.html.

[3GPP19] 3GPP, *Digital cellular telecommunications system (Phase 2+) (GSM); Universal Mobile Telecommunications System (UMTS)*, Report TR 21.915, Stage 2 (Release 15), V15.0.0, Oct. 2019. Available: https://www.tech-invite.com/3m21/tinv-3gpp-21-915.html.

[3GPP20a] 3GPP, *System Architecture for the 5G System*, Internal Report TS 23.501, Stage 2 (Release 16), V16.7.0, Jan. 2021. Available: https://www.tech-invite.com/3m23/tinv-3gpp-23-501.html.

[3GPP20b] 3GPP, *Evolution across three major Releases*, Poster, Feb. 2020 Available: https://www.3gpp.org/ftp/Information/presentations/presentations_2020/Poster_2020_MWC_v6_OPTIMIZED.pdf.

[3GPP21] 3GPP, *5G; NR; Physical channels and modulation*, Internal Report TS 38.211, (Release 16), V16.5.0, Apr. 2021. Available: https://www.tech-invite.com/3m38/tinv-3gpp-38-211.html.

[5GAm17] 5G Americas, "5G Spectrum Recommendations", *5G Americas*, Apr. 2017. Available: https://www.5gamericas.org/5g-spectrum-recommendations/.

[Alco17] A. Alcobia, *LTE radio network deployment design in urban environments under different traffic scenarios*, M.Sc. Thesis, Instituto Superior Técnico, University of Lisbon, Lisbon, Portugal, 2017. Available: https://grow.tecnico.ulisboa.pt/research/publications/#msc-theses.

[AFZT20] G. Athanasiadou, P. Fytampanis, D. Zarbouti, G.V Tsoulos, P. Gkonis and D. Kaklamani "Radio Network Planning towards 5G mmWave Standalone Small-Cell Architectures*", Electronics*, Vol. 9. No. 2, Feb. 2020, pp. 2019-9292 Available: https://doi.org/10.3390/electronics9020339.

[ALTI20] Altice Labs, *5G Intelligent Communications for V2X ecosystems Whitepaper*, Jul. 2020 Available: https://www.alticelabs.com/content/WP_5G_Intelligent_Communications.pdf.

[ANAC20a] ANACOM, *ANACOM creates conditions for consistent and competitive development of 5G in Portugal*, Nov. 2019. Available: https://www.anacom.pt/render.jsp?contentId=1493002.

[ANAC20b] ANACOM, *Auction Regulation for the Allocation of Rights of Use of Frequencies in the 700 MHz, 900 MHz, 1800 MHz, 2.1 GHz, 2.6 GHz and 3.6 GHz bands*, Regulation no. 987-

A/2020, Nov. 2020. Available: https://anacom.pt/render.jsp?contentId=1573881&languageId=1.

[Belc18] I. Belchior, *Evaluation of 5G Cellular Network Implementation Over an Existing LTE One*, M.Sc. Thesis, Instituto Superior Técnico, University of Lisbon, Lisbon, Portugal, 2018. Available: https://grow.tecnico.ulisboa.pt/research/publications/#msc-theses.

[Carv21] A. Carvalho, *Analysis of Strategies for Minimising End-to-End Latency in 4G and 5G Networks*, M.Sc. Thesis, Instituto Superior Técnico, University of Lisbon, Lisbon, Portugal, 2021. Available: https://grow.tecnico.ulisboa.pt/research/publications/#msc-theses.

[Cisc20] Cisco, *Cisco Annual Internet Report (2018–2023)*, White Paper, Cisco Public, Mar. 2020. Available: https://www.cisco.com/c/en/us/solutions/collateral/executive-perspectives/annual-internet-report/white-paper-c11-741490.html.

[CJMN20] J. Campos, G. Jue, M. Millhaem, R. Nichols and K. Sundhar, "The 5G NR Standard", in N. Faubert (ed.), *Engineering the 5G World – Design and Test Insights*, Keysight Technologies, USA, 2020. Available: https://www.keysight.com/zz/en/assets/7119-1223/ebooks/Engineering-the-5G-World.pdf?success=true.

[Corr20] L.M. Correia, *Mobile Communication Systems*, Lecture Notes, Instituto Superior Técnico, University of Lisbon, Lisbon, Portugal, 2021. Available: https://fenix.tecnico.ulisboa.pt/disciplinas/SCM364511132646/2020-2021/2-semestre/lectures.

[DAPS16] E. Dahlman, S. Parkvall and J. Skold, "5G wireless access", in Academic Press, Inc. (ed.), *4G, LTE-Advanced Pro and The Road to 5G*, San Diego, USA, 2016. Available: https://www.academia.edu/36715560/4G_LTE_Advanced_Pro_and_The_Road_to_5G_Third_Edition.

[ERIC18] Ericsson, *Advanced antenna systems for 5G networks*, White Paper, Nov. 2018. Available: https://www.ericsson.com/en/reports-and-papers/white-papers/advanced-antenna-systems-for-5g-networks.

[ERIC21] Ericsson, *Ericsson Mobility Report*, White Paper, Nov. 2021. Available: https://www.ericsson.com/en/reports-and-papers/mobility-report/reports/november-2021.

[FCDY20] M. Fuentes, J. Carcel, C. Dietrich, L. Yu, E. Garro, P. Volker, F. Lazarakis, O.Grondalen, O. Bulakci, J. Yu, W. Mohr and D. Gomez-Barquero "5G New Radio Evaluation Against IMT-2020 Key Performance Indicators", *IEEE Access*, Vol. 8, 2020, pp. 110880-110896. Available: https://ieeexplore.ieee.org/document/9114983.

[GPRC19] M. Giordani, M. Polese, A. Roy, D. Castor and M. Zorzi, "A Tutorial on Beam Management for 3GPP NR at mmWave Frequencies", *IEEE communications surveys & tutorials*, Vol. 21, No. 1, Apr. 2019, pp. 173-196. Available: https://ieeexplore.ieee.org/document/8458146.

[HYW19] N. Hassan, K.A. Yau and C. Wu, "Edge Computing in 5G: A Review", *IEEE Access*, Vol. 7,

Aug. 2019, pp. 127276-127289. Available: https://ieeexplore.ieee.org/document/8821283.

[IAIH18] I. Parvez, A. Rahmati, I. Guvenc, A. Sarwat and H. Dai, "A Survey on Low Latency Towards 5G: RAN, Core Network and Caching Solutions", *IEEE communications Surveys & Tutorials*, Vol. 20, No. 4, May. 2018, pp. 3098–3130. Available: https://ieeexplore.ieee.org/document/8367785.

[ITUR04] ITU-R Radiocommunication Sector ITU, *Adaptive antennas concepts and key technical aspects*, Report ITU-R M.2040-0, Jan. 2004. Available: https://www.itu.int/pub/R-REP-M.2040-2004.

[ITUR15] ITU-R Radiocommunication Sector ITU, *IMT traffic estimates for the years 2020 to 2030,* Report ITU-R M. 2370-0, Jul. 2015. Available: https://www.itu.int/pub/R-REP-M.2370-2015.

[ITUR15a] ITU-R Radiocommunication Sector ITU, *IMT Vision – Framework and overall objectives of the future development of IMT for 2020 and beyond*, Report ITU-R M.2083-0, Sep. 2015. Available: https://www.itu.int/rec/R-REC-M.2083-0-201509-I/en.

[JMJL02] J. Marescaux, J. Leroy, F. Rubino and M. Smith, "Transcontinental Robot-Assisted Remote Telesurgery: Feasibility and Potential Applications", *Annals of Surgery,* Vol. 235, No. 4, Apr. 2002, pp 487–492. Available: https://www.ncbi.nlm.nih.gov/pmc/articles/PMC1422462/pdf/20020400s00005p487.pdf.

[KCFH19] O. Kaddoura, J. Carnero, J. Fernández, R. Hernández, M. Larrubia, L. Ríos, J. Sánchez and R. Barco, "Greenfield Design in 5G FWA Networks", *IEEE Communications Letters*, Vol. 23, No. 12, Dec. 2019, pp. 2422-2426. Available: https://ieeexplore.ieee.org/document/8825811.

[KGE20] M. Khan, A. García-Armada and J. Escudero-Garzás, "Service-Based Network Dimensioning for 5G Networks Assisted by Real Data", *IEEE Access*, Vol. 8, Jul. 2020, pp. 129193-129212. Available: https://ieeexplore.ieee.org/document/9139969.

[KMHZ08] P. Kyösti, J. Meinilä, L. Hentila, X. Zhao, T. Jämsä, C. Schneider, M. Narandzic, M. Milojević, A. Hong, J. Ylitalo, V. Holappa, M. Alatossava, R. Bultitude, Y. Jong, T. Rautiainen, "WINNER II channel models", Article, Feb. 2008. Available: https://www.researchgate.net/publication/234055761_WINNER_II_channel_models.

[Mour21] F. Moura, *Analysis of the Impact of EMF Restrictions on 5G Base Stations Deployment in Existing Networks*, M.Sc. Thesis, Instituto Superior Técnico, University of Lisbon, Lisbon, Portugal, 2021. Available: https://grow.tecnico.ulisboa.pt/research/publications/#msc-theses.

[Mari21] S. Marinheiro, *Analysis of the Implementation of Network Slicing in 5G Radio Networks*, M.Sc. Thesis, Instituto Superior Técnico, University of Lisbon, Lisbon, Portugal, 2021. Available: https://grow.tecnico.ulisboa.pt/research/publications/#msc-theses.

[NAIA14] O. Najm, M. Ismail and G. Abed, "High-Performance Mobile Technology LTE-A using the

Stream Control Transmission Protocol: A Systematic Review and Hands-on Analysis", *Journal of Applied Sciences*, Vol.14, No.19, 2014, pp. 2194-2218 Available: https://scialert.net/abstract/?doi=jas.2014.2194.2218.

[NOKI18] Nokia, *5G deployment below 6 GHz - Ubiquitous coverage for critical communication and massive IoT*, White Paper, Finland, Oct 2018. Available: https://www.rrt.lt/wp-content/uploads/2018/10/Nokia_5G_Deployment_below_6GHz_White_Paper_EN.pdf.

[PSMM17] P. Schulz, M. Matthé, H. Klessig and M. Simsek, "Latency Critical IoT Applications in 5G: Perspective on the Design of Radio Interface and Network Architecture", *IEEE Communications Magazine*, Vol. 55, No. 2, Feb. 2017, pp. 70-78. Available: https://ieeexplore.ieee.org/document/7842415.

[Patr21] S. Patrício, *Influence of Active Antennas on EMF Restrictions in 5G Base Stations Deployment*, M.Sc. Thesis, Instituto Superior Técnico, University of Lisbon, Lisbon, Portugal, 2021. Available: https://grow.tecnico.ulisboa.pt/research/publications/#msc-theses.

[QJGZ18] Q. Zhang, J. Liu and G. Zhao, *Towards 5G Enabled Tactile Robotic Surgery*, Aarhus University, Aarhus, Denmark, Mar. 2018. Available: https://arxiv.org/pdf/1803.03586.pdf.

[Qual18] Qualcomm, *VR and AR pushing the connectivity limits*, Qualcomm Technologies, Oct. 2018. Available: https://www.qualcomm.com/media/documents/files/vr-and-ar-pushing-connectivity-limits.pdf.

[Rodr15] J. Rodriguez, "Small Cells for 5G Mobile Networks", in John Wiley & Sons, Ltd. (ed.), *Fundamentals of 5G Mobile Networks*, United Kingdom, 2015. Available: https://www.researchgate.net/publication/324862482_Fundamentals_of_5G_mobile_networks.

[SeDo19] S. Domingues, *Analysis of the Performance of Multi-Access Edge Computing Network Slicing in 5G*, M.SC thesis, Instituto Superior Técnico, Lisbon, Portugal, Nov. 2019. Available: https://grow.tecnico.ulisboa.pt/wp-content/uploads/2020/07/Thesis_SergioD_vPublic.pdf.

[SFVS20] G. Soos, D. Ficzere, P. Varga and Z. Szalay, *Practical 5G KPI Measurement Results on a Non-Standalone Architecture*, Jan. 2020. Available: https://www.researchgate.net/publication/338992230_Practical_5G_KPI_Measurement_Results_on_a_Non-Standalone_Architecture.

[Skol90] M. Skolnik, *Radar Handbook*, McGraw-Hill, New York, USA, 1990. Available: https://www.geo.uzh.ch/microsite/rsl-documents/research/SARlab/GMTILiterature/PDF/Skolnik90.pdf.

[Tabb19] S. Tabbane, *LTE planning and dimensioning: ITU PITA Workshop on Mobile network planning and security*, Nadi, Fiji Island, Oct. 2019. Available: https://www.itu.int/en/ITU-D/Regional-Presence/AsiaPacific/SiteAssets/Pages/Events/2019/ITUPITA2018/ITU-ASP-

CoE-Training-on-/LTE%20planning%20and%20dimensioning.pdf.

[Viei18] A. Vieira, *Analysis of 5G Cellular Radio Network Deployment over Several Scenarios*, M.Sc. Thesis, Instituto Superior Técnico, University of Lisbon, Lisbon, Portugal, 2018. Available: https://grow.tecnico.ulisboa.pt/research/publications/#msc-theses.

[WJSW17] J. Wang, A. Jin, D. Shi, L. Wang, H. Shen, D. Wu, L. Hu, L. Gu, L. Lu, Y Chen, J. Wang, Y. Saito, A. Benjebbour and Y, Kishiyama, "Spectral Efficiency Improvement With 5G Technologies: Results From Field Tests", *IEEE Journal on Selected Areas in Communications*, Vol. 35, No. 8, Aug. 2017, pp. 1867-1875. Available: https://ieeexplore.ieee.org/document/7944631.

[WLY20] J. Wang, C. Lee and X. Wu, "A Coverage-Based Location Approach and Performance Evaluation for the Deployment of 5G Base Stations," *IEEE Access*, Vol. 8, Jul. 2020, pp. 123320 - 123333. Available: https://ieeexplore.ieee.org/document/9131799/authors.

[YUKI13] S. Yu and S. Kim, "Downlink capacity and base station density in cellular networks", in *2013 11th International Symposium and Workshops on Modelling and Optimisation in Mobile, Ad Hoc and Wireless Networks (WiOpt)*, Tsukuba, Japan, May 2013. Available: https://ieeexplore.ieee.org/document/6576422.